

**REPUBLIC OF TURKEY
HACETTEPE UNIVERSITY
INSTITUTE OF HEALTH SCIENCES**

**EXPRESSION AND FUNCTIONAL ANALYSIS OF CCRL2
ATYPICAL CHEMOKINE RECEPTOR VARIANTS ON BREAST
CANCER CELLS**

Dr. Parisa SARMADI

**Tumor Biology and Immunology
PHD THESIS**

**ANKARA
2014**

**REPUBLIC OF TURKEY
HACETTEPE UNIVERSITY
INSTITUTE OF HEALTH SCIENCES**

**EXPRESSION AND FUNCTIONAL ANALYSIS OF CCRL2
ATYPICAL CHEMOKINE RECEPTOR VARIANTS ON BREAST
CANCER CELLS**

Dr. Parisa SARMADI

**Tumor Biology and Immunology
PhD THESIS**

**Advisor of Thesis
Assoc. Prof. Dr. Güneş ESENDAĞLI**

**ANKARA
2014**

Department: **Basic Oncology**
Program: **Tumor Biology and Immunology**
Dissertation Title: **Expression and Functional Analysis of
CCRL2 Atypical Chemokine Receptor
Variants on Breast Cancer Cells**

Name of the Student: **Parisa SARMADI**

Date of Dissertation Defense: **June 30, 2014**

This study has been accepted and approved as a PhD dissertation in the program of "Tumor Biology and Immunology" by the examining committee, whose members are listed below.

Chairman of the Committee: **Prof. Dr. A. Lale DOĞAN**
Hacettepe University

Advisor of the Dissertation: **Assoc. Prof. Dr. Güneş ESENDAĞLI**
Hacettepe University

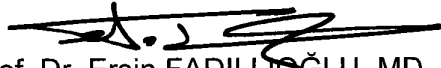
Member: **Prof. Dr. Emin KANSU**
Hacettepe University

Member: **Prof. Dr. Dicle GÜÇ**
Hacettepe University

Member: **Assoc. Prof. Dr. Güldal YILMAZ**
Gazi University

APPROVAL

This dissertation has been approved by the committee above in conformity to the regulations and bylaws of Hacettepe University Graduate Programs and has been accepted by the Board of Directors of the Institute of Health Sciences.


Prof. Dr. Ersin FADILLIOĞLU, MD, PhD
Institute Director

ACKNOWLEDGEMENTS

I would like to express my deepest gratitude and appreciation to my advisor Assoc. Prof. Dr. Güneş ESENDAĞLI for his support, encouragement, and guidance during all parts of my PhD study.

I would like to express my deepest gratitude to Prof. Dr. Emin KANSU for his constitutive support and gentle and kind attitude; also, for his passion in science and transferring it to and inspiring students.

I deeply and faithfully thank Prof. Dr. Dicle GÜÇ for her continuous support, kind-heartedness and guidance and for sharing her knowledge and experiences.

I would like to gratefully thank Prof. Dr. A. Lale DOĞAN for her support, delicacy and kindness.

I would like to cordially express my deepest and infinite gratitude and thankfulness to Asst. Prof. Dr. Hande CANPINAR for her support.

I would like to gratefully thank Assoc. Prof. Dr. Güldal YILMAZ from Pathology Department at Gazi University for the great Immunohistochemistry analysis of breast cancer tissues.

I would like to thank Asst. Prof. Dr. Füsün ÖZMEN for her kind attitude and support.

I would like to gratefully thank Prof. Dr. Petek KORKUSUZ from Histology and Embryology Department and Prof. Dr. Nuhan PURALI from Biophysics Department at Hacettepe University for the important fluorescence microscopic observations.

I would like to thank Basic Oncology students, the secretary, and all Basic Oncology Department family for their help and friendship.

I would like to express my cordial and deepest gratitude to my family for their support. I dedicate this thesis to them.

This study was supported by Eczacıbaşı Research and Awards Fund.

ÖZET

Sarmadi, P. CCRL2 atipik kemokin reseptör varyantlarının meme kanseri hücrelerinde ekspresyonu ve fonksiyonel analizi. Hacettepe Üniversitesi Sağlık Bilimleri Enstitüsü, Tümör Biyolojisi ve İmmünolojisi Programı, Doktora Tezi, Ankara, 2014. Kemokinler ve kemokin reseptörlerin kompleks ağı atipic (decoy) kemokin reseptörleri tarafından regüle edilir. Atipik kemokin reseptörleri inflammatuvar yanıtların sonlandırılmasında rol oynarlar ve CCRL2 en yeni üyedir. CCRL2'nin CCL5, CCL19, ve chemerin'e bağlandığı ve bu kemokinlerin lokal konsantrasyonunu azalttığı öne sürülmüştür. İnsan CCRL2 geninin iki varyantı vardır; CRAM-A ve CRAM-B. Bu çalışmada, CRAM-A ve CRAM-B ekspresyonu RT-PCR yöntemi ile meme kanseri hücre hatlarında, periferik kan mononükleer hücrelerinde (PBMC), ve izole edilmiş immün hücrelerde IFN- γ veya LPS uyarımından sonra belirlendi. pCRAM-A/B-IRES2-EGFP rekombinant DNA'ları oluşturuldu ve PCR, restriksiyon kesimi, ve DNA dizileme analizi ile doğrulandı. Bu plazmid HEK293T hücre hattına, MDA-MB-468 ve BT-474 meme kanseri hücre hatlarına transfekte edildi. Transfeksiyon etkinliği (GFP ekspresyonu) ve rekombinant CRAM ekspresyonu akım sitometri ile analiz edildi. Fonksiyonel analizi için, Ca^{2+} flux, ligand bağlanma, reseptör internalizasyonu, ve ligand uzaklaştırma deneyleri yapıldı. Beklendiği gibi, CCL5, CCL19, ve chemerin hücre içi Ca^{2+} akımını uyarmadı. Meme kanseri hücreleri üzerinde, CRAM-A ekspresyonu özellikle IFN- γ uyarımından sonra arttı. CCL19 hücre dışı ortamdan en etkin şekilde uzaklaştırılan kemokindi. Bu etki rekombinant CRAM-A ile transfekte edilmiş hem HEK293T ve hem BT-474 hücre hatlarında görüldü. Bu sonuçlara göre, CRAM-A ekspresyonunun tümöre doğru T hücre infiltrasyonunu azaltabilen bir immün kaçış mekanizması olarak görev yapabileceği düşünülmüştür.

Anahtar Kelimeler: Atipik kemokin reseptörü, CCRL2, Kemokin, Rekombinant DNA teknolojisi.

Bu çalışma Eczacıbaşı Tıp Ödülleri ve Bilimsel Araştırma Destekleri tarafından desteklenmiştir.

ABSTRACT

Sarmadi, P. Expression and functional analysis of CCRL2 atypical chemokine receptor variants on breast cancer cells. Hacettepe University Institute of Health Sciences, Tumor Biology and Immunology Program, PhD Thesis, Ankara, 2014. The complex network of chemokines and chemokine receptors is regulated by atypical (decoy) chemokine receptors. Atypical chemokine receptors play role in the termination of inflammatory responses and CCRL2 is the newest member. CCRL2 has been suggested to bind CCL5, CCL19 and chemerin and to decrease their local concentration. Human CCRL2 gene has two variants; namely, CRAM-A and CRAM-B. The aim of this work is to investigate the expression and the functions of these variants in breast cancer cells. CRAM-A and CRAM-B expression were determined with RT-PCR in breast cancer cell lines, PBMCs, and purified-immune cells under IFN- γ or LPS stimulation. pCRAM-A/B-IRES2-EGFP recombinant DNAs were constructed and confirmed by PCR, restriction digestion and DNA sequencing analysis, and transfected into HEK293T cell line, and MDA-MB-468 and BT-474 breast cancer cell lines. Transfection efficiency (GFP expression) and recombinant CRAM expression were examined by flow cytometry. For functional analyses; Ca²⁺ flux (FuraRed II staining), ligand binding, receptor internalization and ligand removal assays were performed. As expected, CCL5, CCL19 and chemerin did not stimulate intracellular Ca²⁺ flux. On breast cancer cells, CRAM-A expression was specifically increased upon IFN- γ stimulation. CCL19 was the most efficiently removed chemokine from the extracellular milieu. This effect was observed both in HEK293T and BT-474 cell lines transfected with recombinant CRAM-A. Therefore, CRAM-A expression may serve as an immune evasion mechanism that mitigates T cell infiltration towards the tumor.

Key words: Atypical chemokine receptor, CCRL2, Chemokine, Recombinant DNA technology.

This study was supported by Eczacıbaşı Research and Awards Fund.

CONTENTS

THESIS APPROVAL PAGE	iv
ACKNOWLEDGEMENTS	v
ÖZET	vi
ABSTRACT	vii
CONTENTS	viii
LIST OF ABBREVIATIONS	xi
LIST OF FIGURES	xvi
LIST OF TABLES	xix
1. INTRODUCTION	1
2. LITERATURE REVIEW	5
2.1. Chemokines and Chemokine Receptors	5
2.2. Decoy Chemokine Receptors	8
2.2.1. Duffy Antigen Receptor for Chemokines (DARC)	10
2.2.2. D6	11
2.2.3. CXCR7	12
2.2.4. CCX-CKR	12
2.2.5. CCRL2	13
2.3. Decoy Chemokine Receptors and Cancer	16
2.4. Tumor Immunology	19
2.5. Breast Cancer	22
2.6. Chemokine Network in Breast Cancer	27
2.7. Immune responses in breast cancer	30
3. MATERIALS AND METHODS	35
3.1. Materials Used in This Work	35
3.2. Buffers and Solutions	36
3.3. Molecular Techniques	38
3.3.1. Total RNA Isolation	38
3.3.2. RNase-Free DNase Treatment	39
3.3.3. Spectrophotometric Measurement of Nucleic Acids	40
3.3.4. cDNA Synthesis	40

3.3.5. Polymerase Chain Reaction (PCR)	41
3.3.6. Agarose Gel Electrophoresis	44
3.3.7. Directional Cloning	45
3.3.8. TA Cloning	52
3.3.9. Preparation of Competent Bacteria and Heat Shock Transformation	56
3.3.10. Confirmation of Constructed Recombinant Clones	60
3.4. Cell Culture	62
3.4.1. Culture of Cell Lines and Cells Isolated from Peripheral Blood	62
3.4.2. Thawing Cell Lines	62
3.4.3. Passage of Adherent Cells with Trypsin-EDTA	63
3.4.4. Cell Counting	63
3.4.5. Cryopreserving Cell Lines	64
3.4.6. Stimulation of PBMCs and Breast Cancer Cell Lines	64
3.4.7. Liposomal Transfection	64
3.4.8. Fluorescence Microscopy	65
3.5. Immunological Assays	65
3.5.1. Flow Cytometry	65
3.5.2. Ca ²⁺ Mobilization Assay	67
3.5.3. Analysis of CCRL2 Binding Capacity of 152254 mAb	68
3.5.4. Receptor Internalization Analysis	69
3.5.5. Enzyme-Linked Immunosorbent Assay (ELISA)	69
3.6. Cell Isolation and Sorting	73
3.6.1. Isolation of Lymphoid Cells	73
3.6.2. Isolation of Monocytes and Neutrophils	76
3.7. Immunohistochemistry	78
3.8. Statistical Analysis	79
4. RESULTS	80
4.1. Expression of CCRL2 Variants in Immune Cells	80
4.1.1. Expression of CCRL2 Variants in Immune Cells Under LPS or IFN- γ Stimulation	81
4.2. Expression of CCRL2 Variants in Breast Cancer Cell Lines	82

4.3. Expression of CCRL2-related Genes in MDA-MB-231 Cell Line	83
4.4. Construction of Recombinant CRAM-A and CRAM-B DNA for Eukaryotic Expression	86
4.5. <i>De Novo</i> Expression and Functional Analysis of CRAM-A and CRAM-B	92
4.6. Construction of GFP Hybrids of CRAM-A or CRAM-B Genes	98
4.7. Determination of the Binding Capacity of anti-CCRL2 mAb 152254 in the Presence of CCRL2 Ligands	104
4.8. Determination of Surface Expression Changes of CRAM-A in the Presence of CCL5, CCL19, or Chemerin	107
4.9. The Analysis of CCL5 and CCL19 Chemokine Removal Capacity of CRAM-A	109
4.9.1. In HEK293T Cells	109
4.9.2. In BT-474 Breast Cancer Cells	110
4.10. CCRL2 Expression in Breast Cancer Tissues	116
5. DISCUSSION	119
6. RESULTS AND RECOMMENDATIONS	133
REFERENCES	136
APENDICES	
Appendix 1: Research Ethics Approval	
Appendix 2: Results of DNA sequencing analyses	
Appendix 3: Scientific meetings where the data of this thesis were presented and the related prize	

LIST OF ABBREVIATIONS

aa	Amino acid
ACKR	Atypical chemokine receptor
APC	Antigen presenting cell
APC	Allophycosyanin
B-CLL	B cell chronic lymphocytic leukemia
BSA	Bovine serum albumin
Ca ²⁺	Calcium ion
CC	Cystein motif
CCL	Chemokine ligand
CCR	Chemokine receptor
<i>Ccr1</i> ^{-/-}	CCRL1 knockout mice
CCRL2	Chemokine (C-C motif) receptor-like 2
CCX-CKR	Chemocentryx chemokine receptor
CD	Cluster of differentiation
cDNA	Complementary DNA
ChemR23	Chemerin receptor 23
CMKLR1	Chemokine-like receptor 1
CRAM	Chemokine receptor on activated macrophages
CSF1	Colony stimulating factor 1
CSF1R	Colony stimulating factor 1 receptor
C-terminus	Carboxyl terminus
CTL	Cytotoxic T lymphocyte
CTLA-4	Cytotoxic T lymphocyte antigen-4
D	Aspartic acid
DAPI	4',6-diamidino-2-phenylindole
DARC	Duffy antigen receptor for chemokines
DC	Dendritic cell
DCIS	Ductal carcinoma in situ
DMEM	Dulbecco's modified eagle medium
DNA	Deoxyribonucleic acid

DRYLAIIV	Asp-Arg-Tyr-Leu-Ala-Ile-Val
dNTP	Deoxyrinonucleotide triphosphate
dT	Deoxythymidine
EAE	Experimental autoimmune encephalomyelitis
ECM	Extracellular matrix
ECMV	Encephalomyocarditis virus
<i>E.coli</i>	<i>Escherichia coli</i>
EDTA	Ethylene diamine tetraacetic acid
EGF	Epidermal growth factor
EGFP	Enhanced green fluorescent protein
ELISA	Enzyme-linked immunosorbent assay
ELR	Glutamate-leucine-arginine
ER	Estrogen receptor
FACS	Fluorescence-activated cell sorting
FBS	Fetal bovine serum
FoxP3	Forkhead box P3
FSC	Forward scatter
GBM	Glioblastoma multiforme
GFP	Green fluorescent protein
Gi	G inhibitory protein
GM-CSF	Granulocyte monocyte-colony stimulating factor
GPCR	G protein-coupled receptor
GPR1	G protein-coupled receptor 1
GTP	Guanosine triphosphate
HCR	Human chemokine receptor
HEK	Human embryonic kidney
HER2	Human epidermal growth factor receptor 2
HIF1- α	Hypoxia inducible factor 1-alpha
HIV	Human immunodeficiency virus
HRP	Horseradish peroxidase
HSV TK	Herpes simplex virus thymidine kinase
IDO	Indoleamine 2,3-deoxygenase

IFN- γ	Interferon gamma
IgG	Immunoglobulin G
IL	Interleukin
IRES	Internal ribosome entry site
I-TAC	Interferon-inducible T cell α chemoattractant
kDa	Kilo Dalton
L-CCR	Lipopolysaccharide inducible C-C chemokine receptor
LCIS	Lobular carcinoma in situ
LPS	Lipopolysaccharide
M	DNA size marker
mAb	Monoclonal antibody
MAPK	Mitogen-activated protein kinase
mCCRL2	Murine orthologue to CCRL2
MCP-1	Monocyte chemotactic protein 1
MCS	Multiple cloning site
MDSC	Myeloid-derived suppressor cell
MFI	Mean fluorescent intensity
MHC	Major histocompatibility complex
MIP-3	Macrophage inflammatory protein-3
MMP	Matrix metalloproteinase
MRI	Magnetic resonance imaging
NCBI	National center for biotechnology information
NEB	New England biolabs
Neo ^r	Neomycin resistance gene
NF- κ B	Nuclear factor-kappa B
NK	Natural killer cell
NSCLC	Non-small cell lung carcinoma
N-terminus	Amino-terminus
OD	Optical density
PBMC	Peripheral blood mononuclear cell
PBS	Phosphate buffered saline

PCMV IE	Immediate early promoter of cytomegalovirus
PCR	Polymerase chain reaction
pCR	Pathological complete response
PD	Programmed death
PDGF	Platelet-derived growth factor
PFA	Paraformaldehyde
PI3K	Phosphatidylinositol 3-kinase
PLC	Phospholipase C
PMN	Polymorphonuclear leukocyte
PR	Progesterone receptor
Q	Glutamine
RANTES	Regulated on activation, normal T cell expressed and secreted
RAS	Rat sarcoma
RB	Retinoblastoma
rh	Recombinant human
RNA	Ribonucleic acid
ROS	Reactive oxygen species
RT	Reverse transcriptase
RT-PCR	Reverse transcriptase PCR
SD	Standard deviation
SDF-1	Stromal cell-derived factor 1
SNP	Single nucleotide polymorphism
SSC	Side scatter
STAT	Signal transducer and activator of transcription
SV	Simian virus
TA	Thymine adenine
TAM	Tumor associated macrophage
TBE	Tris borate EDTA
TGF	Transforming growth factor
Th	T helper cell
TIL	Tumor infiltrating lymphocyte

TMB	3,3',5,5'-tetramethylbenzidine
TNBC	Triple negative breast cancer
TNF	Tumor necrosis factor
Treg	Regulatory T cell
UV	Ultra violet
VEGF	Vascular endothelial growth factor

LIST OF FIGURES

1.1. Schematic presentation of the hypothesis proposed	3
2.1. Schematic representation of the four different groups of chemokines	8
2.2. Schematic representation for decoy function of atypical chemokine receptors	10
2.3. Cancer immunoediting: from immunosurveillance to tumor escape	20
3.1. DNA ladders	45
3.2. Schematic representation of pIRES2-EGFP eukaryotic expression vector and its multiple cloning site map	48
3.3. Topoisomerase activity in TOPO [®] cloning	54
3.4. The features of the pcDNA3.1/CT-GFP-TOPO [®] vector diagram	56
3.5. <i>Mlu</i> I restriction digestion points on the recombinant DNA containing CCRL2 insert	61
3.6. Standard curves obtained for CCL5 and CCL19 ELISAs	72
3.7. Gating leukocytes and confirmation by post-sort flow cytometric analysis	75
3.8. Isolated monocytes and neutrophils (polymorphonuclear cells, PMNs) were confirmed by flow cytometry	77
4.1. CRAM-A and CRAM-B gene expression in immune cells	80
4.2. CRAM-A and CRAM-B gene expression in control or in LPS or IFN- γ stimulated PBMCs	81
4.3. Expression of CCRL2 variants, CRAM-A and CRAM-B, in breast cancer cell lines with or without LPS or IFN- γ stimulation	82
4.4. CCRL2-related chemokines and chemokine receptors	84
4.5. CCRL2-related gene expression analysis in control or LPS-stimulated MDA-MB-231 breast cancer cell line	85
4.6. Schematic presentation of the recombinant human CRAM-A or CRAM-B genes cloned into eukaryotic expression vector pIRES2-EGFP and the expression of two intact proteins CRAM-A or -B and EGFP	87

4.7. Amplification of CRAM-A and CRAM-B insert DNA molecules by <i>Pfu</i> DNA polymerase and visualization on agarose gel	88
4.8. Kanamycin resistant <i>E.coli</i> colonies on an LB agar petri dish possibly containing recombinant CCRL2 constructs	89
4.9. A) Confirmation of recombinant DNA products by PCR and B) by <i>NheI-XmaI</i> restriction digestion	90
4.10. Gene expression analysis of CCRL2-related genes in HEK293T cells	93
4.11. Surface expression analysis of recombinant CRAM-A or CRAM-B constructs transfected into HEK293T cells	95
4.12. Ca ²⁺ mobilization analysis in HEK293T cells transfected with the control empty vector pIRES2-EGFP and recombinant plasmids pCRAM-A-IRES2-EGFP or pCRAM-B-IRES2-EGFP	97
4.13. Schematic presentation of human CRAM-A or CRAM-B cloning into pcDNA3.1/CT-GFP eukaryotic expression vector and the resulting CRAM-A/B-GFP hybrid recombinant protein	98
4.14. Amplification of CRAM-A and CRAM-B DNA inserts by <i>Taq</i> DNA polymerase	99
4.15. Ampicillin resistant <i>E.coli</i> colonies on an LB agar petri dish possibly containing recombinant CCRL2 variants hybridized with GFP	100
4.16. Confirmation of recombinant DNA products A) by PCR, and B) confirmation of inserts' orientation by <i>MluI</i> restriction digestion, and examination on agarose gel	101
4.17. Surface expression analysis of recombinant CRAM-A or CRAM-B constructs transfected into HEK293T cells	103
4.18. Fluorescence microscopic observation of A) HEK293T cells transfected with the empty vector pcDNA3.1/CT-GFP and B) HEK293T cells transfected with pcDNA3.1/CRAM-A/B-CT-GFP recombinant plasmids	104
4.19. Binding capacity of anti-CCRL2 antibody 152254 in the presence of CCRL2-specific chemokine ligands	106

4.20. CRAM-A surface levels in the presence of CCL5, CCL19, or chemerin	108
4.21. ELISA results for CCL5 and CCL19	110
4.22. Analysis of CCRL2 expression in CRAM-A-transfected MDA-MB-468 and BT-474 breast cancer cell lines by flow cytometry	112
4.23. Expression analysis of CCRL2-related genes in control BT-474 breast cancer cell line	114
4.24. ELISA results for CCL5 and CCL19	115
4.25. Immunohistochemical determination of CCRL2 on breast cancer tissues	117-118
5.1. Schematic presentation of the hypothesis proposed	132

LIST OF TABLES

2.1. Chemokines and Chemokine Receptors	6
2.2. Decoy chemokine receptors and their ligands	9
2.3. Breast carcinoma subtypes: histopathological, molecular and clinical features	25
3.1. cDNA synthesis reaction components and conditions	41
3.2. The primers' information used in gene expression analyses	42
3.3. Standard PCR components, volumes, and final concentrations	43
3.4. Standard PCR thermal cycler program	44
3.5. Forward and reverse primers, and <i>NheI</i> and <i>XmaI</i> restriction enzyme digestion sites used in directional cloning of CRAM-A and CRAM-B	46
3.6. PCR components, volumes, and final concentrations used for the amplification of insert DNA for cloning	46
3.7. PCR thermal cycler program	47
3.8. Restriction digestion reaction components, volumes, and final concentrations	49
3.9. Ligation reaction components, volumes, and final concentrations	52
3.10. Primers used in TOPO [®] TA cloning	53
3.11. <i>MluI</i> restriction digestion reaction mixture components, volumes, and final concentrations	60
3.12. Antibodies used for flow cytometric analyses	67
4.1. The SNPs detected in cloned CCRL2 genes	91

1. INTRODUCTION

Chemokines or chemoattractant cytokines are a superfamily of small (8-12 kDa) secreted proteins. These proteins primarily promote and regulate the directional migration and trafficking of the cells. Approximately 50 chemokine ligands and 20 chemokine receptors have been identified in humans. These molecules constitute a complex network of ligand-receptor interactions [1]. Generally, upon binding a chemokine receptor to its cognate ligand a signaling pathway is induced via G protein coupling to the receptor. However, because of the modified DRYLAIV motif in the second intracellular loop atypical chemokine receptors do not couple with G proteins and do not induce signal transduction in the cell [2]. Up to date, five decoy chemokine receptors have been identified; namely, DARC, D6, CXCR7, CCX-CKR, and CCRL2 [3]. Except CXCR7, other decoy chemokine receptors regulate cell migration by sequestering their cognate chemokine ligands. Atypical chemokine receptors have been shown to play an important role in cancer by reducing inflammation [4]. CCRL2 is the newest member of atypical chemokine receptor family and binds to CCL5, CCL19, and chemerin. However, CCRL2's internalization upon binding to these ligands or specificity to CCL5 remains controversial and may increase glioblastoma cell's migration and invasion, can regulate B cell chronic lymphocytic leukemia (B-CLL) blasts' migration and reduce their survival [5, 6]. However, a possible link between CCRL2 and breast cancer has not been investigated to our knowledge. The human CCRL2 has two variants named Chemokine Receptor on Activated Macrophages (CRAM-A) and a 12-amino acid shorter, more common variant, CRAM-B. CRAM-B is also known as human chemokine receptor, HCR [7, 8]. Despite their differences in the N-terminus, no clear functional difference has been previously shown between CRAM-A

and CRAM-B. The longer isoform, CRAM-A is only expressed in high order primates.

The preliminary results of this study showed that IFN- γ can specifically up-regulate the expression of the long isoform of CCRL2, CRAM-A, in breast cancer cell lines. CCRL2's specific chemokine ligands CCL5, CCL19, and chemerin can be found in the breast tumor microenvironment. These chemokines mediate the infiltration of NK cells, Th cells, and CTLs into the breast tumor. IFN- γ produced by these immune cells is a critical player in anti-tumor immune responses. Thus, by virtue of these preliminary data and literature knowledge, here CRAM-A can function as an atypical chemokine receptor removing these chemokines from the breast tumor microenvironment. The hypothesis of this study proposes that the long variant of CCRL2, CRAM-A, is upregulated on breast cancer cells upon IFN- γ -mediated immune responses and regulates the immune infiltration into the tumor microenvironment. Therefore, CRAM-A is to be considered as an immunomodulatory receptor which can function in favor of malignancy (Figure 1.1).

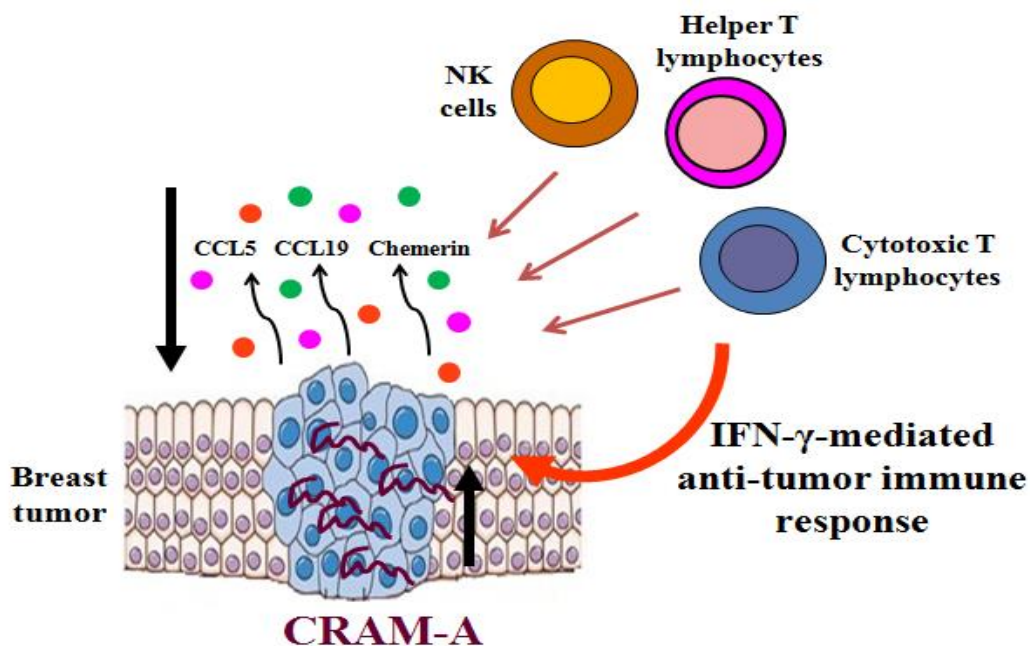


Figure 1.1. Schematic presentation of the hypothesis proposed. NK cells, Th1, and cytotoxic lymphocytes migrate towards CCL5, CCL19, and chemerin gradient supplied by the breast tumors. IFN- γ , the common product of these immune cells, leads to the upregulation of CRAM-A in the breast tumor cells. This results in the chemokine levels reduction; therefore, hampering the infiltration of these anti-tumor effectors.

In this study, molecular techniques such as RNA isolation, cleaning and concentration, cDNA synthesis, polymerase chain reaction (PCR), directional cloning, TA cloning, heat shock transformation, plasmid purification, confirmation of constructed recombinant clones by PCR, restriction enzyme digestion and by DNA sequencing analysis; cell culture and purification techniques such as density gradient and FACS, liposomal transfection; immunological assays such as flow cytometry, analysis of CCRL2 binding capacity of antibody, receptor internalization analysis, and ELISA; Ca^{2+} mobilization assay and fluorescence microscopy were performed.

Here, the expression of CCRL2 variants, CRAM-A and CRAM-B, in purified immune cells and PBMCs and under LPS or IFN- γ stimulation was investigated. Expression of CCRL2 variants in breast cancer cell lines and expression status of CCRL2-related genes, CCL5, CCL19, chemerin, CCR1, CCR3, CCR4, CCR5, CCR7, CCRL1, DARC, D6, CMKLR1, and GPR1, in certain cell lines were analyzed. Human CRAM-A and CRAM-B coding sequences were cloned into eukaryotic expression vectors pIRES2-EGFP and pcDNA3.1/CT-GFP. CRAM-A or CRAM-B was also hybridized with GFP in order to trace its cellular sub-localization; however, this attempt was hampered by the dimness of recombinant protein products' fluorescence intensity. These recombinant constructs were transfected into HEK293T and BT-474 cell lines for *de novo* expression and functional analyses such as Ca²⁺ mobilization capacity, binding capacity of CCRL2 specific monoclonal antibody 152254, and surface expression changes of CRAM-A in the presence of CCRL2 ligands (CCL5, CCL19, and chemerin). In addition, CCL5 and CCL19 chemokine removal capacity of CRAM-A from the extracellular milieu was investigated.

In conclusion, recombinant CCRL2 constructs were successfully expressed in HEK293T and BT-474 cell lines. As expected, CCL5, CCL19 and chemerin did not stimulate intracellular Ca²⁺ flux, whereas ionomycin Ca²⁺ ionophore did. On breast cancer cells, CRAM-A expression was specifically increased upon IFN- γ stimulation. In the presence of chemokine ligands, CRAM-A internalization was determined in ~30 minute-intervals. In addition, CCL19 was the most efficiently removed chemokine from the environment. This effect was observed both in HEK293T and BT-474 cell lines transfected with recombinant CCRL2. Therefore, CRAM-A expression may serve as an immune evasion mechanism that mitigates T cell infiltration towards the tumor.

2. LITERATURE REVIEW

2.1. Chemokines and Chemokine Receptors

Chemokines or chemoattractant cytokines are a superfamily of small (8-12 kDa) secreted proteins. These proteins primarily promote and regulate the directional migration and trafficking of leukocytes, endothelial cells, and epithelial cells. Approximately 50 chemokine ligands and 20 chemokine receptors have been identified in humans, which are listed in Table 2.1 [9]. This system of molecules displays a promiscuous network, in which chemokine receptors interact with different chemokines with variable affinities and multiple chemokines bind to the same receptor [10]. This feature might be important in fine-tuning of chemokine-associated responses. Chemokines and chemokine receptors are divided into four categories on the basis of the sequence around the first two conserved N-terminus cysteine residues namely XC, CC, CXC and CX3C (where C is the amino acid Cysteine and X refers to any amino acid) (Figure 2.1) [11, 12].

The CXC family of chemokines is further divided into ELR⁺ and ELR⁻ categories based on the motif glutamate-leucine-arginine (E-L-R), which is placed upstream of the CXC sequence. CXCL1, CXCL2, CXCL3, CXCL5, CXCL6, CXCL7, and CXCL8 are ELR⁺ chemokines. This is important as the N-terminal portion of the chemokine has been shown to be in charge of neutrophil attraction and angiogenesis. CXCL12 is the only ELR⁻ chemokine which shows angiogenic properties [12]. CXCL4, CXCL9, CXCL10, CXCL11, and CXCL14 function as angiostatic factors and generally hamper the cellular invasion.

Table 2.1. Chemokines and Chemokine Receptors. Adapted from Sarvaiya et al. [9] and Abbas et al. [13].

Chemokine Receptor	Chemokine	Major Function
CC Family		
CCR1	CCL3, CCL4, CCL5, CCL7, CCL9/CCL10, CCL14, CCL15, CCL16, CCL23	Mixed leukocyte recruitment
CCR2	CCL2, CCL7, CCL8, CCL12, CCL13, CCL16	Mixed leukocyte recruitment
CCR3	CCL5, CCL7, CCL8, CCL11, CCL13, CCL15, CCL24, CCL26, CCL28	Eosinophil, basophil, and Th2 recruitment
CCR4	CCL2, CCL3, CCL5, CCL17, CCL22	T cell and bosophil recruitment
CCR5	CCL3, CCL4, CCL5, CCL8, CCL14	T cell, dendritic cell, monocyte, and NK recruitment; HIV coreceptor
CCR6	CCL20	
CCR7	CCL19, CCL21	T cell and dendritic cell migration into parafollicular zones of lymph nodes
CCR8	CCL1, CCL4, CCL17	Monocyte recruitment and endothelial cell migration
CCR9	CCL25	Astrocyte migration
CCR10	CCL27, CCL28	Dermal cell migration
CCR11	CCL2, CCL7, CCL8, CCL12, CCL13, CCL19, CCL21, CCL25	Monocyte recruitment
CXC Family		
CXCR1	CXCL6, CXCL8	Neutrophil recruitment
CXCR2	CXCL1, CXCL2, CXCL3, CXCL5, CXCL6, CXCL7, CXCL8	Neutrophil recruitment
CXCR3	CXCL4, CXCL9, CXCL10, CXCL11	Effector T cell recruitment, platelet aggregation
CXCR4	CXCL12	Mixed leukocyte recruitment; HIV coreceptor
CXCR5	CXCL13, CXCL16	B cell migration into follicles
CXCR6	CXCL16	Fibroblast recruitment
CXCR7	CXCL12, CXCL11	Regulation of CXCR4 activity, endothelial progenitor cell recruitment

		and glioma cell migration
C Family		
XCR1	XCL1, XCL2	T cell and NK cell recruitment
CX₃C Family		
CX ₃ CR1	CX ₃ CL1	T cell, NK cell, and macrophage recruitment; CTL and NK cell activation

Chemokines can also be divided into two sub-groups based on their functions: homeostatic/developmental chemokines and inflammatory chemokines [9, 14]. Homeostatic chemokines are constitutively expressed and have crucial roles in embryonic development, general organogenesis, stem cell migration, lymphoid organogenesis, and immune surveillance [14]. The expression of inflammatory chemokines can be induced by inflammatory stimuli such as tumor necrosis factor (TNF), interferon- γ (IFN- γ), microbial products or trauma; and play a vital role in maintenance of innate and adaptive immunity to tissue damage, infection, and other physiological abnormalities [1]. Their expression is temporary and ceases with the resolution of the inflammation. Some chemokines can function in both groups depending on the biological status or on the pathological circumstances [15].

Chemokine receptors are of seven transmembrane G protein-coupled chemokine receptors (GPCR) family [9, 16]. CC-chemokines bind to receptors CCR1 to CCR11, CXC-chemokines bind to CXCR1 to CXCR7, and XCR1 is the receptor for lymphotactin, and CX₃CR1 is the receptor for fractalkine [12, 17]. Upon specific ligand binding, a cascade of downstream signals, including calcium mobilization and the activation of mitogen-activated protein kinase (MAPK), phospholipase-C (PLC), phosphatidylinositol 3-kinase (PI3K), RAS, the RHO family of GTPases, and NF- κ B begins [18].

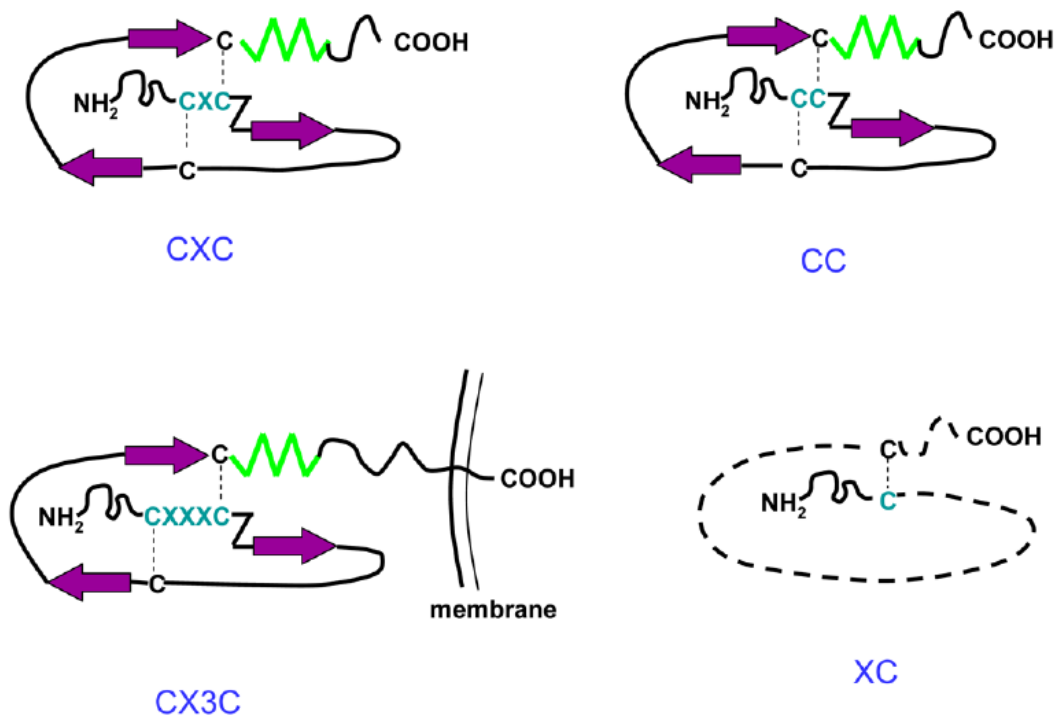


Figure 2.1. Schematic representation of the four different groups of chemokines. Taken from Ali and Lazennec [13].

2.2. Decoy Chemokine Receptors

The sophisticated system of chemokines and chemokine receptors is adjusted by the group of atypical or decoy chemokine receptors including Duffy Antigen Receptor for Chemokines (DARC), D6, Chemocentryx Chemokine Receptor (CCX-CKR, CCRL1), CXCR7, and C-C Chemokine Receptor-Like 2 (CCRL2, Chemokine Receptor on Activated Macrophages, CRAM) [2]. Recently, these families of decoy chemokine receptors have been adapted to a new nomenclature. In this naming system DARC was renamed as ACKR1, D6 as ACKR2, CXCR7 as ACKR3, CCRL1 as ACKR4, and CCRL2 as ACKR5 [3]. Table 2.2 shows decoy chemokine receptors and their ligands.

Table 2.2. Decoy chemokine receptors and their ligands.

Decoy Chemokine Receptors	Proposed or Specific Ligands
DARC	CCL2, CCL5, CCL7, CCL11, CCL13, CCL14, CCL17, CXCL1, CXCL2, CXCL5, CXCL6, CXCL7, CXCL8, CXCL11
D6	CCL2, CCL3, CCL4, CCL5, CCL7, CCL8, CCL11, CCL13, CCL14
CXCR7	CXCL12, CXCL11
CCRL1	CCL19, CCL21, CCL25, CXCL13
CCRL2	CCL5, CCL19, Chemerin

These receptors structurally resemble to the seven transmembrane G protein- coupled receptors. However, they do not elicit signal transduction, because they contain a modified DRYLAIV motif in their second intracellular loop that prevents them from coupling with G proteins (e.g. DKYLEIV instead of DRYLAIV amino acid sequence in D6) [2]. Decoy chemokine receptors bind their cognate chemokine ligands with high affinity and effectively internalize them; thus, they act as scavengers [2]. Internalized chemokines become degraded by lysosomal enzymes in endocytic vesicles (Figure 2.2). This decoy function of atypical chemokine receptors regulates and modifies the chemokine gradient and bioavailability in the microenvironment. In addition, this function indirectly regulates the surface expression of the specific receptor. After the ligands are degraded in the vesicle, the receptor recirculates to the cell membrane [2].

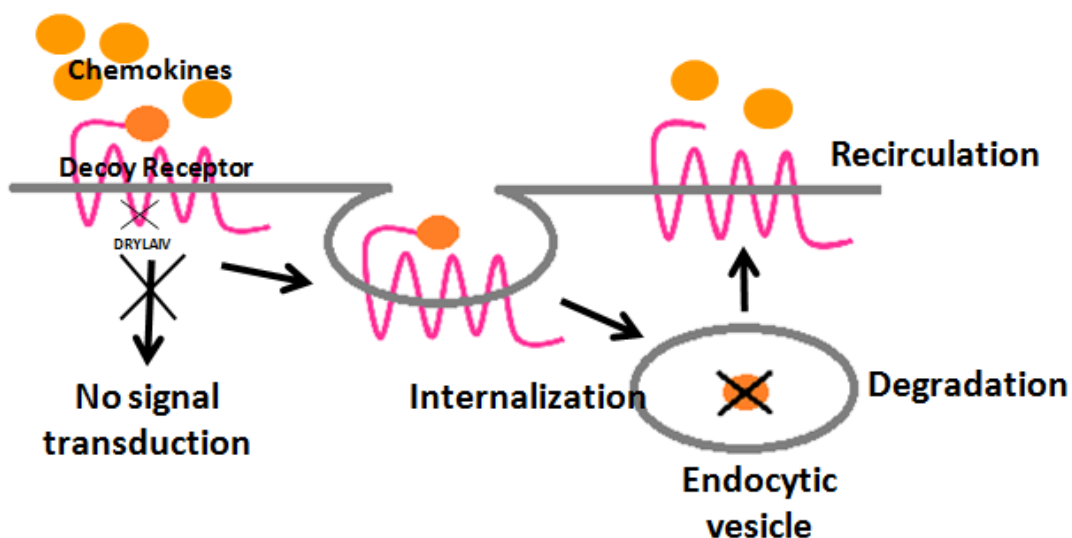


Figure 2.2. Schematic representation for decoy function of atypical chemokine receptors.

Studying the roles of decoy chemokine receptors shows that they have been investigated in different types of cancers. For example, DARC has been studied in lung, breast, and prostate cancers, D6 has been studied in lung and breast cancers, CXCR7 in different cancer types, including glioma, lung, breast, prostate, and liver cancers, CCRL1 in breast and cervix cancers, and CCRL2 in glioblastoma and B-cell CLL. As it can be seen, all of these decoy chemokine receptors have been studied in breast cancer except for CCRL2.

2.2.1. Duffy Antigen Receptor for Chemokines (DARC)

DARC was primarily identified as Duffy blood group antigen, the erythrocyte receptor for malaria parasite *Plasmodium vivax*; and later, it was described as an erythrocyte receptor for CXCL8. Other than erythrocytes of the Duffy antigen positive individuals, DARC is also found on the vascular endothelial cells lining post-capillary venules, collective venules and small

veins in different tissues such as spleen and lymph nodes, on the epithelial cells of kidneys and lungs, and expressed by neurons in discrete anatomic sites of the brain including Purkinje cells [19]. DARC does not contain intracellular signaling motifs and does not induce signaling or migration cascades. This silent receptor has important functions in chemokine transcytosis, clearing chemokines from the blood stream and leukocyte tethering to the endothelium, thus regulating plasma chemokine concentration [20]. DARC expression is up-regulated during inflammation and it binds both pro-inflammatory CC (e.g. CCL2, CCL5) and CXC (e.g. CXCL1, CXCL3, CXCL5, CXCL6, CXCL8) families of chemokines, but not the homeostatic chemokines [21]. DARC is the only mammalian chemokine receptor that binds ligands from more than one chemokine subfamily [22].

2.2.2. D6

D6 is the second best characterized member of atypical chemokine receptors. It is expressed in placenta, on lymphatic endothelial cells (in gut, skin, lung, and liver) and on immune cells. This atypical receptor binds many inflammatory CC chemokines (CCL2, 3L1, 4, 5, 7, 8, 11-14, and 22) and weakly CCL17. Upon ligation, D6 undergoes rapid internalization and the internalized ligand becomes degraded while the receptor recycles onto the cell surface. The lack of D6 expression has been correlated with impaired chemokine clearance, uncontrolled and continuous inflammation in various inflammatory models such as *Mycobacterium tuberculosis* infection, phorbol ester-induced cutaneous inflammation, and inflammatory bowel disease. In addition to lymphatic endothelial cells, different populations of immune cells including dendritic cells (DCs), macrophages and B cells express D6. It has been reported that in contrast to its classical function on lymphatic endothelium, when expressed on the leukocytes D6 can also promote inflammatory reactions in certain experimental models [23].

2.2.3. CXCR7

Coupling of CXCR7 with G proteins is still controversial [24]. In several cell types, CXCR7 functions as a signaling receptor as evidenced by phosphorylation of MAPKs or serine/threonine kinase Akt [24]. Recently, CXCR7 has also been classified as a member of the atypical chemokine receptor family [3]. The ligands of CXCR7 are CXCL12 (stromal cell-derived factor 1, SDF-1) and CXCL11 (interferon-inducible T cell α chemoattractant, I-TAC). CXCR7 expression is found on T cells, differentiated neurons, activated tumor-associated endothelial cells, and in many types of tumors. It has been shown to be important for proliferation and survival of the tumor cells [25, 26]. CXCR7 has a nearly 10 times higher binding affinity for CXCL12 as compared with CXCR4 [27]. In contrast to CXCR4, CXCR7 does not activate intracellular signaling upon interaction with CXCL12 or CXCL11 [28]. Other than competing for CXCL12 binding, CXCR7 can modulate CXCR4-mediated processes directly by crosstalking and forming heterodimers with CXCR4 [29-31]. Alternatively, it is interesting that CXCR7 was shown to induce signals that influence the cell proliferation and migration in different types of tumor cells, primary interneurons, primary rodent astrocytes, and human glioma cells [27, 32, 33].

2.2.4. CCX-CKR

CCX-CKR (Chemocentryx Chemokine Receptor, Chemokine CC motif Receptor-Like 1, CCRL1) was recently discovered and is predominantly expressed in the epithelial cells of heart and lung [34]. CCX-CKR binds the homeostatic chemokines CCL19, CCL21, CCL25, and weakly CXCL13 [35]. It is involved in the regulation of homeostatic lymphocyte trafficking and of immune responses [36]. By efficiently binding CCL19 and CCL21, CCX-CKR especially regulates the CCR7/CCL19/CCL21 axis. Binding of CCL19 to

CCR7 ends with its internalization and degradation, then the receptor becomes desensitized. On the other hand, following CCL21 ligation, CCR7 remains stable at the cell surface but its signaling capacity is limited [6]. In the absence of CCX-CKR, CCL19 and CCL21 levels rise in tissues and lymph nodes [37]. In mice lacking CCX-CKR, DC migration to lymph nodes is impaired and immune responses become weakened in the draining lymph nodes. These aspects might demonstrate the regulatory functions of CCX-CKR on CCR7-mediated responses. Following immunization for experimental autoimmune encephalomyelitis (EAE), *Ccr11*^{-/-} mice show earlier disease onset and irregular T_H17 responses. Herein, high levels of CCL21 induce IL-23 synthesis in DCs that promote the pathogenic differentiation [38]. Thus, a complicated relationship exists between CCX-CKR and CCR7 axis in the peripheral immune system. CCX-CKR is also expressed in the thymus and affects thymic stroma, thymic chemokine localization, and negative selection of thymocytes indicating its role in the maintenance of tolerance [39].

2.2.5. CCRL2

CCRL2 (Chemokine CC motif Receptor-like 2) was first cloned from a polymorphonuclear leukocyte (PMN) cDNA library as an orphan receptor called Human Chemokine Receptor (HCR) with the molecular weight of 39 KDa, in 1997 [40]. CCRL2 gene was mapped by fluorescence *in situ* hybridization to the p21-23 region of chromosome 3, in the main cluster of the CC chemokine receptor genes. CCRL2 shares over 40% sequence homology with CCR1, CCR2, CCR3, and CCR5 [5, 8]. The human gene *CCRL2* is transcribed into two variants deriving from alternative splicing named Chemokine Receptor on Activated Macrophages (CRAM-A) and a 36 base pair shorter, more common variant, CRAM-B. CRAM-B is also known as human chemokine receptor, HCR [7, 8]. The protein sequence of CRAM-A is twelve amino acid longer at the N-terminus than that of CRAM-B [40].

mCCRL2, the murine orthologue to CRAM (lipopolysaccharide inducible C-C chemokine receptor, L-CCR-related gene) only shares 51% sequence homology with the human gene. There is only one CCRL2 variant in murine species, which shares a higher homology with human CRAM-B variant. It has been stated that L-CCR binds CCL2, -5, -7, and -8, but this remains controversial [41].

Like other members of the atypical chemokine receptor family, CCRL2 holds a modified DRYLAIV motif, with a glutamine (Q) at position 127 instead of aspartic acid (D), replacing an acidic residue with a neutral one preventing coupling to the Gi protein. Therefore, interaction of CCRL2 with its ligands does not induce any classical signaling response. Also, it has been shown that CCRL2 expression was associated with reduced MAPK activity [6].

CCRL2 displays a narrow binding spectrum. This atypical receptor couples with chemerin, an adipokine and chemotactic factor agonist for chemokine-like receptor 1 (CMKLR1) (also known as ChemR23) and G protein-coupled receptor 1 (GPR1). Binding of chemerin to CMKLR1 triggers calcium mobilization, receptor and ligand internalization, and cell migration. Whereas, coupling of chemerin with CCRL2 does not induce this classical receptor activation. On the other hand, CCRL2 concentrates chemerin on the cell surface and presents it to cells in the vicinity. Thus, CCRL2 can regulate chemerin bioavailability. The consequences of chemerin binding to GPR1 has not been clearly known. However, it does not support cell migration [41].

It has been shown that CCRL2 expression may change in the presence of CCL5. CCL5 is suggested to be a ligand for CCRL2. Hartmann et al. demonstrated that the surface expression of CCRL2 is dependent on the maturation stage of the B lymphocytes. Furthermore, it is upregulated upon stimulation with the inflammatory chemokine CCL5, as CCL5 induced MAPK activation [7]. On the other hand, no calcium response upon CCL5 stimulation or migration towards CCL5 was detected in Nalm6 cells, a

CCRL2⁺ pre-B acute lymphoblastic leukemia cell line. These authors have also claimed that CCL5 can induce high actin polymerization and MAPK activation in both CRAM-A and CRAM-B transfected cells. They proposed that these capacities are important signs for receptor recycling [7]. However, there are several other reports that contradict with decoy functions of CCRL2. It has been reported that mCCRL2/HEK293 transfected cells respond functionally to chemokine ligands CCL2, CCL5, CCL7, and CCL8 through intracellular calcium mobilization and transwell chemotaxis [42]. On the other hand, in a study done by Zabel et al. to investigate possible functional roles for CCRL2 and to identify CCRL2 ligands, the chemokines CCL2, CCL5, CCL7, and CCL8 were applied on mCCRL2-transfected L1.2 cells, the mouse pre-B lymphoma cell line. These chemokines did not induce cell migration in transwell chemotaxis assays. In addition, other chemokines tested (CCL11, CCL17, CCL22, CCL25, CCL27, CCL28, CXCL9, and CXCL13) did not result in chemotaxis activity [43].

CCL19 is a specific ligand for CCRL2. Upon binding CCL19, CCRL2 internalization occurs but the receptor constitutively recycles back to cell surface. These properties suggest a regulatory role for CCRL2 in immune responses and homing processes [8]. Leick et al. reported that beside CX-CKR, CRAM-B is another atypical chemokine receptor that has some relevance to the CCR7 axis, since it can bind and internalize CCL19 [8, 37]. CCRL2 shows a constitutive cycling activity, which results in CCL19 internalization. Therefore, it is an effective modulator of CCR7 functions [6]. In the beginning, CCRL2 might compete with CCR7 to bind CCL19, but later it may favor CCL19 presentation to CCR7- expressing cells of the B lymphocyte origin [6].

CCRL2 is expressed on almost all human hematopoietic cells including monocytes, macrophages, basophils, mast cells, PMNs, CD4⁺ and CD8⁺ T cells, pro- and pre-B cells (depending on the maturation stage), DCs,

NK cells, and CD34⁺ progenitor cells [44]. At mRNA level, CCRL2 expression is up-regulated on human PMNs, in response to LPS or TNF; on human monocyte-derived iDCs in response to LPS+IFN- γ and CD40L; and, on human T cells upon stimulation with anti-CD3 or IL-2 [45]. In addition, CCRL2 mRNA is also detected in human pre-B acute lymphoblastoid leukemia cell lines, Nalm6, G2, and in mouse astrocytes and microglia cells [45]. It has been reported that CCRL2 expression is induced during DC maturation, both *in vitro* and *in vivo* [46].

In order to investigate the biological relevance of CCRL2 in migration and maturation of lung DCs in airway allergy and inflammation, Otero et al. generated CCRL2-deficient mice (CCRL2^{-/-}). These mice were used in a model of airway hypersensitivity [46]. In this study, CCRL2^{-/-} mice showed a dramatic reduction in the total number of lung leukocytes, in particular of eosinophils and lymphocyte/mononuclear cells, in comparison with wild type animals. A significant reduction in DC migration to mediastinal lymph nodes was also apparent. This observation was not directly related with CCRL2 involvement in the recruitment of these cells, but was associated with the reduction of CCL11 and CCL17 chemokines levels in CCRL2^{-/-} mice. This may underline an important role of CCRL2 in directing DC migration to draining lymph nodes and Th2 priming in the lung [46].

2.3. Decoy Chemokine Receptors and Cancer

Chemokines and chemokine receptors are key players in the cancer-related inflammation [47]. Unresolved pathogen infections and chronic inflammation are closely related with cancer development. These fundamental molecules can be produced by tumor and stromal cells in the tumor microenvironment. In the progressive way of carcinogenesis, chemokines and their receptors are factors mediating the recruitment of

tumor-promoting cells such as myeloid-derived suppressor cells (MDSCs), tumor-associated macrophages (TAMs) and tumor-infiltrating lymphocytes (TILs). Chemokine systems welcome directional migration and metastasis of tumor cells together with leukocytes to specific target tissues. They can mediate the leukocytes' effects on cancer cell survival, metastasis, and regulation of angiogenesis [47]. Chemokines and chemokine receptors are up-regulated in different types of cancers. Type and amount of the secreted chemokines specify character and quantity of immune cell infiltration in the tumor microenvironment [48].

DARC and D6, the two best characterized members of atypical chemokine receptors may serve as a systemic barrier to metastasis of cancer cells through the two main spreading (hematogenous and lymphatic) ways. DARC is broadly expressed on erythrocytes and vascular endothelial cells and D6 is expressed on lymphatic endothelial cells [49]. Experimental studies have demonstrated that DARC expression has a negative influence on tumor metastasis and angiogenesis [50]. DARC is the essential modulator of prostate cancer progression by clearing angiogenic chemokines from the tumor microenvironment and reducing angiogenesis. It has been shown that in humans who lack erythroid DARC, prostate cancer progression and mortality was increased [12]. In breast cancer, D6 expression attenuates lymph node metastasis and is negatively correlated with clinical tumor stage [51]. D6 expression is significantly decreased in colon tumors compared to non-tumor tissue from the same individual. Moreover, D6 expression was lower in advanced tumors. Hence, tumor cells can benefit D6 down-regulation as a mechanism to shape the regional chemokine network to favor tumorigenesis and spread [22].

CXCR7 expression is higher in transformed cells as compared to their normal non-transformed counterparts [24]. CXCL12-CXCR7 or CXCL12-CXCR4 interactions mediate recruitment of endothelial progenitor cells and

sustain neo-angiogenesis in tumors [52]. CXCR7 is high on breast and lung cancer cells. Hypoxia induces its expression on endothelial and tumor-associated vessels. This correlates with cell proliferation, neo-angiogenesis, vascularization, and metastatic potential. CXCR7 has been found to be up-regulated on prostate cancer cells and on aggressive tumors. This correlates with cell proliferation, survival, adhesion, chemotaxis and increases the expression of pro-angiogenic factors such as IL-8, vascular endothelial growth factor (VEGF) and transforming growth factor (TGF)- β . CXCR7 expression level is suppressed by CXCR4 activation in prostate cancer cells. Thus, CXCR7 expression on tumor cells can be an important factor in promoting tumor cell proliferation and angiogenesis [53].

In breast cancer, CCX-CKR overexpression restricts cell proliferation and invasion, *in vitro*; and tumor progression and metastasis, *in vivo*. In contrast, low levels of CCX-CKR expression are correlated with poor prognosis in breast cancer patients [22]. Recent studies on breast and gastric cancer tissues have shown that co-expression of DARC, D6, and CCX-CKR is significantly lower in invasive breast cancer compared to non-invasive breast cancer and healthy breast tissues. The presence of these markers is indicative of relapse-free and improved overall survival both in breast and gastric cancers [22, 54].

The role of CCRL2 in human cancers is not fully determined and understood. There are limited studies on the relationship between CCRL2 and cancer. One of these studies demonstrated a substantial CCRL2 expression in human glioma tissues and cell lines. Overexpression of CCRL2 augmented glioblastoma multiforme (GBM) cell migration and invasion [5]. In B cell chronic lymphocytic leukemia (B-CLL), CCL19-CCR7 interaction motivates the formation and maintenance of germinal center-like proliferative foci. By scavenging CCL19, CCRL2 modifies CCL19's availability and

regulates function of CCR7 [6]. Thus, CCRL2 expression may modulate cancer biology and immunology.

2.4. Tumor Immunology

Upon acquisition of sustained proliferative signals, evasion of growth suppressors, resistance to cell death, having replicative immortality, activation of invasion, metastasis, and angiogenesis processes and resistance to anti-tumor immune responses; transformed cells gain complete capacity to form advanced cancers [55, 56]. The initiation and progression of cancer involve several interactions between tumor cells and immune cells. DCs are one of the most important antigen presenting cells (APCs) that function both in innate and adaptive immune responses. Immature DCs sample foreign molecules as well as tumor antigens in the peripheral non-lymphoid tissues. They begin to mature and migrate to secondary lymphoid organs, where they present the peptide antigen via major histocompatibility complex (MHC) molecules to stimulate naïve T cells [56, 57]. Thus, upon efficient presentation of tumor antigens, cognate T cells become activated and eliminate the tumor. Whether newly transformed tumor cells' antigens are enough to induce anti-tumor immune responses or whether their expression can be modulated following interaction with the immune system is not clearly known. Models employing newly generated tumors from primary cells have shown that cancer progression is the result of a T-cell-dependent immunoselection process leading to the outgrowth of tumor cell clones displaying reduced immunogenicity (according to immune selection hypothesis) [58].

The immune system acts as a guardian to detect and eliminate transformed cells through a process called immunosurveillance. However, during this battle, beside protective role of the immunity against tumor,

immune system-tumor interaction may promote the development of cancer [58]. Here, the concept of “cancer immunoediting” is defined by three key stages: Elimination, Equilibrium and Escape. In this model, “Elimination” phase serves as cancer immunosurveillance, where tumors are recognized and subverted by different components of the immune system. During the “Equilibrium” phase, both the tumor and the immune cells are interacting to shape each other and generate a balance. Eventually, some tumor cells “Escape” the immune system and grow uncontrollably (Figure 2.3) [59, 60].

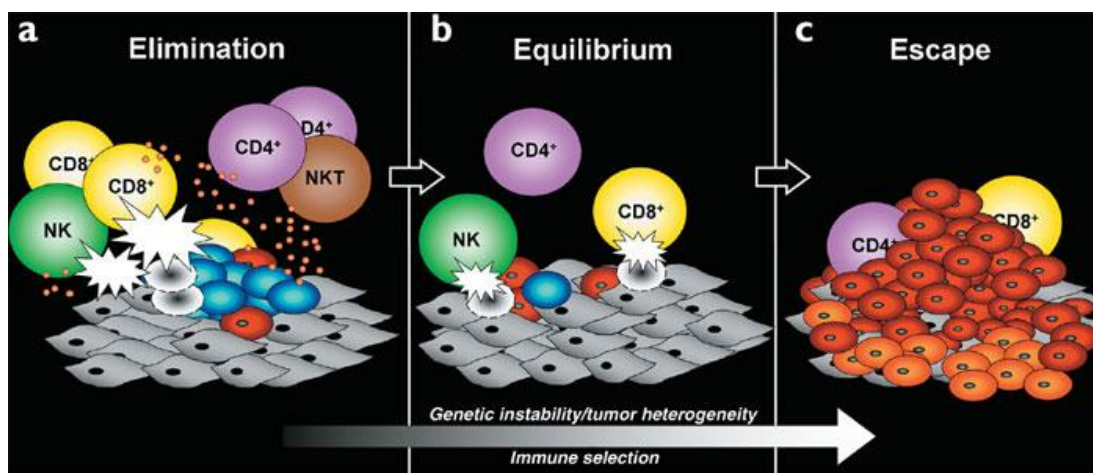


Figure 2.3. Cancer immunoediting: from immunosurveillance to tumor escape. Taken from Dunn et al. [60].

The immunosurveillance/elimination mechanism can be more successful in eradication of certain cancers and control the tumor removal by taking advantage of both cellular and molecular components of the innate and adaptive immune system. The major anti-tumor components include NK cells, CD4⁺ T (especially Th1 type) cells and CD8⁺ cytotoxic T lymphocytes (CTLs), and IFN- γ , perforin, granzyme, Fas/FasL, TRAIL and NKG2D molecules. NK cells eliminate tumor cells by recognizing the malignantly transformed/DNA-damaged tumor cells (i.e. stressed cells) or the activating

ligands (e.g. NKG2D ligands) on tumor cells. Activated NK cells can directly kill the tumor cells, secrete inflammatory cytokines (mainly IFN- γ to activate M1 and Th1-mediated immune responses). CD4⁺ helper T cells play roles in anti-tumor immune responses following the recognition of tumor antigens through class II MHC molecules. They provide cytokines for effective CTL development, secrete TNF and IFN- γ , and allow efficient macrophage activation. CD8⁺ CTLs perform the surveillance function by recognizing peptides derived from mutant/oncogenic cellular proteins via class I MHC molecules and kill the malignant cells [58].

The molecular mechanisms mediating the equilibrium phase (tumor dormancy) are hardly modeled and poorly understood. Some studies showed a possible role for Th1 immunity. The immune-mediated equilibrium may be a very prolonged process with tumor cells persisting for years or even decades with minimal outcome. Critically, the balance between IL-12 that promotes elimination and IL-23 that promotes persistence may function in the maintenance of tumors in equilibrium. It has been shown that silent cancers in the equilibrium state contain high ratios of CD8⁺ T cells, NK cells, $\gamma\delta$ T cells and low ratios of NKT cells, Foxp3⁺ Treg cells and MDSCs in their microenvironment. This supports the concept that the balance between immune cells and immunosuppressive cells is correlated with the tumor dormancy. However, the factors that shift this balance in favor of tumor escape are not well known; but, lack of the tumor specific antigens or of the capacity to present them can be crucial in this process. This is further supported by findings that by IFN- γ and TNF production tumor antigen-specific T cells can inhibit the growth of a pancreatic tumor in mice [58]. In the absence of either TNFR1 or IFN- γ signaling, the same T cells promote angiogenesis and carcinogenesis [61]. Additionally, while IFN- γ and TNFR1 signaling are strictly required in cancer cell senescence, TNFR1^{-/-} cancer cells resist cytokine-induced senescence and grow aggressively. Therefore, as IFN- γ and TNF stimulate tumor cell senescence in different cancers, this

may be a general mechanism for arresting cancer progression and escape [62].

Tumor escape can emerge through several mechanisms. One of these mechanisms is reduced immune recognition through the decrement or failure of presenting tumor antigens, downregulation of class I MHC molecules or costimulatory molecules. Another mechanism of tumor escape can be resistance or survival through increased expression of STAT3 or anti-apoptotic molecule Bcl2. Tumor can also escape from the immune system by reconstruction of an immunosuppressive tumor microenvironment rich in immunosuppressive molecules such as VEGF, TGF- β , PD-1/PD-L1, IL-10, or recruitment of immunoregulatory cells such as Tregs and MDSCs [58, 63]. These changes may render the tumor cells invisible to T lymphocytes yet result in ineffective immune responses. Immunosuppression can activate dormant tumor cells and shift the equilibrium towards the escape phase [64].

2.5. Breast Cancer

Breast cancer is the most common cancer in women. More than 1.3 million women are affected by breast cancer every year and it is related with 14% of cancer-related deaths [65]. Breast cancer is a heterogeneous disease. Gene expression analyses and molecular characterizations in different breast cancer cell lines have indicated that there are several oncogenic mutations in breast cancer [66]. Mutations in PI3K pathway and/or p53 and RB tumor suppressor genes are frequent among all types of breast cancers. Mutation profile in the cancers with luminal properties frequently involves *E-cadherin*, *MAPK* gene mutations and amplifications of *CyclinD1*, *ERBB2*, and *HDM2*, while the basal-like cancers' mutation profile commonly involves *BRCA1*, *RB1*, *RAS*, and *BRAF* [66]. Estrogen receptor (ER), progesterone receptor (PR), and ERBB2/HER2 are important markers for

classification of breast cancer subtypes and for targeted therapies [67]. With the use of gene expression profiling and DNA microarray analyses, breast cancer has been classified into 5 major molecular subtypes: luminal type A, luminal type B, basal-like, HER2 type, and normal breast-like types.

I. Luminal-A tumors represent 50-60% of breast carcinomas. Luminal-A subtype is ER-positive, PR-positive and HER2-negative and share expression markers with luminal epithelial layer of cells lining normal breast ducts. They show low histological grade, favorable prognosis, and less lymph node involvement [65-67].

II. Luminal-B subtype ranges between 10-30% of breast cancers and displays rapid proliferation, sustained oncogene amplification (e.g. *MYC*), and less favorable prognosis. Luminal-B tumors are ER-positive, PR-positive or -negative, and HER2- positive or -negative. They also share expression markers with breast luminal epithelial cells. Patients with hormone receptor-positivity represent better prognosis than those with hormone receptor-negative breast cancer. Proteomic analyses have shown that luminal-B tumors are generally associated with high plasma CCL5, EGF, PDGF, and TGF- β levels [65].

III. Basal-like breast cancer subtype represents a prevalence of approximately 10-20%. Basal-like tumors show primarily triple negative breast cancer (TNBC) phenotype that expresses neither ER or PR, nor HER2. They share expression markers with the underlying basal (myoepithelial) layer of normal breast ducts, carry frequent chromosome segmental gain/loss, and BRCA1 gene mutations. Basal-like breast cancers display high histological grade (more likely to be grade III), are diagnosed in younger women, show early metastasis (but show less lymph node involvement), and are associated with poor prognosis with limited therapeutic options. The proteins involved in cytokine and growth factor signaling such as

STAT1, CCL5, and VEGF are abundant in the plasma and lead to increased migration and invasion [65, 68].

IV. Approximately 4-7% of the breast carcinomas can be categorized as HER2-enriched subtype. HER2 (ERBB2)-enriched tumors are associated with overexpression and amplification of *HER2* (epidermal growth factor receptor) oncogene and related genes. HER2-positive tumors show increased cell proliferation and motility, increased angiogenesis and tumor invasiveness and decreased apoptosis. HER2-overexpressing cells which are ER- and PR-negative are manifested with high histological grade, younger age, advanced disease at the time of diagnosis, more lymph node involvement, increased risk of metastasis preferentially to lung, liver and brain, negative hormone receptor status, and short survival rate [68]. The proteins involved in lipid and glucose metabolism, stress-mediated chaperones, detoxification, and proteins related with tumor survival, chemoresistance, and poor prognosis are upregulated in HER2-overexpressing tumors [65].

V. Normal breast-like cancers are not well distinguished in the literature, but these tumors share expression markers with normal breast tissue [66, 67]. Normal breast-like gene expression pattern show the highest expression of many genes expressed by adipose tissue and other non-epithelial cell types (fibroblasts, macrophages, and lymphocytes). This subtype also exhibits strong expression of basal epithelial genes and low expression of luminal epithelial genes [69].

Breast cancer classification according to the gene expression analyses has led to the clinical characterization representing correlation with survival, disease relapse, site of preference of metastatic spread and chemotherapy response (Table 2.3) [65].

Table 2.3. Breast carcinoma subtypes: histopathological, molecular and clinical features. Taken from Lam et al. [65].

Molecular subtype	Prevalence ^a	IHC definition ^b	Additional markers	Genes	Histological grade	TP53 mutation	Prognosis	Consensus recommendation for (Neo) adjuvant systemic treatment ^b
Luminal A	50-60%	ER+ and/or PgR+ HER2- Ki-67 low	CK8/18+ FOXA1+	<i>ESR1, GATA3, KRT8, KRT18, XBP1, FOXA1, TFF3, CCND1, LIV1</i>	Good differentiation	Low	Good	Endocrine therapy alone ^d
Luminal B	10-30%	-	FGFR1 and ZIC3 amplification	<i>ESR1, GATA3, KRT8, KRT18, XBP1, FOXA1, TFF3, SQLE, LAPTM4B</i>	Moderate differentiation	Intermediate high	Intermediate -	-
Luminal B (HER2 negative)	15-20%	ER+ and/or PgR+ HER2- Ki-67 high	-	Not examined ^c	-	-	-	Endocrine therapy ± chemotherapy ^e
Luminal B (HER2 positive)	6%	ER+ and/or PgR+ Any Ki-67 HER2+	-	Not examined ^c	-	-	-	Endocrine + cytotoxic + anti-HER2 therapy
HER2-enriched	10-15%	HER2 + ER- and PgR-	CK5/6+ GRB7+	<i>ERBB2, GRB7</i>	Poor differentiation	High	Poor	Chemotherapy + anti-HER2 therapy ^f
Basal-like	10-20%	ER- and PgR- HER2-	EGFR+ CK5/6+ CK14+ CK17+ HER1+ Cyclin E+ CDKN2A+ RB1: low/- BRCA1: low/- FGFR2: amplification	<i>KRT5, CDH3, ID4, FABP7, KRT17, TRIM29, LAMC2, ITGB4</i>	Poor differentiation	High	Poor	Chemotherapy for triple negative breast cancer (ductal)

Breast tumor staging according to the histopathological properties and TNM (primary tumor, regional nodes, metastasis) of the tumor is also very important for accurate prognosis and therapeutic decision making [70, 71].

The proliferation of malignant epithelial cells inside the breast ducts is called ductal carcinoma in situ (DCIS). Untreated DCIS likely develops invasive breast cancer within 5 years. Prognostic features such as extensive disease, necrosis, poor nuclear grade, and presence of hormone receptors overexpression of HER2 may help to identify the risk for local recurrence after conventional (surgery and/or radiation) therapies [70-72].

The proliferation of malignant cells inside the breast lobules is called lobular neoplasia or lobular carcinoma in situ (LCIS). It has been shown that approximately 30% of patients whose lesions had been removed developed cancer after 15-20 years. Lobular neoplasia can be defined as a

pre-malignant lesion that likely develops breast cancer. Molecular analysis of these patients' biopsies can be a good indicator to detect patients who are at the risk of further progression [70].

Invasive breast carcinoma have been divided into five groups; invasive ductal carcinoma, invasive lobular carcinoma, medullary carcinoma, colloid carcinoma, and tubular carcinoma.

Majority of breast cancers (70-80%) fall into the group called invasive ductal carcinoma. In most ductal carcinomas, normal breast fat is replaced with fibrous or connective tissue. Lymphovascular invasion is common. About two third of invasive ductal carcinoma express estrogen or progesterone receptors, and about one third overexpress HER2 [73, 74].

Cells of the invasive lobular carcinoma invade individually into the surrounding stroma and form strands or chains. This growth pattern is correlated with mutations in E-cadherin. Lobular carcinoma specifically invades cerebrospinal fluid, serosal surfaces, gastrointestinal tract, ovary, uterus, and bone marrow. Nearly all of these carcinomas express hormone receptors, but HER2 overexpression is rare [73].

Medullary carcinoma incidence is less than 1%. These cancer cells form sheets of large neoplastic cells with high lymphocytic infiltrates. Women with BRCA1 mutations manifest increased frequency for medullary carcinoma. These carcinomas do not express estrogen and progesterone receptors and do not overexpress HER2. Therefore, they demonstrate a triple negative phenotype [73, 74].

Colloid (mucinous) carcinoma also is a rare cancer. These tumor cells produce high quantities of extracellular mucin, which spreads into the stroma. They form soft and gelatinous masses. They express hormone receptors, but do not overexpress HER2 [73].

Tubular carcinoma accounts for 10% of invasive carcinomas smaller than 1 cm. They show irregular densities with well-formed tubules, rare lymph node metastasis, and good prognosis. They express hormone receptors and no HER2 overexpression [73].

2.6. Chemokine Network in Breast Cancer

Chemokines and chemokine receptors play vital roles in breast cancer progression and metastasis, including proliferation, invasion, migration, senescence, angiogenesis, and regulation of immune responses [49]. Many chemokines are expressed by normal breast epithelium at low levels. These include CXCL1, CXCL2, CXCL5, CXCL6, CXCL8, CXCL20, CX3CL1, CCL2, and CCL7. CXCL1-3 and CXCL5-8 are also detected in human milk. In many cases, chemokines are detected at higher levels in breast cancer tissues compared to normal tissues. There is accumulating evidence on the roles of CXCL8 (IL-8), CCL2 (MCP-1), CCL4, and CCL5 (RANTES) in breast cancer [12].

Elements of the tumor microenvironment (cytokines, growth factors, stromal cells, and malignant tumor cells) are in a dynamic interaction with tumor infiltrating immune cells, which can support or restrict tumor growth [75]. Basically, infiltrating immune cells function in elimination of tumor cells, however factors in the tumor microenvironment modify these cells and suppress anti-tumor immunity. The major immune cell types found in breast cancer microenvironment are macrophages, myeloid-derived suppressor cells, and T lymphocytes.

Tumor associated macrophages (TAMs) are one of the most important immune cells that infiltrate tumor and are found in the tumor microenvironment in different types of cancer, including breast cancer. Tumor cells release colony stimulating factor-1 (CSF-1) and the chemokine CCL2.

These factors are the major growth factors and chemoattractants for TAMs. TAMs in turn produce high amounts of immune-suppressive IL-10 in the tumor microenvironment [76].

CCL5 can be produced by breast tumor cells and other cells of the tumor microenvironment (i.e. bone marrow as metastatic foci) including osteoblasts and mesenchymal stem cells. Beside TAMs and Tregs, CCL5 promotes the infiltration and differentiation of myeloid derived suppressor cells (MDSCs) to breast tumor microenvironment [77].

CCR5 and its ligands CCL3, CCL4, and CCL5 are also important factors for CD4⁺ helper T cells and CD8⁺ cytotoxic T cells infiltration, DC activation, antigen cross presentation, and anti-tumor immune responses in tumor microenvironment [78]. CXCL10 overexpression by basal breast cancer cells, activated T lymphocytes, endothelial cells, fibroblasts, monocytes, and keratinocytes attracts other immune cells which express CXCR3, including NK cells, monocytes, and more activated T lymphocytes [79].

CCR7 expression on breast tumors has been correlated with poor prognosis [80]. Intratumoral CCL21 can increase T cell infiltration in breast cancer. CCL21 in combination with IFN- γ are positively correlated with good prognosis [81]. Beside CCL21, CCR7 is activated by binding CCL19. Under normal conditions, naïve T cells use CCL19 to enter into the lymph nodes. Thus, it is likely that CCR7-expressing tumors use these chemokines to metastasize to lymph nodes. An *in vivo* study showed that CCR7 directed the migration of breast tumor cells to lymph nodes, preferentially those that are located in the lung [80].

There are several studies associated with chemerin and cancer progression [82-84]. However, there is less known about the role and expression of chemerin in breast cancer. Rama et al. reported that neither

chemerin nor CMKLR1 was detected in 4T1 breast cancer cell line, *in vitro*; however, both genes were highly expressed in the tumors established with this cell line, *in vivo* [85].

Among tumor infiltrating lymphocytes (TILs), $\gamma\delta$ T cells are one of the important IFN- γ -mediated anti-tumor immune cells. *In vitro* studies have shown that human $\gamma\delta$ T cells migrate toward CCL2, CCL3, CCL4, CCL5, CXCL10, CXCL11, and CXCL12. A recent study has demonstrated that CCL2/CCR2 signaling is an important pathway in $\gamma\delta$ T cell infiltration toward tumors and V δ 1 T cells (a subset of $\gamma\delta$ T cells) infiltration in breast cancer [86].

IFN- γ can induce CXCL9 and CXCL10 production; whereas, CCL2 expression was decreased in the presence of Th1 cells co-cultured with breast cancer cell lines. CCL2 is essential in chemotaxis of monocytes and Tregs and inhibits CD8⁺ CTL effector functions [87].

The formation of metastatic tumors is a non-random process. Tumor cells also utilize chemokines and chemokine receptors to migrate and metastasize to distant target tissues and organs. Expression of chemokine receptors CXCR4, CCR7, and CCR10 in breast cancer are associated with metastasis. Among these chemokine receptors, CXCR4 plays an important role in the lymph node trafficking of hematopoietic progenitors and endothelial cells [88]. CCR4 is also identified as an important chemokine receptor in breast tumor metastasis to lungs. CCR4 expression both on breast tumor cells and on CCR4⁺ Tregs was correlated with breast cancer cells' spread [88].

2.7. Immune Responses in Breast Cancer

Depending on their maturation stage and on the properties of tumor microenvironment, immune cells can both restrict or promote cancer progression [89].

Macrophages are important components of the tumor microenvironment. Tumor associated macrophages (TAMs) are a heterogeneous population of cells influenced by oxygen availability, stages of tumor progression, and the factors found in the tumor microenvironment. The macrophages with M1 phenotype that has the tumoricidal capacity can polarize into M2 immunosuppressive and tumorigenic phenotype under immune modulating factors [90]. High densities of macrophages have been detected in breast cancer stroma. TAMs promote tumor progression, induce angiogenesis, and reduce anti-tumor immune responses. It has been found that high infiltration of TAMs is associated with poor prognosis, decreased overall survival, and increased risk of recurrence for most solid tumors including breast cancer [90]. In breast cancer, TAMs exhibit a clear M2 phenotype, which is associated with more aggressive histopathological characteristics, high tumor grade, metastasis, and decreased overall survival [91, 92].

Like in other solid malignancies, during breast tumor angiogenesis newly formed vessels contain leaky endothelial lining that does not supply enough oxygen pressure in the tumor, hence hypoxia develops. Hypoxia leads to the necrosis of cells in the area, which provides a factor for attraction of macrophages. Accumulation of TAMs in poorly vascularized and hypoxic areas of breast cancer has been positively correlated with aggressive tumor behavior [93]. Hypoxic conditions in the tumor microenvironment upregulate HIF-1 α and VEGF by macrophages. In these conditions, TAMs secrete more immunosuppressive cytokines such as IL-10 and produce matrix metalloproteinases (MMP-2 and MMP-9), degrading the extracellular matrix

(ECM) and allowing the tumor cells to metastasize. These factors link breast cancer with more metastatic, aggressive malignant behavior, and increased patient mortality. Tumor associated macrophages also produce collagen fibers that can facilitate tumor cell migration and tumor invasiveness [93].

Myeloid-derived suppressor cells (MDSCs) are a heterogeneous population of immature myeloid cells that display different maturation levels [92]. MDSCs exert their suppressive functions by disturbing both innate and adaptive immune responses using immunosuppressive cytokines (TGF- β , IL-10, IL-6), proinflammatory mediators (VEGF and GM-CSF), and enzymes (arginase and indoleamine 2,3-deoxygenase (IDO)) [94]. Protumorigenic factors can also be released by MDSCs during tumor development, supporting tumor cell survival, and suppressing effector T cells, inhibiting anti-tumor immune responses. The number of MDSCs is elevated in peripheral blood of breast cancer patients. Additionally, circulating MDSCs in metastatic breast cancer are significantly correlated with worse overall survival [92]. In addition, the total count of white blood cells and especially increased neutrophil to lymphocyte ratio is correlated with poor prognosis in breast cancer [95].

DCs in the peripheral blood and tumor-draining lymph nodes of breast cancer patients are decreased, express low levels of MHC, costimulatory molecules, and IL-12 and are dysfunctional. Breast cancer lymph node metastasis is correlated with maturation arrest and apoptosis of DCs and poor interaction with CD8⁺ T cells [94].

The presence of intratumoral lymphocytes and lymphocyte predominant breast cancers were associated with an increased pathological complete response (pCR) in comparison with patients without any lymphocytic infiltration [92]. High levels of tumor infiltrating lymphocytes (TILs) are associated with better prognosis in primary triple-negative breast cancer [96]. The majority of TILs in solid tumors consist of CD4⁺ helper T

cells, including Th1 and Th2 cells, regulatory T cells (Tregs), and CD8⁺ cytotoxic T lymphocytes (CTLs) [92]. CD8⁺ CTLs mediate tumor cell killing through recognition of MHC I-associated tumor-specific antigens and production of perforin and granzyme molecules for tumor cell lysis. However, antigen processing defects in tumor cells have a negative effect on T cell recognition and activation [97]. T cells with high affinity for normal breast tissue antigens are believed to be deleted by central tolerance during the thymic education or by peripheral tolerance due to antigen load in the case of breast cancer metastasis or they may not be efficient enough to fight against cancer due to tumor (self) antigen recognition. However, some of the T cells specific for tumor antigens may escape thymic deletion and migrate to the tumor site [94]. It has been found that IL-4 expressing CD4⁺ T lymphocytes support invasion and metastasis of breast cancer cells through TAM activation [94].

CD4⁺CD25⁺FoxP3⁺ Tregs are thymus-derived lymphocytes that are induced in the tumor microenvironment. These cells use several mechanisms that suppress immune responses including immunosuppressive cytokines secretion, modulation of the tumor microenvironment and surface receptors. Tregs fundamentally secrete immunosuppressive cytokines including transforming growth factor- β (TGF- β) and IL-10 and express cytotoxic T lymphocyte antigen-4 (CTLA-4), a family of co-inhibitory receptors expressed on T cells. TGF- β suppresses IFN- γ production by Th1 and CD8⁺ T cells, blocking an effective immune response and encouraging tumor progression [92]. High level of TGF- β in circulation is associated with enhanced metastasis and poor prognosis. TGF- β has the capacity to inhibit the activation of CTLs, NK cells, macrophages, and convert naïve CD4⁺ T cells into Tregs [98]. TGF- β provides Treg accumulation in the tumor microenvironment and inhibits dendritic cell-T cell cross talk, necessary for T cell activation [98]. The forkhead box P3 (FoxP3) transcription factor controls the expression of CD25, CTLA-4, and other molecules responsible for

mediating Tregs' suppressive functions, and activates transcription of oncogenes. Tregs constitutively express IL-2 receptor (CD25) that promotes their high proliferation rate. Tregs stimulate down-regulation of APC functions through inhibitory signals by CTLA-4 expression [99]. Treg frequency is increased in the blood circulation of breast cancer patients. Accumulation of CD4⁺FOXP3⁺CD25^{high} Treg in the blood circulation is correlated with suppression of anti-tumor immune responses, tumor grade, poor prognosis, and reduced survival [94, 95]. In breast cancer, Treg quantity correlates significantly with the aggressiveness of the disease (high tumor grade, node positivity), shorter overall survival, and decreased recurrence-free survival [92]. CTLA-4, an essential regulator of T cell activation, maintains self tolerance and limits immune reaction by binding CD80 or CD86 costimulatory molecules. Its expression has been detected in breast tissue and peripheral blood of breast cancer patients [92]. While high number of TILs indicate general activation and response of the immune system, the ratio between effector T cells and Tregs may display a better prognostic indicator for breast cancer survival [100]. On the other hand, high CD8⁺ and low FoxP3⁺ T cell infiltrates after chemotherapy are positively correlated with increased disease-free survival. Tumor-specific CTLs tend to have low proliferation, to differentiate in the breast tumor microenvironment, and to produce high levels of IFN- γ and low levels of TGF- β [94]. A high Th1 and CTL response relative to Th2 and Treg responses are identified with favorable disease outcome. Molecular profiling of breast cancers has demonstrated that aggressive breast tumors (most frequently triple-negative) show high expression of Th2 and Treg genes and a low Th1/Th2 gene ratio [94]. Tumor infiltrating B7-H1⁺/PD-1⁺ T cells and Tregs indicate high risk in breast cancer [94].

Activated T cells display high levels of specific cytotoxicity by circulating Th1 cytokines. Th1 cells are the fundamental source of IFN- γ that functions as a major anti-tumor agent. It has been demonstrated that

activated T cells and IFN- γ in Th1-enriched breast tumor microenvironment have induced smaller tumor size and reduced the number of MDSCs [87]. Conversely, IFN- γ produced by tumor-specific T lymphocytes may also induce MDSC differentiation. However, Th1 cells are rendered inactive or change phenotype into Foxp3-expressing Tregs by immunosuppressive factors in the tumor microenvironment [87, 98].

B cells or plasma cells have also been shown in breast cancer. Immunoglobulin G (IgG) that present in the tumor stroma can be an immune biomarker for prognosis and chemotherapy response in breast cancer. B cell infiltrates have been correlated with better prognosis in breast cancer [95]. On the other hand, the presence of tumor-specific antibodies (specially IgM) were associated with reduced tumor-specific T cell responses, increased intratumoral TGF- β , and advanced tumor stage [94].

3. MATERIALS AND METHODS

This work has been done in Hacettepe University Cancer Institute, Department of Basic Oncology Laboratories through November 2010-February 2014.

3.1. Materials Used in This Work

Chemical and biological materials used in this study are listed below:

Phosphate buffered saline (PBS) (Calbiochem, USA); Agarose, low glucose (1g/L glucose)/high glucose (4.5 g/L glucose) Dulbecco's Modified Eagle Medium (DMEM), RPMI medium, Fetal Bovine Serum (FBS), Ficoll 1077 (Lonza, USA); β -mercaptoethanol, Ethidium Bromide, Ficoll 1119, hydrocortisone, insulin (Sigma-Aldrich, USA); LPS, rhIFN- γ , rhCCL5, rhCCL19, rhchemerin (R&D Systems, USA); CCL5 and CCL19 ELISA assay kits (RayBiotech, USA); EDTA disodium salt, FuraRedII reagent (Invitrogen, USA); Human Embryonic Kidney (HEK293T) Cell Line (gift from Dr. Ihsan Gursel, Bilkent University, Turkey); MDA-MB-231, MDA-MB-468, MCF-7 (gift from Dr. Alison Benham, Oxford University, UK); BT-474 (gift from Dr. Elif Erson-Bensan, METU, Turkey); HCC38, SK-BR-3, T-47D, ZR-75-1 breast cancer cell lines, and MCF-12A normal breast cell line (ATCC, USA); *Taq* DNA polymerase, 10X *Taq* buffer (NH_4)₂SO₄, MgCl₂ (25 mM), 6X loading dye, Oligo (dT)₁₈ primer, deionized nuclease-free water, RT reaction buffer (5X), dNTP mix (10 mM), Ribonuclease inhibitor, Reverse transcriptase, *Mlu*I restriction digestion enzymes, 10X NEB buffer, 10X Bovine Serum Albumin (BSA), buffer R (10X) with BSA, T4 DNA ligase, T4 DNA ligase buffer, 50 bp DNA ladder, 1 Kb DNA ladder, dNTP mixture (2 mM), *Pfu* DNA polymerase, 10X *Pfu* buffer, Mr. Frosty Freezing container Nalgene (Fermentas, Lithuania); DyNzyme DNA polymerase, 10X buffer for Dynazyme DNA polymerase (Finnzymes, Finland); *Xma*I, *Nhe*I, *Phu*sion DNA polymerase, 5X

Phusion buffer (New England BioLabs, USA); Primer oligonucleotides (Alpha DNA, Canada); 10X Tris-Borate-EDTA (TBE) buffer (Dr. Zeydanli, Turkey); Tris base, Boric acid (Sigma, USA); pIRES2-EGFP vector (BD Biosciences Clontech, USA); DH5a *E.coli* competent bacteria, NaC₂H₃O₂·3H₂O (Merck, USA); CaCl₂ anhydrate, MnCl₂·4H₂O (Applichem, USA); Yeast extract, Tryptone, Bacto Agar (BD, USA); Sodium chloride (NaCl) (Merck, Germany); Kanamycin, Ampicillin, Wizard[®] Plus Minipreps DNA Purification System (Promega, USA); L-glutamine, Penicillin-Streptomycin, Puromycin, Trypsin-EDTA, non-essential amino acids solution (PAA, Austria); cell culture flasks, 15/50 mL falcon tubes, cryovial tubes (Corning, USA); 6-well plate, 96-well plate (Costar, USA).

3.2. Buffers and Solutions

TBE Buffer: 1X TBE buffer was either diluted from 10X TBE buffer or was freshly prepared. In order to prepare 10X TBE buffer, 108 gr of Tris base, 55 gr of Boric acid, and 7.5 gr of EDTA were dissolved in 1 liter dH₂O.

Luria Bertanni (LB) Broth and LB Agar: 2.5 gr Yeast extract, 5 gr Tryptone, and 2.5 gr NaCl were mixed and completed to 500 mL with dH₂O. To prepare LB agar, 2.5 gr Yeast extract, 5 gr Tryptone, and 2.5 gr NaCl were dissolved in dH₂O, and then 7.5 gr Agar was added, mixed, and completed to 500 mL with dH₂O. Then, they were sterilized using autoclave. After cooling, the media were stored at 4°C.

For LB agar plates, 25 mL LB agar was poured into each plate. These plates contained either 50 µg/mL kanamycin or 100 µg/mL ampicillin.

Competent Solution: This solution contained: 40 mM NaC₂H₃O₂·3H₂O, 100 mM CaCl₂ anhydrate, and 70 mM MnCl₂·4H₂O in 50 mL with dH₂O. pH of the solution was adjusted to 5.5, filtered using a 0.22 µm filter, and stored at 4°C.

RNase-Free DNase: Lyophilized DNase enzyme (QIAGEN, Germany) was reconstituted with RNase-DNase-free dH₂O, aliquoted as 30 µL volumes into RNase-DNase-free tubes and stored at -20°C.

Full DMEM (low or high glucose): In order to prepare full cell culture medium; into 500 mL DMEM, 10% (55 mL) heat-inactivated fetal bovine serum (FBS), 1% (5.5 mL) L-glutamine, and 1% (5.5 mL) penicillin and streptomycin were added and mixed well. Completed media were stored at 4°C.

Full RPMI Medium: In order to prepare full serum cell culture medium, into 500 mL RPMI medium; 10% (55 mL) heat-inactivated fetal bovine serum (FBS), 1% (5.5 mL) L-glutamine, and 1% (5.5 mL) penicillin and streptomycin were added and mixed well. Completed media were stored at 4°C.

Full DMEM-F12 Medium for MCF-12A: 500 mL DMEM-F12 medium containing L-glutamine was mixed with 1X MEM non-essential amino acid solution, 20 µg/mL EGF, 0.01 mg/mL bovine insulin, 500 ng/mL hydrocortisone, 10% FBS, and 1% penicillin-streptomycin. Completed media were stored at 4°C.

Full McCoy5A Medium: 500 mL medium containing L-glutamine was mixed with 10% FBS and 1% penicillin-streptomycin. Completed media were stored at 4°C.

FBS Heat Inactivation: FBS was thawed at 4°C or at room temperature. After thawing, it was incubated at 56°C for 30 min. Then, 10 mL aliquots were prepared and stored at -20°C.

Preparation of Recombinant Proteins: rhCCL5 was reconstituted at 100 µg/mL in sterile PBS containing 0.1% bovine serum albumin (BSA). rhCCL19 was reconstituted at 25 µg/mL in sterile PBS containing 0.1% BSA. rhChemerin was reconstituted at 100 µg/mL in sterile PBS containing 0.1%

BSA. rhIFN- γ was reconstituted at 200 $\mu\text{g}/\text{mL}$ in sterile dH_2O . These recombinant proteins were aliquoted and stored at -86°C .

LPS Solution: 1 mg LPS was weighted and dissolved in RPMI 1640 medium at 10 $\mu\text{g}/\text{mL}$ final concentration. LPS solution was aliquoted and stored at -20°C .

3.3. Molecular Techniques

3.3.1. Total RNA Isolation

RNA Isolation from Cells: In order to isolate total RNA (QIAamp[®] RNA Blood Mini Kit, QIAGEN, Germany) from cells, they were washed with 1X PBS and centrifuged at 2000 rpm for 5 min (Jouan CR3, UK). Supernatant was discarded, 350 μL buffer RLT+ β -merceptoethanol (10%) mixture was added onto the pellet and mixed. 350 μL of 70% ethanol was added, the mixture was put into a QIAamp spin column, and centrifuged at 10000 rpm for 20 sec. 350 μL buffer RW1 was added to the column and centrifuged at 10000 rpm for 20 sec (Eppendorf, USA). Flow through was discarded. 80 μL DNase digestion mixture (70 μL buffer RDD+10 μL DNase) (QIAGEN, Germany) was directly added onto the membrane and incubated at room temperature for 45 min. After completion of incubation, 350 μL buffer RW1 was added into the column and centrifuged at 10000 rpm for 20 sec. Flow through was discarded. 500 μL buffer RPE was added into the column and centrifuged at 10000 rpm for 20 sec. Flow through was discarded. 500 μL buffer RPE was added into the column and centrifuged at 13000 rpm for 4 min. The column was placed in a new 2 mL collection tube and centrifuged at 14000 rpm for 1 min. The column was transferred into a 1.5 mL DNase- and RNase- free microcentrifuge tube. 30 μL RNase-free water, provided by the kit, was added directly onto the membrane and centrifuged at 10000 rpm for 1 min. RNA samples were stored at -86°C .

RNA Isolation from Blood: Peripheral blood was diluted with 1X PBS. 5X volumes of erythrocyte lysis (EL) buffer was added. Sample was incubated on ice for 12 min and meanwhile vortexed (Clifton Cyclone, UK) 3 times (10 sec each). Sample was centrifuged at 1400 rpm for 10 min at 4°C. Supernatant was discarded. Again, pellet was resuspended with 1X PBS, 2X volume of EL buffer was added, and vortexed. Sample was centrifuged at 1400 rpm for 10 min at 4°C. Supernatant was discarded. 350 µL buffer RLT+β-mercaptoethanol mixture was added on the sample and vortexed. The mixture was added into a QIAshredder spin column and centrifuged at 13000 rpm for 2 min at 4°C. Column was discarded. 350 µL of 70% ethanol was added to the flow through and mixed. The mixture was added to a QIAamp spin column and centrifuged at 10000 rpm for 20 sec and the protocol was continued as the same for “RNA isolation from cells”.

3.3.2. RNase-Free DNase Treatment

Each total RNA sample (16 µL) was used for DNase treatment (Ambion, USA). 2 µL of buffer was added to RNA and then 2.2 µL of recombinant DNase1 (2 U/µL) was added. Sample was slowly mixed and incubated at 37°C for 45 min. 4.8 µL of DNase inactivation reagent was added to the sample and mixed well. Sample was incubated at room temperature for 2 min and meanwhile slowly mixed. The sample was centrifuged at 13000 rpm for 90 sec. Supernatant was collected in a new DNase-RNase-free tube. DNase-treated RNA samples were stored at -86°C. In order to check the presence of DNA in RNA samples, 1 µL of each RNA sample was used in β-actin PCR. If RNA samples were not free of genomic DNA (i.e. PCRs were not negative), they were re-treated with RNase-free DNase treatment and again checked by PCR. PCR conditions are given in Section 3.3.5.

In order to concentrate (pool) the isolated RNAs, all RNAs isolated from the same cell were mixed in the tube containing the highest RNA concentration (Zymo Research, USA). 2 volumes RNA binding buffer was added and mixed. 1 volume of 100% ethanol was added and mixed. The mixture was added into a spin column and centrifuged at 13000 rpm for 1 min. Flow through was discarded. 400 μ L RNA prep buffer was added and centrifuged at 13000 rpm for 1 min. Flow through was discarded. 800 μ L RNA wash buffer was added and centrifuged at 13000 rpm for 30 sec. Flow through was discarded. 400 μ L RNA wash buffer was added and centrifuged at 13000 rpm for 30 sec. Flow through was discarded and centrifuged at 13000 rpm for 2 min. The spin column was transferred to an RNase-DNase-free tube. RNase-free water was added (putatively calculated to give at least 40 ng/ μ L final RNA concentration). Tube was incubated at room temperature for 1 min and centrifuged at 10500 rpm for 30 sec.

3.3.3. Spectrophotometric Measurement of Nucleic Acids

The concentration and quality of the isolated RNA and DNA were measured with an UV spectrophotometer (NanoDrop ND-1000, USA) at 260 nm, 230 nm, and 280 nm. Quality of nucleic acids was determined by using A_{260}/A_{280} and A_{260}/A_{230} ratios. These ratios for RNA purity is accepted in the range of 1.9 – 2.0 and for DNA purity is between 1.8 - 1.9.

3.3.4. cDNA Synthesis

Single chain complementary DNA (cDNA) was synthesized from total RNA by using RevertAid™ First Strand cDNA Synthesis Kit (Fermentas, Lithuania). cDNA synthesis reaction components and conditions are shown in Table 3.1. The cDNA products were stored at -20°C.

Table 3.1. cDNA synthesis reaction components and conditions.

Component	Amount	Final Concentration
RNA	290 ng	
Oligo (dT)₁₈ Primer (0.5 µg/µl)	1 µl	0.025 µg/µl
Deionized Water	Complete to 12 µl.	
Incubation		65°C, 5 min.
RT Reaction Buffer (5X)	4 µl	1 X
dNTP mix (10 mM)	2 µl	1 mM
Ribonuclease Inhibitor (20 u/µl)	1 µl	1 u/µl
M-MuLV Reverse Transcriptase (200 u/µl)	1 µl	10 u/µl
Incubation	42°C, 60 min. &	70°C, 10 min.
Final Volume	20 µl	

3.3.5. Polymerase Chain Reaction (PCR)

Primers used for gene expression analyses by PCR are listed in Table 3.2.

Table 3.2. The primers' information used in gene expression analyses.

Gene	Forward (F) and Reverse (R) Primer Sequences	Product (bp)	Annealing Temperature (°C)	Gene Bank No.
CRAM-A	F:5' ACGTCTCAGCTGTCACAGGAA 3' R:5' CTGGGCGTCATACTTGCACA 3'	200	64	NM_001130910.1
CRAM-B	F:5' AAAGGAGGGCATCCACTGTC 3' R:5' CTGGGCGTCATACTTGCACA 3'	208	61	NM_003965.4
CCRL1	F:5' GGACACTCATGAAGATGCC 3' R:5' TGCTCATGTTGCAGCTGGT 3'	161	60	NM_178445.1
D6	F:5' TTGTGTCTTGGTGAGGCTG 3' R:5' CTGTTACCTGGAGTGCCTAG 3'	190	59	NM_001296.4
DARC	F:5' AGGCCACACACACTGTAGC 3' R:5' TAGAACCACCCCATGAGGC 3'	161	60	NM_001122951.2
CCR1	F:5' TGACCAGCATCTACCTCTGAAC 3' R:5' GTGGAAGCTGTTTCAGGCTCTGA 3'	402	62	NM_001295.2
CCR3	F:5' AGAGCACTGATGGCCAGTTTG 3' R:5' CTGGAGGCATTTCCACACTCTGA 3'	527	60	NM_178329.2
CCR4	F:5' AGGTTCTCAGCTCCCTGGAA 3' R:5' ACTTCTAGCTCCACCAGGGT 3'	219	60	NM_005508.4
CCR5	F:5' ACCAAGCTATGCAGGTGACAGAG 3' R:5' CGAGCGAGCAAGCTCAGTTTACA 3'	192	64	NM_000579.3
CCR7	F:5' TGTC AAGATGAGGTACGGACG 3' R:5' CACGCAACTTTGAGCGCAACA 3'	709	62	NM_001838.3
GPR1	F:5' GCATCCTGATCTCCAGTAGGCA 3' R:5' TGTGGTGAATGGTGAGCTCC 3'	114	62	NM_005279
CMKLR1	F:5' ATCGTGTGCAAACACTGCAGCG 3' R:5' GCTCTAGGAGGTTGAGTGTGTTGG 3'	130	62	NM_001142343
CCL5	F:5' TCATTGCTACTGCCCTCTGCGCT 3' R:5' AGCAGTCGTCTTTGTCACCCGA 3'	167	60	NM_002985.2
CCL19	F:5' CCAATGATGCTGAAGACTGCTGC 3' R:5' ACGCATCATCCAGAGACTGCA 3'	193	60	NM_006274.2
Chemerin	F:5' TGGGCCTTCCAGGAGACCAGTG 3' R:5' TTCCGGCAGCTTGTCTGCTG 3'	104	62	NM_002889
β-actin	F: 5' CTGGAACGGTGAAGGTGACA 3' R: 5' AAGGGACTTCCTGTAACAATGCA 3'	139	60	BC013835

Prior to performing PCR, pipettes, pipette tips, the bench, and other materials were sterilized. PCR reagents were thawed at room temperature. In order to prepare PCR mixture, a master mix containing Forward and reverse

primers, dNTP mixture, *Taq* DNA polymerase, *Taq* buffer, MgCl₂, and distilled water (dH₂O) was prepared and distributed equally into each PCR tube. The polymerase enzyme was added into the master mix lastly. cDNA (template DNA) for each gene of interest was added separately into each PCR tube, mixed, and placed into the thermal cycler plate (Thermo Scientific, Arktik Thermal Cycler, USA). PCR optimizations were performed by changing the concentration of different PCR reagents (especially the amount of template cDNA or final concentration of MgCl₂) or the annealing temperature or the annealing time. General conditions used for PCRs are given in Table 3.3 and Table 3.4.

Table 3.3. Standard PCR components, volumes, and final concentrations.

Component	Volume	Final Concentration
dH ₂ O	30.7 µl	
Taq Buffer (10X) with (NH ₄) ₂ SO ₄	5 µl	1X
MgCl₂ (25 mM)	5 µl	2.5 mM
dNTP mix (2 mM)	5 µl	0.2 mM
Primer F (5 µM)	1.5 µl	0.15 µM
Primer R (5 µM)	1.5 µl	0.15 µM
Taq DNA Polymerase (5u/µl)	0.3 µl	0.03 u/µl
Template DNA	1 µl	
Final Volume	50 µl	

Table 3.4. Standard PCR thermal cycler program.

Initial denaturation	95°C	5 min	
Denaturation	94°C	30 sec	} 35 cycles
Annealing	Specific for each primer. ¹	30 sec	
Extension	72°C	30 sec	
Final extension	72°C	10 min	

¹ Primers and their annealing temperatures are listed in Table 3.2.

3.3.6. Agarose Gel Electrophoresis

In order to prepare 1% or 2% (w/v) agarose gel, 1 gr or 2 gr agarose was weighted and mixed with 100 mL of 1X TBE buffer. Agarose was melted in microwave oven (Imperial, USA). After moderate cooling, 10 mg/mL ethidium bromide was added to obtain a 250 µg/mL final concentration and poured into a gel casting tray equipped with a comb. After gelling, the comb was removed, gel was put inside the tank, and 1X TBE was added over the gel to completely cover it. 20 µL volume of PCR product was mixed with 6X DNA loading dye (1X final concentration) and loaded into wells. To determine DNA size, 0.5 µg DNA ladder per lane was used. Figure 3.1 shows band sizes (bp) of the DNA markers used. Products were run with 120V constant voltage. At the end of agarose gel electrophoresis, DNA products were observed under UV light using Kodak gel Logic 1500 (Molecular Imaging System-Carestream Health, Inc).

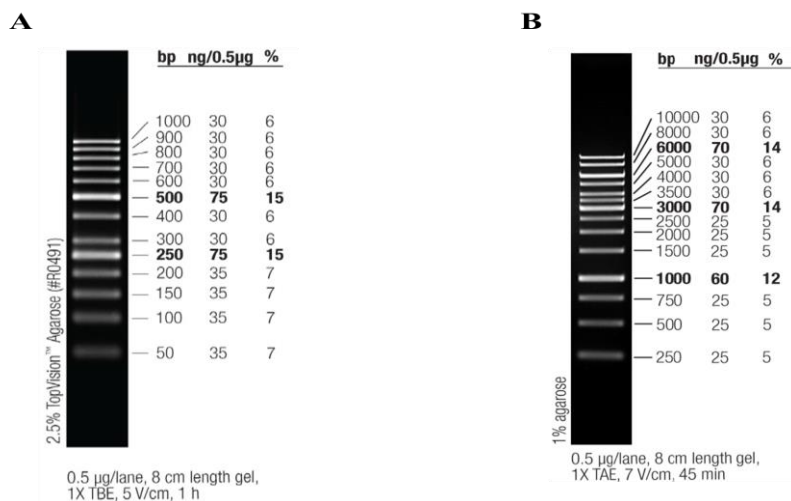


Figure 3.1. **A)** 50 bp DNA ladder, **B)** 1 Kb DNA ladder (Fermentas, Lithuania).

3.3.7. Directional Cloning

For cloning of human CRAM-A and CRAM-B genes into pIRES2-EGFP (BD, USA) eukaryotic expression vector (Figure 3.3), forward and reverse primers containing *NheI* and *XmaI* restriction sites were designed for CRAM-A and CRAM-B genes (Table 3.5). RNA was isolated, as explained in Section 3.3.1, from PBMCs and/or MDA-MB-231 cell line. cDNA was synthesized as described in Section 3.3.4. CRAM-A and CRAM-B coding sequences were amplified by using *Pfu* DNA polymerase with PCR reaction and program as given in Table 3.3 and Table 3.4, respectively. PCR products were run on agarose gel electrophoresis and isolated from the gel.

Table 3.5. Forward and reverse primers, and *NheI* and *XmaI* restriction enzyme digestion sites used in directional cloning of CRAM-A and CRAM-B.

Gene	Forward (F) and Reverse (R) Primer Sequences	Product (bp)	Annealing Temperature (°C)	Gene Bank No.
CRAM-A	F:5' GAGTGAG ^G <u>CTAGC</u> ATGCAGAAATTATGATCTAC 3' <i>NheI</i> R:5' CTCACTC ^C <u>CCGGG</u> TTACACTTCGGTGGAAT 3' <i>XmaI</i>	1106	55	NM_001130910.1
CRAM-B	F:5' GAGTGAG ^G <u>CTAGC</u> AAGATGGCCAATTACACGC 3' <i>NheI</i> R:5' CTCACTC ^C <u>CCGGG</u> TTACACTTCGGTGGAAT 3' <i>XmaI</i>	1070	56	NM_003965.4

Table 3.6. PCR components, volumes, and final concentrations used for the amplification of insert DNA for cloning.

Component	Volume	Final Concentration
dH ₂ O	30.5 µl	
Pfu Buffer (10X)	5 µl	1X
MgSO ₄ (25 mM)	6 µl	3 mM
dNTP mix (2 mM)	5 µl	0.2 mM
Primer F (5 µM)	1 µl	0.1 µM
Primer R (5 µM)	1 µl	0.1 µM
Pfu DNA Polymerase (2.5 u/µl)	0.5 µl	0.025 u/µl
Template DNA	1 µl	
Final Volume	50 µl	

Table 3.7. PCR thermal cycler program.

Initial denaturation	95°C	5 min
Denaturation	95°C	30 sec
Annealing	55°C for CRAM-A, 56°C for CRAM-B.	30 sec
Extension	72°C	30 sec
Final extension	72°C	5 min

} 35 cycles

pIRES2-EGFP Eukaryotic Expression Vector [101]

pIRES2-EGFP vector (Clontech, BD, USA) contains the internal ribosome entry site (IRES) of the encephalomyocarditis virus (ECMV) between the multiple cloning site (MCS) and the enhanced green fluorescent protein (EGFP) coding region (Figure 3.2). This permits both the gene of interest (cloned into the MCS) and the EGFP gene to be translated from a single bicistronic mRNA. pIRES2-EGFP is designed for the efficient selection (by flow cytometry or other methods) of transiently transfected mammalian cells expressing EGFP and the protein of interest. This vector can also be used to express EGFP alone or to obtain stably transfected cell lines without time-consuming drug and clonal selection.

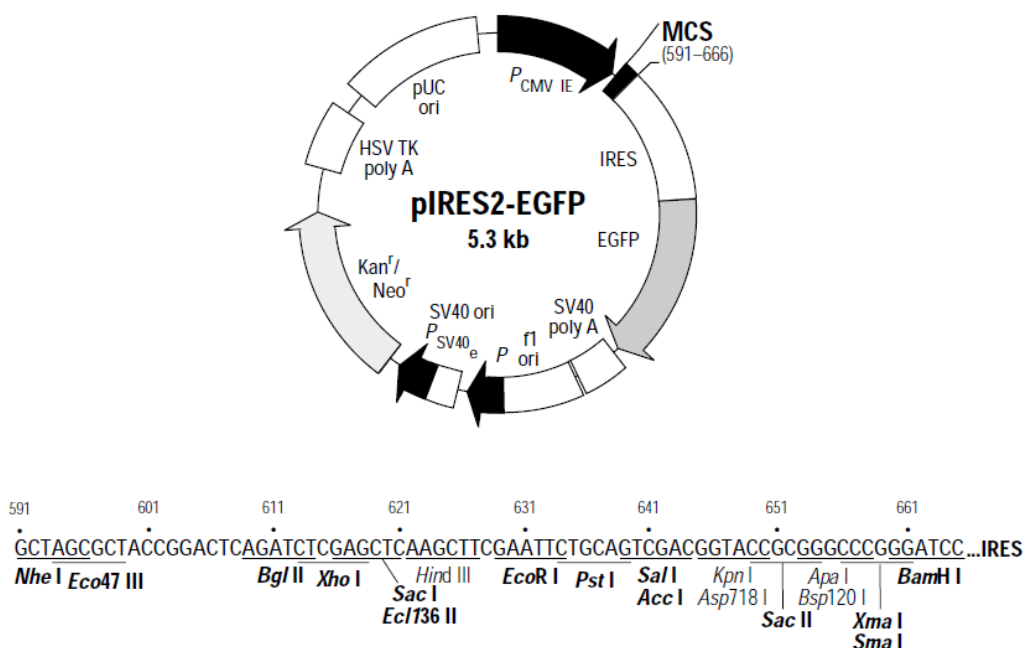


Figure 3.2. Schematic representation of pIRES2-EGFP eukaryotic expression vector and its multiple cloning site map. Taken from Becton, Dickinson and Company [101].

EGFP is a red-shifted variant of wild-type GFP which has been optimized for brighter fluorescence and higher expression in mammalian cells. (Excitation maximum = 488 nm; emission maximum = 507 nm.) EGFP encodes the GFPmut1 variant which contains the double-amino-acid substitution of Phe-64 to Leu and Ser-65 to Thr. The coding sequence of the EGFP gene contains more than 190 silent base changes which correspond to human codon-usage preferences. Sequences flanking EGFP have been converted to a Kozak consensus translation initiation site to further increase the translation efficiency in eukaryotic cells. The MCS in pIRES2-EGFP is between the immediate early promoter of cytomegalovirus (PCMV IE) and the IRES sequence. SV40 polyadenylation signals downstream of the EGFP gene direct proper processing of the 3' end of the bicistronic mRNA. The vector backbone also contains an SV40 origin for replication in mammalian

cells expressing the SV40 T antigen. A neomycin-resistance cassette (Neo^r), consisting of the SV40 early promoter, the neomycin/kanamycin resistance gene of Tn5, and polyadenylation signals from the herpes simplex virus thymidine kinase (HSV TK) gene, allows stably transfected eukaryotic cells to be selected using G418. A bacterial promoter upstream of this cassette expresses kanamycin resistance in *E.coli*. The pIRES2-EGFP backbone also provides a pUC origin of replication for propagation in *E.coli* and an f1 origin for single-stranded DNA production.

Restriction Enzyme Digestion

In order to generate sticky ends at the 5' and the 3' ends of the vector and the insert DNA, *NheI* and *XmaI* restriction enzymes were used in a reaction mixture as shown in Table 3.8.

Table 3.8. Restriction digestion reaction components, volumes, and final concentrations.

Component	Volume	Final Concentration
dH₂O		
Buffer Tango (10X)	4 µl	1X
DNA	500 ng	12.5 ng/µl
NheI (10 u/µl)	2 µl	0.5 u/µl
XmaI (10 u/µl)	4 µl	1 u/µl
Final Volume	40 µl	

Samples were incubated at 37°C for 5 hours. Later, digested products were purified either directly from the tube or from a slice of agarose gel after electrophoresis.

Isolation of DNA from Agarose Gel

For isolation of DNA from agarose gel (Gel Purification Kit, RTA, Turkey), the gel slice containing the amplified gene was cut, placed in a 1.5 mL microcentrifuge tube, and weighed. 4 times gel volume of Solution A was added (e.g: to 100 mg gel slice, 400 μ L Solution A is added). 20 sec vortex was done. Gel was incubated at 60°C for 5-10 min until it was completely melted. 10 μ L Gel Modifier was added and mixed 20 sec by vortex. After the mixture was quickly spun, it was transferred into a spin column in a collecting tube provided by the kit and centrifuged at 10000 x g for 1 min. Collection tube containing the flow-through was discarded and spin column was transferred to a new collection tube. 500 μ L Solution WA was added and centrifuged at 10000 x g for 1 min. The flow-through was discarded, column was put on the same collection tube, and centrifuged at 14000 rpm for 30 sec. The spin column was transferred to a 1.5 mL collection tube. According to the DNA concentration, 50-100 μ L dH₂O was directly added on the membrane and incubated at room temperature for 3 min. Sample was centrifuged at 14000 rpm for 1 min. Spin column was discarded. The elution contained the purified DNA.

Isolation of DNA from PCR Products and Other Enzymatic Reactions

In order to isolate DNA from PCR product and other enzymes, RTA PCR Purification Kit (RTA, Turkey) was used. In a 1.5 mL eppendorf tube, 6 times volume of the sample was added to Solution A (e.g: to 100 μ L sample, 600 μ L Solution A was added) and vortexed well. 200 μ L of ethanol (96-100%) was added and mixed well by vortexing. After a short spin (MiniSpin, eppendorf, Germany), the sample was added into a spin column and centrifuged at 10000 x g for 1 min. The collection tube containing the flow-through was discarded and the column was put on a new collection tube. 500

μL Solution WA was added and centrifuged at 10000 x g for 1 min. The flow-through was discarded, the column was put on the same collection tube, and centrifuged at 14000 rpm for 30 sec. The spin column was transferred to a new 1.5 mL collection tube. According to the DNA concentration, 50-100 μL dH_2O was directly added on the membrane and incubated at room temperature for 3 min. Sample was centrifuged at 14000 rpm for 1 min. Spin column was discarded. The elution contained the purified DNA.

Ligation with T4 DNA Ligase Reaction

In order to obtain an efficient ligation, vector:insert ratio was mixed at 1:3. To calculate the amount of human CRAM-A and CRAM-B coding DNAs (insert), Formula 3.1 was used. Digested and purified insert and vector DNA molecules were ligated by using T4 DNA ligase enzyme (Fermentas, Lithuania) in a reaction mixture (Table 3.9). The positive control of the ligation experiment was the circular empty vector pIRES2-EGFP. Reactions were incubated at room temperature for 15 min.

(3.1)

$$\text{Insert DNA amount (ng)} = \frac{\text{Vector amount (ng)} \times \text{Insert length (kb)} \times \text{Vector:Insert}}{\text{Vector length (kb)}}$$

Table 3.9. Ligation reaction components, volumes, and final concentrations.

Component	Volume	Final Concentration
dH₂O		
T4 DNA Ligase Buffer (10X)	2.5 μ l	1X
Insert DNA	240 ng	9.6 ng/ μ l
Vector DNA	80 ng	3.2 ng/ μ l
T4 DNA Ligase (3 u/μl)	1.2 μ l	0.144 u/ μ l
Final Volume	25 μ l	

3.3.8. TA Cloning

In order to clone human CRAM-A and CRAM-B genes into pcDNA3.1/CT-GFP-TOPO[®] (Invitrogen, USA) eukaryotic expression vector (Figure 3.4), TOPO[®] TA cloning was performed. Primers were designed (Table 3.10) and CRAM-A and CRAM-B inserts were amplified by RT-PCR as described in Section 3.3.7. GFP Fusion TOPO[®] TA Cloning provides a highly efficient, 5-minute, one-step cloning strategy ("TOPO[®] Cloning") for the direct fusion of *Taq* polymerase-amplified PCR products to the green fluorescent protein (GFP). No ligase, post-PCR procedures, or PCR primers containing specific sequences are required. Once cloned, analyzed, and transfected, the GFP fusion protein will express directly in mammalian cell lines. In this cloning, C-terminal (CT-GFP Fusion TOPO[®] TA Expression Kit) was used to provide creation of C-terminal expression of GFP fusion.

Table 3.10. Primers used in TOPO[®] TA cloning.

Gene	Forward (F) and Reverse (R) Primer Sequences	Product (bp)	Annealing Temperature (°C)	Gene Bank No.
CRAM-A	F:5' GCAATGCAGAAATTATGATCTACACCCG 3' R:5' GCACTTCGGTGGAATGGTCAG 3'	1082	64	NM_001130910.1
CRAM-B	F:5' GCAATGGCCAATTACACGCTGG 3' R:5' GCACTTCGGTGGAATGGTCAG 3'	1038	60	NM_003965.4

The vector pcDNA3.1/CT-GFP-TOPO used in this cloning was supplied linearized by the company. In this cloning, also named as TA cloning, the linearized vector has single overhanging 3' deoxythymidine (T) residues. *Taq* DNA polymerase used in this cloning has the capacity to add a single deoxyadenosine (A) to the 3' ends of PCR products. This allows the efficient ligation of PCR products with the vector [102].

In this cloning, topoisomerase I is the enzyme that binds to the vector's duplex DNA and cleaves the phosphodiester backbone after 5'-CCCTT. The energy from the broken phosphodiester backbone is conserved by formation of a covalent bond between the 3' hydroxyl of the cleaved vector strand and the tyrosyl residue (Tyr-274) of the topoisomerase I. The phospho-tyrosyl bond between the vector and the enzyme can be attacked by the 5' phosphate of the PCR strand, releasing topoisomerase, and efficiently cloning the PCR product into the vector (Figure 3.3). In this cloning, GFP reporter protein will be expressed as attached to the carboxyl terminal, CT, of the insert DNA.

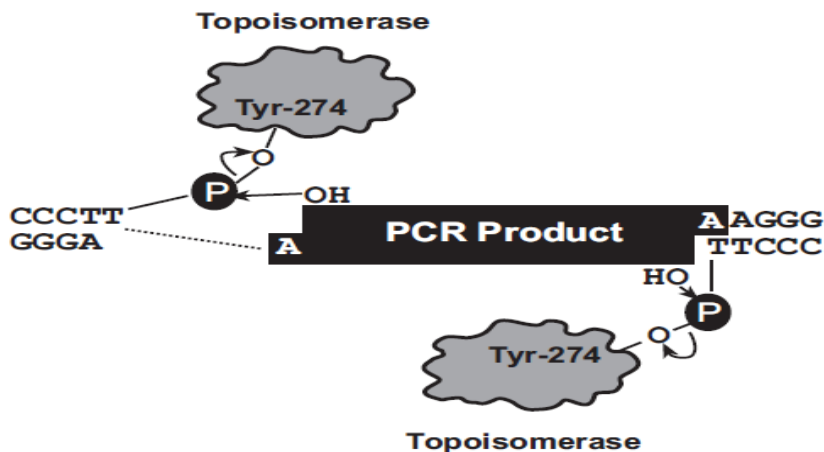


Figure 3.3. Topoisomerase activity in TOPO[®] cloning. Taken from CT-GFP Fusion TOPO[®] TA Expression Kit Protocol, Invitrogen, USA.

In order to perform TA cloning, 3 μL of PCR product, 1 μL of Salt Solution (supplied by the kit), 2 μL sterile water, and 1 μL of pcDNA3.1/CT-GFP-TOPO[®] vector were mixed and incubated at room temperature (22-23°C) for 3 min. The mixture was then placed on ice. The TOPO[®] cloning reaction mixture was added into a vial (50 μL) of one shot[®] TOPO10 chemically competent *E.coli*, gently mixed, and incubated on ice for 20 min. Cells were heat-shocked for 30 seconds at 42°C and immediately transferred to ice. 250 μL of room temperature SOC medium (Life technologies, USA) was added into the cells and incubated in 200 rpm shaker at 37°C for 1 hour. 25-200 (100) μL of the transformed cells was spread on a selective antibiotic (Ampicillin, 100 $\mu\text{g}/\text{mL}$) petri dish and incubated at 37°C overnight. Colonies were selected and plasmids were isolated.

pcDNA3.1/CT-GFP-TOPO[®] Eukaryotic Expression Vector [102]

The schematic representation of pcDNA3.1/CT-GFP-TOPO[®] eukaryotic expression vector is shown in Figure 3.4. The vector was supplied linearized between base pairs 953 and 954 (TOPO[®] cloning site). Human

cytomegalovirus (CMV) immediate-early promoter/enhancer permits efficient, high-level expression of the recombinant protein. T7 promoter allows for *in vitro* transcription in the sense orientation and sequencing through the insert. TOPO® cloning site allows insertion of the PCR product and its fusion with GFP. GFP reverse priming site permits sequencing of the insert from GFP into the insert. GFP open reading frame (ORF) allows fusion of GFP to the C-terminus of the PCR product. BGH reverse priming site permits sequencing through the insert. Bovine growth hormone (BGH) polyadenylation signal provides the efficient transcription termination and polyadenylation of mRNA. f1 origin allows rescue of single-stranded DNA. SV40 promoter and origin allows efficient and high-level expression of the neomycin resistance gene in cells expressing the SV40 large T antigen. Neomycin resistance gene promotes selection of stable transfectants in mammalian cells. SV40 polyadenylation signal allows efficient transcription termination and polyadenylation of mRNA. pUC origin promotes high-copy number replication in *E.coli*. Ampicillin resistance gene provides selection of vector in the bacteria.

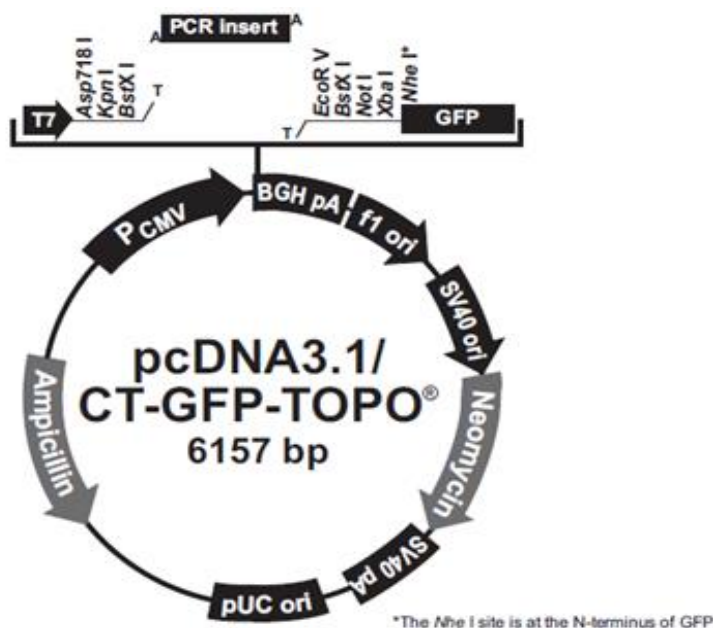


Figure 3.4. The features of the pcDNA3.1/CT-GFP-TOPO[®] vector diagram. Taken from CT-GFP Fusion TOPO[®] TA Expression Kit Protocol, Invitrogen, USA.

3.3.9. Preparation of Competent Bacteria and Heat Shock Transformation

Preparation of Competent *E.coli* DH5a Bacteria

To 3 mL LB broth, 1 colony of DH5a *E.coli* was inoculated and incubated at 30°C for 18 hours in a shaker (Grant, Germany) at 200 rpm. After the incubation, 400 µL of the overnight bacterial culture was taken and inoculated into 50 mL LB broth in Erlenmeyer flask and incubated at 37°C shaker nearly for 2 hours. During this incubation time 1 mL of the bacterial culture was taken and added into a spectrophotometry cuvette and measured at 600 nm wavelength (Molecular Devices, USA). This procedure was done until the OD of the bacterial culture reached to 0.4. The blank was LB broth. As soon as the OD reached to 0.4, bacterial culture was incubated on ice at

4°C for 2 hours. The bacterial culture was poured into a 50 mL falcon tube and centrifuged at 3000 rpm for 10 min at 4°C (Jouan MR22, USA). Supernatant was discarded at 4°C and the pellet was very gently resuspended with 1 mL of the competent solution explained in section 3.2. 24 mL of the competent solution was added, mixed, and incubated on ice in 4°C for 45 min. The sample was centrifuged at 2500 rpm for 15 min at 4°C. Supernatant was discarded and the pellet was very gently resuspended with 1.5 mL of the competent solution. In order to prepare glycerol stocks of the competent bacteria, 800 µL of the competent DH5a *E.coli* were gently mixed with 200 µL of 80% glycerol. The stocks were aliquoted (200 µL/each tube) and stored at -86°C.

Heat Shock Transformation

5 µL of ligated pCRAM-A/B-IRES2-EGFP plasmids or positive (circular vector) or negative (linear vector ligated without insert DNA) were taken, completed to 50 µL with dH₂O, added into 150 µL ice-thawed competent DH5a *E.coli*, and incubated at 37°C water bath shaker for 5 min. 450 µL LB broth was added to the mixtures and incubated at 37°C for 1,5 hours at 200 rpm. Then, ligated plasmids, positive control, and negative control empty vector-transformed bacterial mixtures were spread on 50 µg/mL kanamycin-containing LB agar petri dishes and incubated at 37°C overnight.

In order to transform bacterial cells with pcDNA3.1/CRAM-A/B-CT-GFP-TOPO recombinant plasmids, 25 µL of the ligation product was added into a 50 µL vial of One Shot® Top10 chemically competent *E.coli* (Invitrogen, USA), gently mixed, and incubated on ice for 20 min. Bacteria were heat-shocked at 42°C for 30 sec and immediately transferred on ice. 250 µL of room temperature SOC medium was added and bacteria were incubated at 37°C, 200 rpm shaker for 1 hour. 100-200 µL from each transformation was

spread on a pre-warmed selective antibiotic (Ampicillin, 100 µg/mL) plate and incubated at 37°C overnight.

Minipreps Plasmid Purification

LB broth (3 mL/tube) was added into 15 mL falcon tubes and was supplemented with kanamycin (50 µg/mL final volume) or ampicillin (100 µg/mL final volume). One colony of transformed DH5a or Top10 *E.coli* was taken and cultured in each falcon. Falcon tubes were incubated in 200 rpm shaker overnight. Meanwhile, bacteria were also spread on an agar plate as the experiment's back-up control. Plates were also incubated at 37°C incubator overnight.

Minipreps plasmid purification was performed using Wizard[®] Minipreps (Promega, USA). Overnight bacteria grown in liquid condition were harvested by centrifugation at 11000 rpm for 2 min in 1.5 mL eppendorf tubes. 200 µL in order of Cell Resuspension Solution, Lysis Solution, and Neutralization Solution were added onto the pellets and mixed. 7 min centrifugation was done at 11000 rpm and purification was continued with supernatants. The kit-provided mini-columns were placed on 2 mL eppendorf tubes and 2.5 mL injectors were connected to the columns. 1 mL Miniprep DNA Purification Resin solution was added into the injectors and supernatants were added onto resin. Pistons were put on injectors and slowly pressed, allowing mixtures to pass the columns. 2 mL wash solution was added into injectors and passed through columns same as for resin. Columns were centrifuged at 11000 rpm for 2 min. 50 µL of 57°C-heated dH₂O was directly added onto the membranes inside the columns and incubated in room temperature for 1 min. By centrifugation at 11000 rpm for 20 seconds, plasmids were eluted from the columns and stored at -20°C.

Midipreps Plasmid Purification

Midipreps plasmid purification was performed by using QIAGEN plasmid midi kit (QIAGEN, USA). Into a 50 mL LB broth containing kanamycin or ampicillin, 150 μ L of the overnight grown bacteria was added and incubated at 37°C in 200 rpm shaker overnight.

The bacteria culture was poured into a 50 mL falcon tube and centrifuged at 6000xg for 15 min at 4°C. Meanwhile, a cap was attached to a QIAfilter Cartridge. Supernatant was discarded and the pellet was resuspended with 6 mL Buffer P1. 6 mL Buffer P2 was added and the tube was capped immediately to prevent acidity. The mixture was mixed and turned blue. It was incubated at room temperature for 3 min. 6 mL Buffer P3 was added to the mixture and mixed. The mixture was added into the QIAfilter Cartridge and incubated at room temperature for 10 min. Meanwhile, the “Midi Tip” was placed on a 50 mL falcon tube. 4 mL Buffer QBT was added into the “Midi Tip” and pressed by an injector. The mixture passed and plasmids stayed on the filter. Later, 20 mL Buffer QC was added into the “Midi Tip” and incubated until all the buffer passed. The “Midi Tip” was placed on a 50 mL falcon tube. 5 mL Buffer QF (elution buffer) was added into the “Midi Tip” and incubated until the buffer passed by gravity flow. 3.5 mL isopropanol was added to the eluted product, mixed, and incubated at room temperature for 5 min. A “QIA precipitator module” was placed on a 50 mL falcon tube. A 20 mL syringe was attached on the module. The eluted product was poured into the syringe and pressed by piston. Flow-through was discarded. In order to fix plasmids, 2 mL of 70% ethanol was added into the syringe and pressed. A 5 mL syringe was attached on the module. 1 mL dH₂O was added into the syringe and pressed into a 1.5 mL eppendorf tube. The elution contained the isolated plasmids.

3.3.10. Confirmation of Constructed Recombinant Clones

By PCR: The constructed recombinant clones pCRAM-A-IRES2-EGFP, pCRAM-B-IRES2-EGFP, pcDNA3.1/CRAM-A-CT-GFP, or pcDNA3.1/CRAM-B-CT-GFP were confirmed by using PCR as described in Section 3.3.5. Specific primers (Table 3.2) and PCR conditions (Table 3.3) used for cloning was also used in this PCR confirmation.

By Restriction Enzyme Digestion: The constructed recombinant clones pCRAM-A-IRES2-EGFP and pCRAM-B-IRES2-EGFP were confirmed by *NheI* and *XmaI* restriction digestion enzymes as described in Section 3.3.7.

The constructed recombinant clones pcDNA3.1/CRAM-A-CT-GFP and pcDNA3.1/CRAM-B-CT-GFP were confirmed by *MluI* restriction digestion enzyme. *MluI* restriction digestion enzyme was also used to confirm the correct orientation (5'-3') of CRAM-A/B inserts in pcDNA3.1/CT-GFP vector. The restriction digestion reaction mixture is shown in Table 3.11. The restriction digestion reaction mixture was incubated at 37°C for 3.5 hours.

Table 3.11. *MluI* restriction digestion reaction mixture components, volumes, and final concentrations.

Component	Volume	Final Concentration
dH₂O	Completed to 20 μ l	
Buffer R (10X) with BSA	2 μ l	1X
MluI (10 u/μl)	2 μ l	1 u/ μ l
Plasmid (300 ng/μl)	150 ng	7.5 ng/ μ l
Final Volume	20 μ l	

MluI restriction digestion enzyme cuts the recombinant plasmid pcDNA3.1/CRAM-A/B-CT-GFP at two points. Beside the correct orientation of the insert, in TA cloning, the insert also has the tendency to bind to the vector in the opposite direction (3'-5'). Upon *MluI* restriction digestion, the correct insert orientation generates three bands with 5000, 1199, and 985 bp length for CRAM-A insert. Upon *MluI* restriction digestion, the correct insert orientation generates three bands with 5000, 1199, and 941 bp length for CRAM-B insert (Figure 3.5).

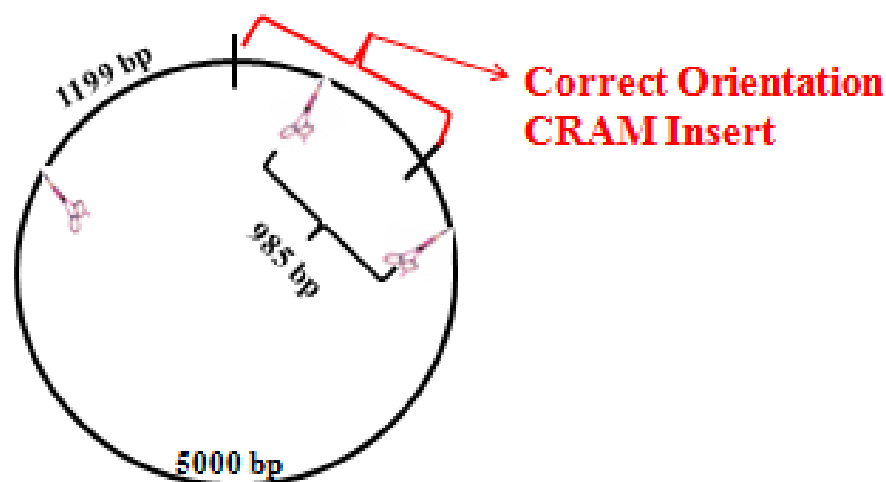


Figure 3.5. *MluI* restriction digestion points (designated with scissors) on the recombinant DNA containing CCRL2 insert. The digestion of the plasmid with correct insert orientation generates three DNA fragments (approximately 1199 bp, 985 bp, 5000 bp).

By DNA Sequencing Analysis: Cloned human pCRAM-A-IRES2-EGFP and pCRAM-B-IRES2-EGFP recombinant constructs were sequenced and confirmed using DNA sequencing by using the sense 5'-ACTCCGCCCCATTGACGCAAATG-3' and the anti-sense 5'-

AGACAAACGCACACCGGCCT-3' sequencing primers for pIRES2-EGFP by lontek biotechnology company (Istanbul, Turkey).

Cloned human pcDNA3.1/CRAM-A-CT-GFP-TOPO and pcDNA3.1/CRAM-B-CT-GFP-TOPO recombinant constructs were sequenced by using 5'-TAATACGACTCACTATAGGG-3' forward sequencing primer (T7 sequencing primer) and 5'-GGGTAAGCTTTCCGTATGTAGC-3' reverse sequencing primer (GFP reverse primer) by lontek biotechnology company (Istanbul, Turkey).

3.4. Cell Culture

3.4.1. Culture of Cell Lines and Cells Isolated from Peripheral Blood

Human embryonic kidney, HEK293T, cell line was cultured in full high glucose DMEM.

MCF-12A normal breast epithelial cell line was cultured in full DMEM-F12; MCF-7, MDA-MB-231, MDA-MB-468, and BT-474 breast cancer cell lines were cultured in full DMEM with 1 g/L Glucose; SK-BR-3 in full McCoy's 5A medium; T-47D in full RPMI supplemented with 0.1% insulin; ZR-75-1 and HCC38 in full RPMI media. PBMCs were also cultured in full RPMI medium. All cell lines and PBMCs were incubated at 37°C, 5% CO₂ in a humidified incubator (Thermo Scientific, USA).

3.4.2. Thawing Cell Lines

Into a small beaker 30 mL dH₂O, warmed to 37°C, was added. Cell line stock was removed from liquid nitrogen tank and put into 37°C water. By using a Pasteur pipette, a small volume of full medium was added into the cryovial, mixed gently and added into a 50 mL falcon tube containing full

medium. Later, this cell mixture was added into a cell culture flask and incubated at 37°C. When the cells reached 80% confluency, they were passaged and new full medium was added.

3.4.3. Passage of Adherent Cells with Trypsin-EDTA

First, the culture medium was removed, 1X PBS was added onto the cells to cover them, and washed several times. Then, cells were covered with trypsin-EDTA solution (1:250). After 3-5 min incubation at 37°C, the culture flask was removed from the incubator and tapped with palm to detach all cells. The flask was examined under an inverted microscope to be sure that all cells left the growth surface. Full medium was added to inactivate trypsin. The cell culture was mixed by pipette to separate cells from each other.

3.4.4. Cell Counting

A cover slip was put on a hemacytometer (Fuchs Rosenthal, USA). 10 µL of the cell suspension obtained by trypsinization of adherent cell lines or the PBMCs was mixed with 10 µL trypan blue and added to the Neubauer hemacytometer with capillary effect. Cells present on four 4x4 squares of the hemacytometer were counted. Mean value of these cells were calculated by using Formula 3.2 to estimate the cell number in each mL of the suspension. Dilution factor was usually 2 because of 1:1 dilution with trypan blue stain.

(3.2)

Cell Count= Average number of cells in one large square x Dilution factor x 10⁴

3.4.5. Cryopreserving Cell Lines

Cell suspensions (2 mL) obtained by trypsinization of an 80% confluent culture were added into a 50 mL falcon tube. Heat inactivated FBS (4 mL) and full medium (3 mL) were added into the tube and mixed. Lastly, 1 mL dimethyl sulfoxide (DMSO) was added, mixed gently, and 1 mL of the final mixture was added into cryovials. Tubes were put in the Mr. Frosty™ freezing container and incubated at -86°C for 3 hours. Cryovial tubes were stored in liquid nitrogen tanks.

3.4.6. Stimulation of PBMCs and Breast Cancer Cell Lines

LPS (1 µg/mL) or IFN-γ (150 ng/mL) were added into PBMCs (87000 cells/mL) or breast cancer cell cultures (4×10^5 cells/7 mL in T25 cell culture flasks) and incubated (stimulated) at 37°C for 24 hours.

3.4.7. Liposomal Transfection

Liposomal transfection was done by using Lipofectamine2000™ (Invitrogen, USA). One day before transfection process, 5×10^5 cells per well were cultured in full medium in a 6-well plate. On the day of transfection, 37°C 250 µL serum-free medium containing recombinant plasmid or empty vector DNA was prepared. According to the plasmid DNA:liposome ratio (1µg:3µL), Lipofectamine reagent was added to serum-free medium in a separate eppendorf tube with a final volume of 250 µL, mixed gently, and incubated at room temperature for 5 min. Plasmid DNA and liposome suspensions were mixed gently and incubated at room temperature for 20 min. Meanwhile, medium was removed from the cells cultured in 6-well plate wells and 1.5 mL serum-free medium was added slowly. The transfection mixture was drop-wise added onto the cells. Plate was gently mixed to let the

mixture reach every point on the cells. Plate was incubated at 37°C, 5% CO₂ for 5 hours. Then, a mixture of FBS, L-glutamine, and penicillin-streptomycin was gently added to the cells and mixed to complete the media and terminate transfection process. Plate was incubated at 37°C, 5% CO₂ for 48 hours. Then, the transfected cells were harvested and analyzed for transfection efficiency and protein expression using flow cytometry.

3.4.8. Fluorescence Microscopy

After the liposomal transfection, cells were harvested and cultured on chamber slides (Lab-Tek® Chamber Slide™ System 177380 2 Well Glass Slide, USA) overnight at 37°C. Culture medium was removed. In order to fix the cells, 4% paraformaldehyde (PFA) was added onto the cells and incubated in room temperature for 2-3 min. Cells were slightly washed with 1X PBS. Cells were covered with 10 mg/mL of 4',6-diamidino-2-phenylindole (DAPI) DNA stain, covered with lamel, and immediately observed under fluorescence microscopy. Fluorescence microscopic observations were performed in Hacettepe University, Department of Histology and Embryology.

3.5. Immunological Assays

3.5.1. Flow Cytometry

In order to harvest the adherent cells for the flow cytometric analysis, culture medium was removed and cells were covered with 1X PBS. Cells were detached from the surface by using a scraper or by flushing with a Pasteur pipette, filtered from a 47 µm mesh into a 5 mL tube. Cells were centrifuged at 2000 rpm for 5 min. Supernatant was discarded, 200 µL of 1X PBS was added and mixed by vortexing. Appropriate amounts of monoclonal antibodies were added into the tubes and mixed by pipeting and by vortex.

List of used antibodies and their amounts is given in Table 3.12. Cells were incubated at 4°C for 40 min. Then, 1-2 mL of 1X PBS was added onto the cells and centrifuged at 2000 rpm for 5 min. Supernatant was discarded. 300 µL of 1X PBS was added on the cell pellet, mixed by vortex, and analyzed by using FACS Aria II flow cytometer (BD, USA). In these analyzes, isotype staining was used as the experimental control. Isotype antibody is non-specific for the molecule of interest, so positive cells can be compared with the control. The percentage of positive cells was calculated by comparison with the appropriate isotype-matched control antibodies. Mean fluorescent intensity (MFI) values were also calculated for at least three independent analyses.

Table 3.12. Antibodies used for flow cytometric analyses.

Antibody	Clone	Supplier	Fluorochrome	Volume per Test
anti-CCRL2 (recognizes both CRAM-A and B)	152254	R&D, USA	APC	10 μ l (0.25 μ g/100 μ l)
IgG1, κ Isotype	MOPC-21	BioLegend, USA	APC	5 μ l (0.125 μ g/100 μ l)
anti-CD3 ¹	SK7	BD, USA	FITC	30 μ l
anti-CD16 ¹	B73.1		PE	
anti-CD56 ¹	NCAM16.2		PE	
anti-CD45 ¹	2D1		PerCP	
anti-CD19 ¹	SJ25C1		APC	
anti-CD4 ²	SK3	BD, USA	FITC	25 μ l
anti-CD8 ²	SK1		PE	
anti-CD3	17A2	R&D USA	APC	25 μ l (0.2 μ g/100 μ l)
anti-CD13	L138	BD, USA	PE	25 μ l
anti-CD14	M5E2	BD, USA	FITC	25 μ l
anti-CD66b	G10F5	BD, USA	FITC	25 μ l

^{1, 2} These antibodies were supplied in a cocktail.

In addition to immunophenotyping analyses, Ca²⁺ mobilization with FuraRedII and GFP expression were also evaluated by flow cytometry.

3.5.2. Ca²⁺ Mobilization Assay

The fluorescent probe FuraRedII was used for the determination of intracellular Ca²⁺ mobilization. As this dye binds intracellular Ca²⁺ ions, a decrease in the fluorescence intensity can be measured by flow cytometry

[103]. In this analysis, HEK293T cells transfected with control (empty) pIRES2-EGFP vector or recombinant constructs carrying CRAM-A/CRAM-B cDNA inserts were incubated with 6 μ M final concentration of FuraRedII reagent for 30 min at 37°C in the dark. After the incubation, cells were washed with serum-free culture medium, centrifuged at 2000 rpm for 5 min, supernatant was discarded, cells were resuspended at 1×10^6 cells/mL with 1X PBS, and placed on ice. Meanwhile, the flow cytometry was adjusted to 488 nm, at PerCP vs. green channel (GFP) at 37°C. Cells were started to be read by flow cytometry for 3 min, the device was paused, and CCRL2's specific chemokine ligands (0.4 μ g/mL rhCCL5, 0.1 μ g/mL rhCCL19, and 20 ng/mL rhchemerin) were added onto the cells. In order to observe whether there is a change in the intracellular Ca^{2+} between the absence and the presence of ligands, the cells were continued to be read for 4 min and the device was paused again. Ionomycin Ca^{2+} ionophore (2 μ g/mL) was used as the experimental positive control. After the addition of ionomycin, cells were read for another 3 min. The change in FuraRedII fluorescence was plotted against time and MFI values were also determined.

3.5.3. Analysis of CCRL2 Binding Capacity of 152254 mAb

In order to analyze the capacity of anti-hCCRL2 mouse antibody (mAb) with the clone number 152254 to recognize CCRL2 receptor in the presence of specific chemokine ligands, HEK293T cells transfected with control (empty) pIRES2-EGFP vector or recombinant constructs carrying CRAM-A/CRAM-B cDNA inserts were incubated with rhCCL5 (0.6 μ g/mL), rhCCL19 (0.16 μ g/mL), or rhChemerin (20 ng/mL) in the presence of the APC-labeled antibody on ice for 60 min, washed with 1XPBS analyzed by flow cytometry, and the difference in MFI values was observed.

3.5.4. Receptor Internalization Analysis

In this assay, cells were divided into four groups, each group containing four tubes for control, rhCCL5 (0.6 µg/mL), rhCCL19 (0.16 µg/mL), and rhChemerin (20 ng/mL). Cells (10^5 cells/100 µL) were added into each tube and incubated on ice. Chemokine ligands were added into each corresponding tube. The first group (control) was held on ice during the entire assay. The second group was incubated at 37°C for 10 min. The third group was incubated at 37°C for 30 min. The fourth group was incubated at 37°C for 60 min. After the completion of each group's incubation time, they were immediately replaced on ice. Then, the cells were labeled with APC-labeled anti-hCCRL2 mAb on ice as described in Section 3.5.3, and analyzed by using flow cytometry.

3.5.5. Enzyme-Linked Immunosorbent Assay (ELISA)

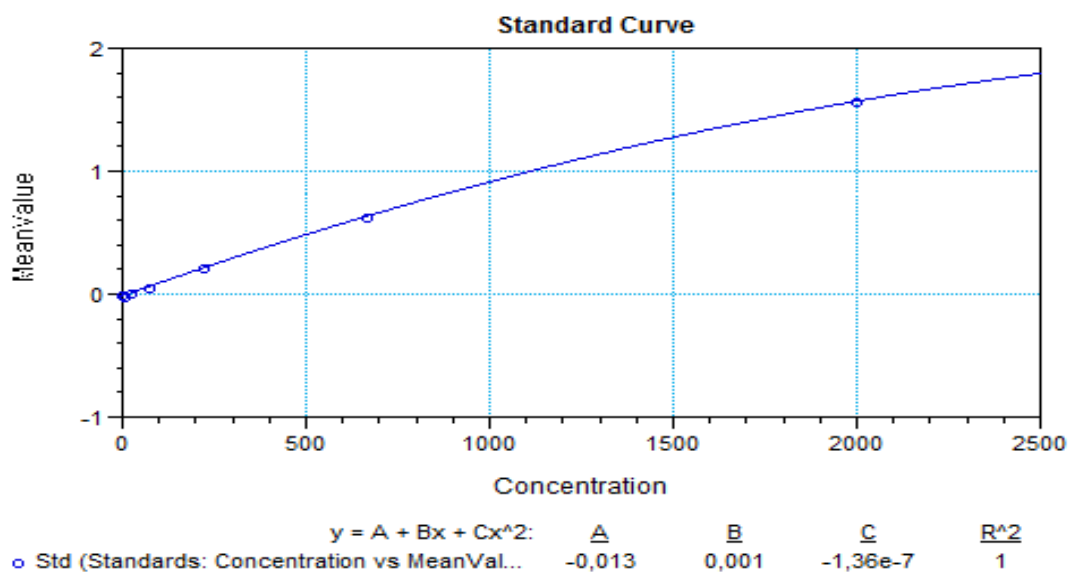
HEK293T cells or BT-474 breast cancer cells transfected with the control (empty) pIRES2-EGFP vector or the recombinant construct carrying CRAM-A cDNA insert were cultured as 5×10^4 cells/well in full media in 96-well plates overnight at 37°C. Cells were incubated with control isotypic IgG mAb or unconjugated anti-human CCRL2 (clone: 152254) for 15 min at 37°C. The ligands (rhCCL5, 2 ng/mL; rhCCL19, 0.5 ng/mL; or rhChemerin, 2 ng/mL) were added into corresponding wells and incubated for 20 min at 37°C. Then, the cell culture media was collected from each well and centrifuged at 2000 rpm for 5 min at 4°C. The supernatants were collected and stored at -86°C until the CCL5 (RANTES) and CCL19 (MIP-3 beta) ELISA assays were performed.

ELISA assay kits were used according to the manufacturer's instructions (RayBiotech, USA). Briefly, 96-well plates coated with anti-human CCL5 or anti-human CCL19 antibodies were provided by the kit. All

reagents and samples were brought to room temperature (18-25°C) before use. If the samples needed to be diluted, 1X Assay Diluent B (Item E) was used for dilution of culture supernatants. Assay Diluent B was diluted 5-fold with distilled water. For preparation of standards, standards (recombinant human RANTES or recombinant human MIP-3 beta) (Item C) were briefly spun. 1X Assay Diluent B was added into the standard vial (Item C) to prepare a 50 ng/mL standard and mixed. 40 µL RANTES or MIP-3 beta standard from the vial of Item C was added into a tube with 960 µL of 1X Assay Diluent B to prepare a 2000 pg/mL stock standard solution. 400 µL of 1X Assay Diluent B was pipetted into each tube. The stock standard solution was used to produce a dilution series. Each tube was mixed thoroughly before the next transfer. 1X Assay Diluent B served as the zero standard (0 pg/mL). If the Wash Concentrate (Item B) contained visible crystals, it was warmed to room temperature and mixed gently until dissolved. 20 mL of Wash Buffer Concentrate was diluted by distilled water to yield 400 mL of 1X Wash Buffer. The Detection Antibody (Item F) was briefly spun before use. 100 µL of 1X Assay Diluent B was added into the vial to prepare a detection antibody concentrate and mixed. The detection antibody concentrate was diluted 80-fold with 1X Assay Diluent B for use in assay procedure. The HRP-Streptavidin concentrate vial (Item G) was briefly spun before use. HRP-Streptavidin concentrate was diluted 300-fold with 1X Assay Diluent B. All standards and samples were run in duplicate. 100 µL of each standard and 100 µL of each sample were added into appropriate wells. Plates were covered and incubated for 2.5 hours at room temperature with gentle shaking. The solution was discarded and wells were washed 4 times with 1X Wash Solution. Wash was done by filling each well with Wash Buffer (300 µL) using autowasher. After each wash, any remaining Wash Buffer was removed by tapping for good performance. 100 µL of 1X biotinylated antibody was added to each well, covered, and incubated for 1 hour at room temperature with gentle shaking. The solution was discarded and again

washed as described above. 100 μ L of HRP-Streptavidin solution was added to each well. Plates were covered and incubated for 45 min at room temperature with gentle shaking. The solution was discarded and again washed as described before. 100 μ L of 3,3',5,5'-tetramethylbenzidine (TMB) in buffered solution (TMB one-step substrate reagent) was added to each well. Plates were covered and incubated for 30 min at room temperature in the dark with gentle shaking. 50 μ L of Stop Solution was added to each well and immediately read at 450 nm. In order to quantify the amount of chemokines, standard curves were drawn for CCL5 and CCL19 (Figure 3.6 A and B).

A)



B)

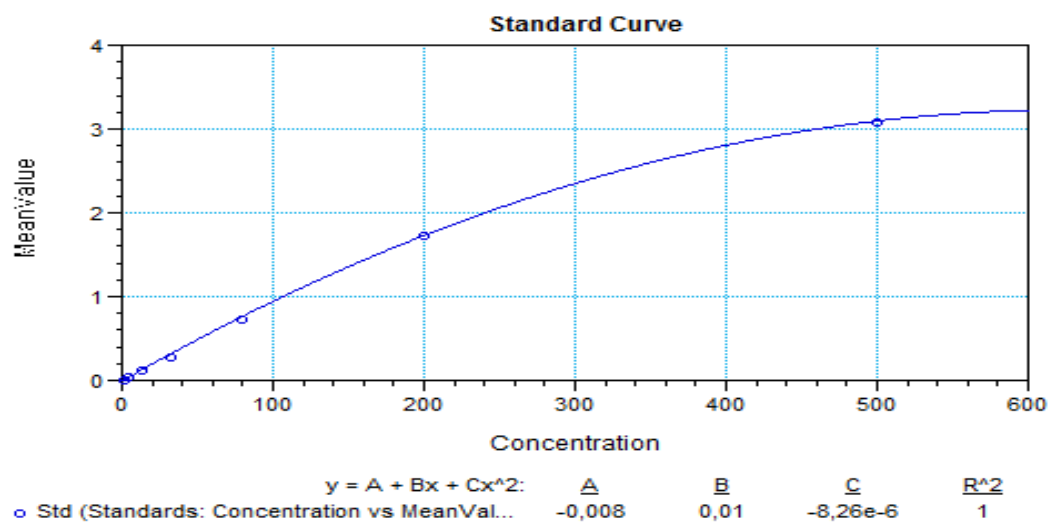


Figure 3.6. Standard curves obtained for **A)** CCL5 and **B)** CCL19 ELISAs.

3.6. Cell Isolation and Sorting

3.6.1. Isolation of Lymphoid Cells

In order to isolate peripheral blood mononuclear cells (PBMCs), peripheral blood was taken from healthy volunteers. 2-3 mL RPMI 1640 was mixed with the blood. 3 mL Ficoll 1077 was added into the bottom of a 15 mL falcon tube. Blood was added onto Ficoll by a Pasteur pipette slowly flushing against the tube wall. Tubes were centrifuged (Thermo Scientific Suprafuge 22, Germany) at 1700 rpm (400xg) for 25 min. PBMCs were collected using a Pasteur pipette, put into a 50 mL falcon tube, washed with 1X PBS, and centrifuged at 2000 rpm for 5 min. Supernatant was discarded and pellet was resuspended with 1 mL 1X PBS. In order to isolate NK and B lymphocytes, PBMCs were labeled with 30 μ L anti-CD45-PerCP, anti-CD3-FITC, anti-CD16/CD56-PE, and anti-CD19-APC antibody cocktail. In order to isolate helper T cells and cytotoxic T cells, PBMCs were labeled with 25 μ L anti-CD3-APC, anti-CD4-FITC, and anti-CD8-PE antibody cocktail (Table 3.12). PBMCs were incubated with antibodies at room temperature for 30 min in dark. After completion of the incubation, 2 mL full RPMI was added into the tubes and filtered using 70 micron sterile strainers (Corning, USA) to remove any aggregates.

In the flow cytometric gating strategy, initially, lymphocytic cells were gated according to their side scatter (SSC) and forward scatter (FSC) properties (region P2, Figure 3.7A). Then, for the isolation of CD3⁻CD19⁻CD16/56⁺ NK cells (region P4) and CD3⁻CD19⁺CD16/56⁻ B lymphocytes (region P5), CD45⁺ leukocytes were gated (region P3) (Figure 3.7B). For the isolation of CD3⁺CD4⁺CD8⁻ helper (region Q1) and CD3⁺CD4⁻CD8⁺ cytotoxic T cells (region Q4), CD3⁺ T lymphocytes were gated (region P6) (Figure 3.7C). Isolation of the targeted cell types was performed by Fluorescence activated cell sorting (FACS) on FACS Aria II flow cytometer. Later, isolated

lymphocytes' purity was analyzed by post-sort analysis on flow cytometry (Figure 3.7B and C).

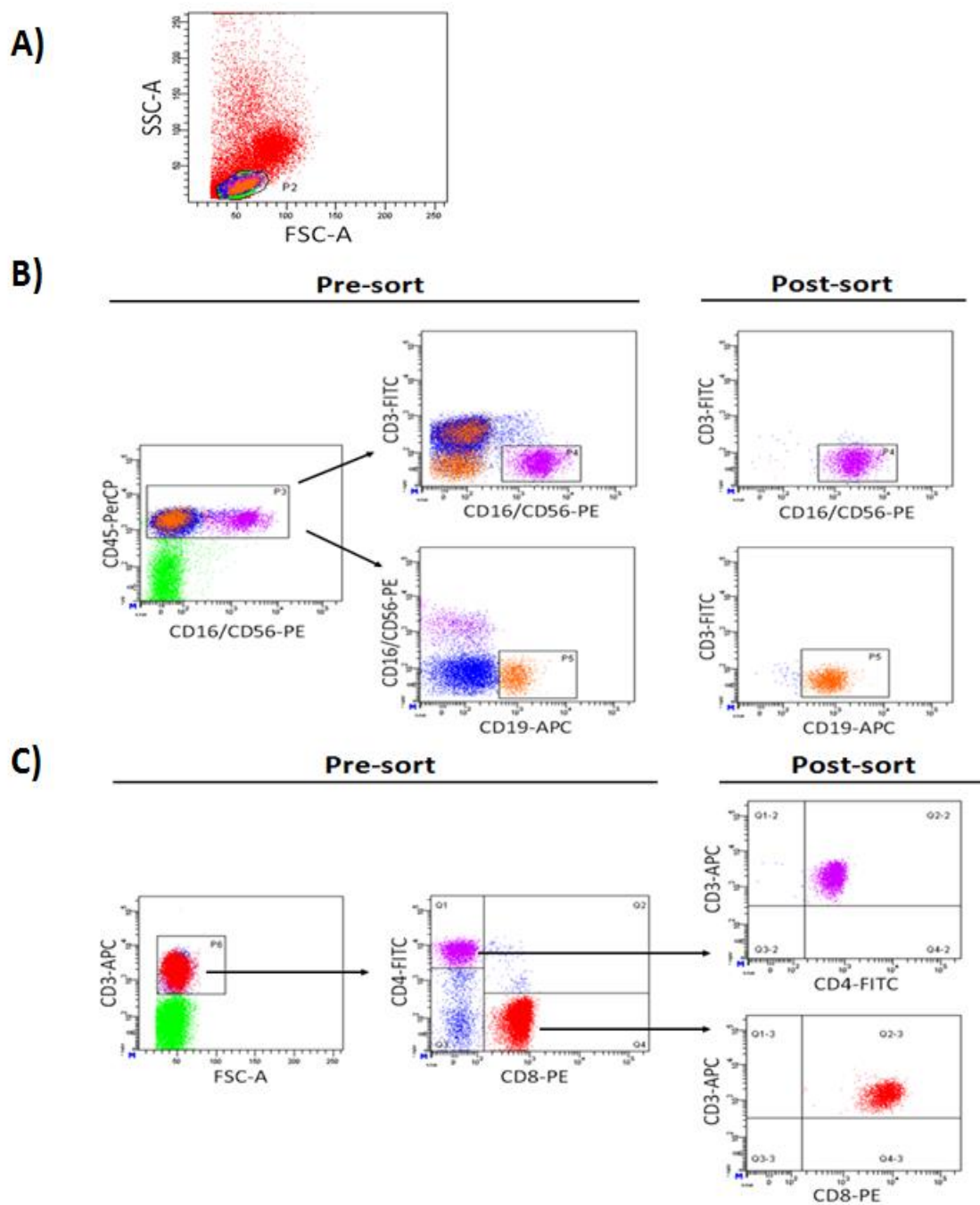


Figure 3.7. **A)** Gating lymphoid cells. **B)** Gating over leukocytes, NK cells and B lymphocytes and confirmation by post-sort flow cytometric analysis. **C)** Gating over CD3 positive T cells and sorting CD4⁺ and CD8⁺ T cells and confirmation by post-sort flow cytometric analysis.

3.6.2. Isolation of Monocytes and Neutrophils

For monocyte isolation, PBMCs were isolated from peripheral blood as explained in Section 3.6.1. PBMCs were cultured in T25 flasks containing full RPMI medium and incubated at 37°C overnight. Non-adherent cells and medium were discarded. Cells that were attached onto the flask's bottom were considered as monocytes and extensively washed with 1X PBS to remove remaining non-adherent cells. Adherent cells were scraped and labeled with anti-CD13-PE and anti-CD14-FITC antibodies. These isolated cells were analyzed with flow cytometry and their monocyte origin was confirmed (Figure 3.8).

For the isolation of neutrophils, in a 15 mL falcon tube, 3 mL Ficoll 1119 in the bottom and 2.5 mL Ficoll 1077 on the top was added. Then, the blood was layered onto Ficoll 1077 by a Pasteur pipette slowly flushing against the tube wall. Centrifugation was done at 700xg for 20 min at 20°C. Leukocytes over Ficoll 1077 were discarded and leukocytes over Ficoll 1119 were considered as PMNs and were isolated by a Pasteur pipette, washed by 1X PBS, and centrifuged at 2000 rpm for 5 min. Supernatant was discarded. Cells in the pellet were resuspended and labeled with anti-CD13-PE and anti-CD66b-FITC antibodies. These isolated cells were analyzed with flow cytometry and confirmed as neutrophils (Figure 3.8).

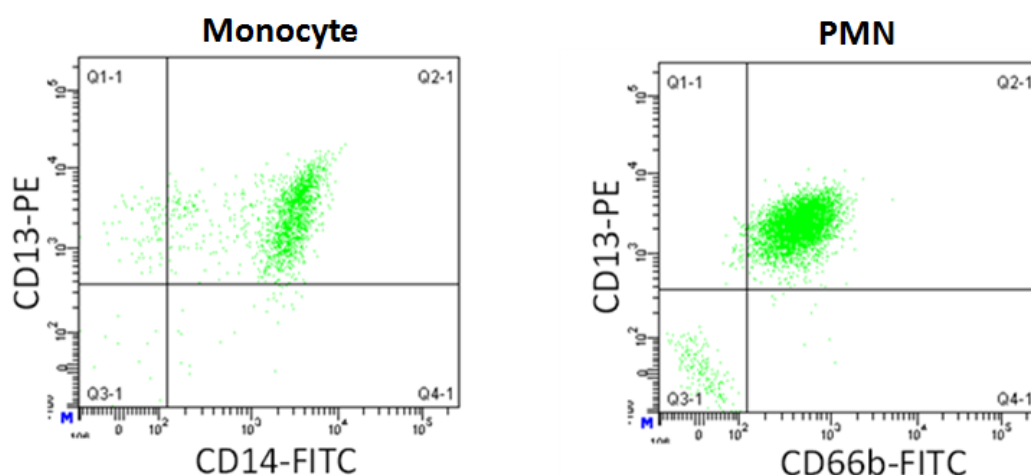


Figure 3.8. Isolated monocytes and neutrophils (polymorphonuclear cells, PMNs) were confirmed by flow cytometry.

After the isolation of immune cells (NK cells, B lymphocytes, T lymphocytes, monocytes, and neutrophils), cells were washed with 1X PBS and RNA was isolated as described in Section 3.3.1. In order to obtain good quality and appropriate RNA concentrations, for NK cells, B lymphocytes, and CD4⁺ helper T lymphocytes RNA was isolated from 5 independent donors; for CD8⁺ cytotoxic T lymphocytes RNA was isolated from 9 independent donors; for monocytes RNA was isolated from 8 independent donors; and for polymorphonuclear (PMN) neutrophils RNA was isolated from 10 independent donors. The RNA samples from each isolation were pooled (concentrated) and treated with RNase-free DNase prior to cDNA synthesis (as described in Section 3.3.2).

3.7. Immunohistochemistry

All breast tissues were fixed in 10% formalin and paraffinized. Samples were obtained from normal breast tissues (n=5) obtained from reduction mammoplasty operations. Invasive ductal carcinoma (grade 1/3, n=5; grade 2/3, n=5; grade 3/3, n=5) tissues with high ER positivity, and triple-negative (ER⁻, PR⁻, HER2⁻) invasive ductal carcinoma tissues (n=9) was used. In order to determine CCRL2 expression, streptavidin-biotin triple indirect immunoperoxidase method was applied. Liver tissue was selected as a positive control.

From the paraffin blocks of the tissues, 4 µm thick slices were taken on polylysine covered slides and deparaffinized at 56°C for 12 h. Samples were incubated in xylene for 30 min. In order to hydrate the tissues, they were incubated in serial (100%, 95%, and 90%) ethanol dilutions for 5 min. Samples were washed with water. In order to block endogenous peroxidase, samples were incubated in 3% hydrogen peroxide solution at room temperature for 10 min. Following the washing with PBS (pH 7.6) for 5 min, samples were incubated in citrate buffer (pH 6.0) in microwave oven for 20 min, for antigen retrieval process and were incubated in room temperature for 30 min. Then, they were washed with distilled water 3 times, incubated in non-immune protein blocking serum for 10 min, and covered with anti-CCRL2 primary antibody (1:100 dilution) and incubated in room temperature for 1 h. After washing with PBS and drying, the samples were incubated with secondary antibody (Multi-species ultra streptavidin detection system-HRP, Lab Vision, USA) at room temperature for 10 min and washed 3 times with PBS each for 5 min. Samples were incubated with streptavidin-biotin complex for 10 min (Lab Vision, USA) and washed 2 times with PBS. Addition of diaminobenzidine (DAB) (Lab Vision, USA) for 10 min revealed the staining. Counter staining method was performed with Harris hematoxyline. In order to dehydrate the samples, slices were again

incubated in 90%, 95%, and 100% ethanol 5 min each and brighted in xylene.

In order to evaluate immunohistochemical staining, every region of tissue was examined under light microscopy (Olympus CX41, USA). CCRL2 cytoplasmic expression in the tumor cells, staining distribution, and severity were determined. CCRL2 staining was categorized as, >50%, diffuse; <50% was regarded as focal. For staining intensity, observations were performed at 40X magnification was used, 100X for moderate staining, and 200X magnification for low intensity. Immunohistochemistry analyses were performed in Gazi University, Department of Pathology.

3.8. Statistical Analysis

Statistical analyses were carried out by using Microsoft Office Excel 2003 program. All values were expressed by arithmetic mean \pm standard deviation (SD). Statistical difference between experimental groups was determined using Student's paired or unpaired *t-test* where appropriate. Differences were regarded as statistically significant when $P \leq 0.05$.

The probability of SNPs determined in recombinant DNA constructs by DNA sequencing (Section 3.3.10) on protein function damage was determined using PolyPhen-2 computer program publicly available online [104].

4. RESULTS

4.1. Expression of CCRL2 Variants in Immune Cells

Expression of CCRL2 transcript variants, CRAM-A and CRAM-B in different immune cells was investigated by RT-PCR. Since the quality (OD_{260}/OD_{280} 1.15; OD_{260}/OD_{230} 0.31) and concentration (1.8 ng/ μ L) of RNA isolated from monocytes were not optimal, it was not used in gene expression analyses. The results of CRAM-A and CRAM-B gene expression in the $CD3^+CD4^+$ helper T cells, $CD3^+CD8^+$ cytotoxic T cells, $CD45^+CD3^-CD19^-CD16/56^+$ NK cells, $CD45^+CD3^-CD19^+CD16/56^-$ B cells, and $CD13^+CD66b^+$ polymorphonuclear cells are shown in Figure 4.1. β -actin was amplified as housekeeping gene.

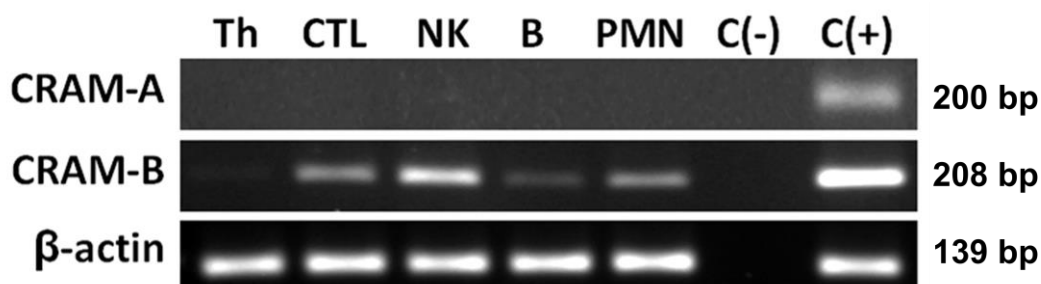


Figure 4.1. CRAM-A and CRAM-B gene expression in immune cells. Th, helper T lymphocytes; CTL, cytotoxic T lymphocytes; NK, natural killer cells; B, B lymphocytes; PMN, polymorphonuclear leukocytes; C(-), negative control; C(+), positive control. cDNA obtained from MDA-MB-231 cell line was used as positive control.

CRAM-A expression was not detected in these immune cells. A slight CRAM-B expression band was obtained with Th cells, but it was clearly detectable in all the other immune cells including CTLs, B lymphocytes,

PMNs, and most prominently in NK cells. This result shows that CRAM-A was not expressed in these immune cells under steady state (control) conditions. However, CRAM-B was widely expressed in unstimulated immune cell types.

4.1.1. Expression of CCRL2 Variants in Immune Cells Under LPS or IFN- γ Stimulation

In order to investigate the expression of CRAM-A and CRAM-B in immune cells under inflammatory conditions, PBMCs were stimulated with LPS or IFN- γ for 24 h. RT-PCR results of CRAM-A and CRAM-B expression are shown in Figure 4.2.

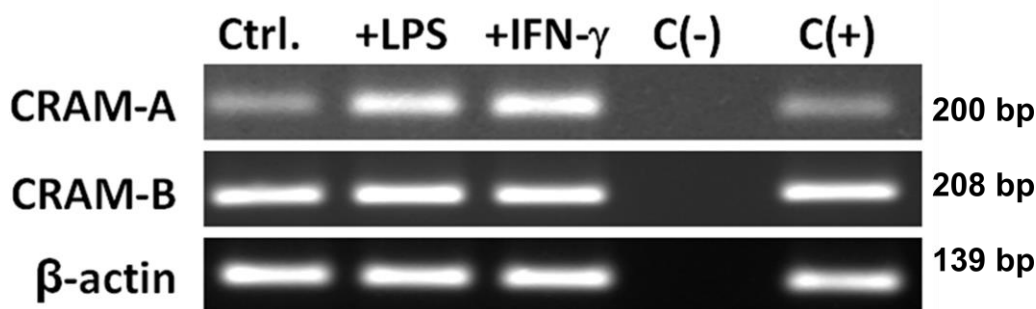


Figure 4.2. CRAM-A and CRAM-B gene expression in control or in LPS- or IFN- γ -stimulated PBMCs. Ctrl., control; +LPS, LPS stimulation; +IFN- γ , IFN- γ stimulation; C(-), negative control; C(+), positive control. cDNA obtained from MDA-MB-231 cell line was used as positive control.

CRAM-B expression was still highly present under LPS or IFN- γ stimulation, not changed. On the other hand, CRAM-A became apparent in

PBMCs stimulated either with LPS or IFN- γ . Whereas, its expression was barely low in control PBMCs.

4.2. Expression of CCRL2 Variants in Breast Cancer Cell Lines

CRAM-A and CRAM-B expression in unstimulated (control) or LPS- or IFN- γ -treated breast cancer cell lines (MCF-12A normal breast, MCF-7, SK-BR-3, MDA-MB-468, MDA-MB-231, BT-474, T-47D, ZR-75-1, and HCC38) were investigated (Figure 4.3).

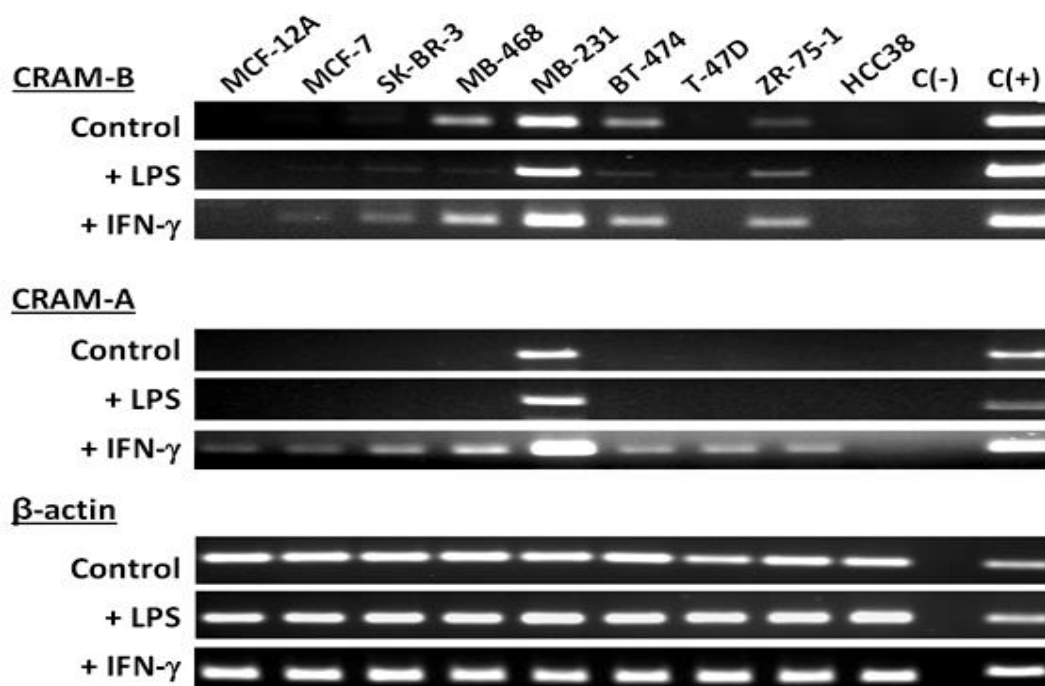


Figure 4.3. Expression of CCRL2 variants, CRAM-A and CRAM-B, in breast cancer cell lines with or without LPS or IFN- γ stimulation. C(-), negative control; C(+), positive control. cDNA obtained from MDA-MB-231 cell line was used as positive control.

CRAM-B expression was clearly observed in control MDA-MB-468, MDA-MB-231, BT-474, and ZR-75-1. After LPS stimulation, CRAM-B expression tended to decrease especially in MDA-MB-468 and BT-474 cell lines. After IFN- γ stimulation, CRAM-B expression was induced in MCF-7 and SK-BR-3 cell lines. No CRAM-B expression was detected in MCF-12A, T-47D, and HCC38 cell lines even under stimulatory conditions.

Amongst control or LPS-stimulated cell lines, CRAM-A was only detected in MDA-MB-231 cells. However, upon IFN- γ stimulation, CRAM-A expression was induced in all of these breast cancer cell lines except for HCC38 and showed pronounced expression in MDA-MB-231 cells (Figure 4.3).

4.3. Expression of CCRL2-related Genes in MDA-MB-231 Cell Line

Since both CRAM-A and CRAM-B were constitutively expressed in MDA-MB-231 cell line, it was questioned whether “CCRL2-related genes” were also constitutively expressed in this cell line.

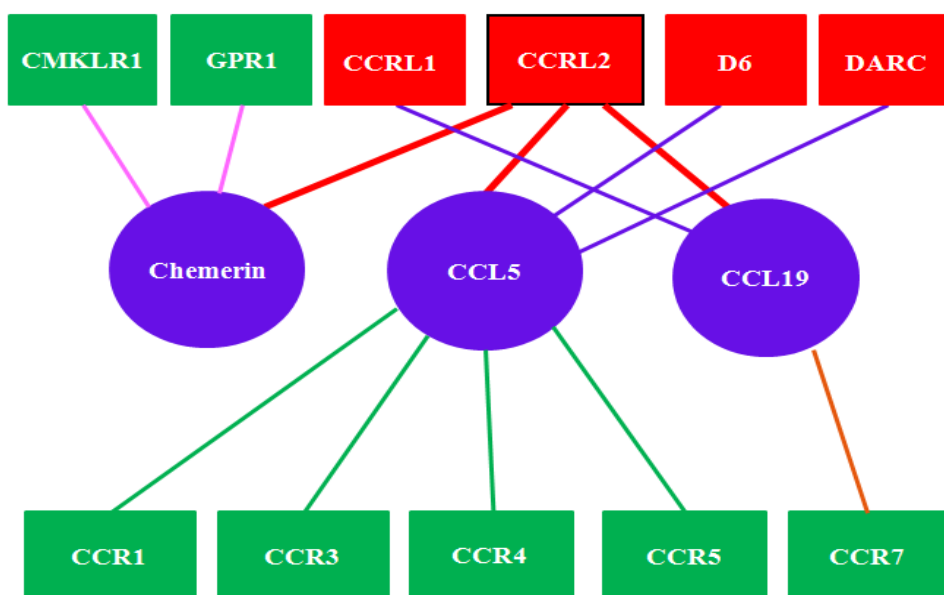


Figure 4.4. CCRL2-related chemokines and chemokine receptors. CCRL2's specific chemokine ligands are shown in purple, canonical signal transducer chemokine receptors are shown in green, and atypical non-signaling chemokine receptors are shown in red. Lines represent ligand-receptor interactions.

CCRL2-related genes include the specific ligands for CCRL2 and the classical and atypical chemokine receptors that share chemokine ligands with CCRL2. CCRL2's specific chemokine ligands are CCL5, CCL19, and chemerin. CCL5 binds CCR1, CCR3, CCR4, and CCR5 canonical signal transducer chemokine receptors and DARC and D6 atypical non-signaling chemokine receptors. CCL19 binds CCR7 canonical signal transducer and CCRL1 atypical chemokine receptors. Chemerin binds CMKLR1 and GPR1 signal transducer chemokine receptors. These genes can be related with the expression and/or with the function of CCRL2. CCRL2-related chemokines and chemokine receptors are displayed in Figure 4.4.

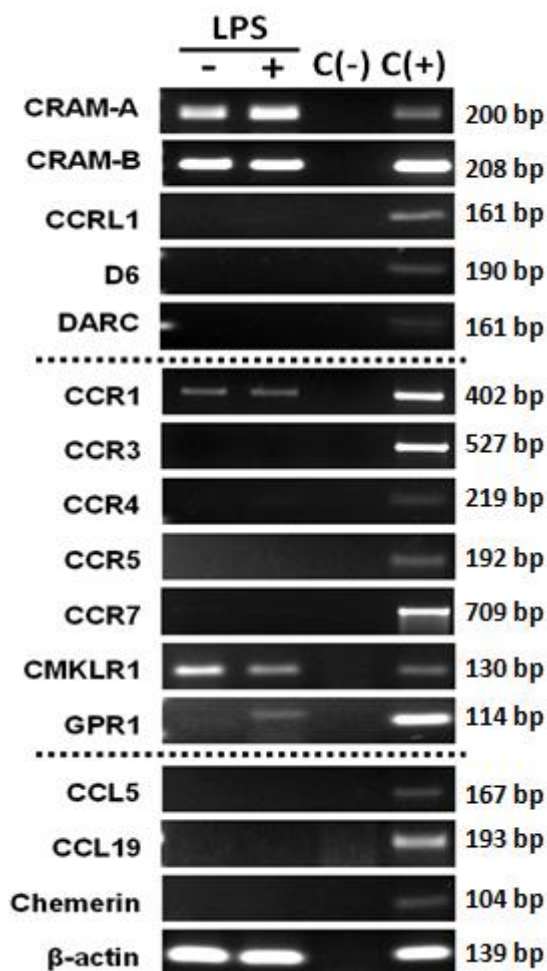


Figure 4.5. CCRL2-related gene expression analysis in control or LPS-stimulated MDA-MB-231 breast cancer cell line. LPS (-/+), unstimulated control or stimulated with LPS; C(-), negative control; C(+), positive control. cDNA obtained from control or LPS-stimulated PBMCs was used as positive controls.

There was no obvious and important relation between constitutive expression of CRAM-A and CRAM-B and other CCRL2-related genes in MDA-MB-231. Since CCRL2 expression is not distinctly changed under LPS stimulation, MDA-MB-231 cells stimulated with LPS were also a stimulated control used to check if LPS affects the expression of CCRL2-related genes.

CRAM-A and CRAM-B were highly expressed in MDA-MB-231 cells, while other decoy chemokine receptors, CCRL1, D6, and DARC, were not expressed. Among the CCRL2-related conventional chemokine receptors only CCR1 and CMKLR1 expression was observed in control or LPS-stimulated cells. A slight GPR1 expression was only observed after LPS stimulation. The cognate chemokines for CCRL2, CCL5, CCL19, and chemerin, were not expressed (Figure 4.5). These results show that there might not be a direct relationship between the constitutive expression of CRAM-A or CRAM-B with the expression of CCRL2-related genes in MDA-MB-231 breast cancer cell line.

4.4. Construction of Recombinant CRAM-A and CRAM-B DNA for Eukaryotic Expression

In order to obtain two separate and intact CRAM-A or CRAM-B and EGFP proteins, human CRAM-A or CRAM-B genes were cloned into the eukaryotic expression vector pIRES2-EGFP (Figure 4.6).

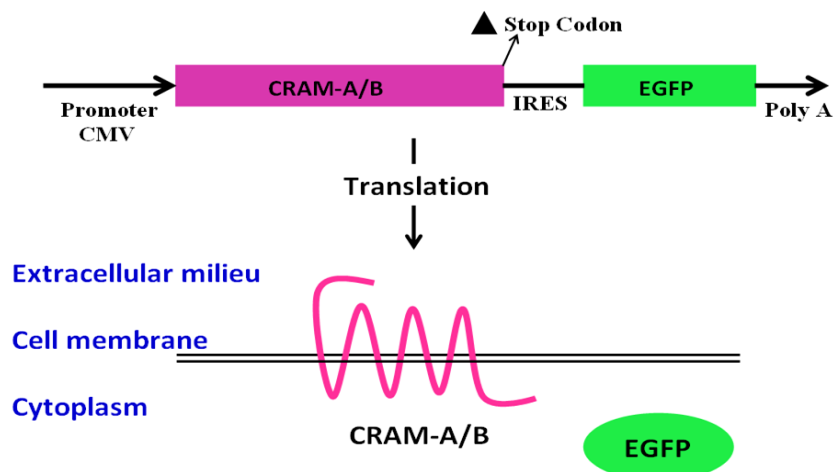


Figure 4.6. Schematic presentation of the recombinant human CRAM-A or CRAM-B genes cloned into eukaryotic expression vector pIRES2-EGFP and the expression of two intact proteins CRAM-A or -B and EGFP. EGFP, Enhanced green fluorescent protein.

RNA was isolated from peripheral blood and/or MDA-MB-231 breast cancer cell line. cDNA was synthesized by RT-PCR. CRAM-A and CRAM-B coding sequences were amplified by *Pfu* DNA polymerase. Amplified DNAs were examined by using agarose gel electrophoresis (Figure 4.7). CRAM-A and CRAM-B amplicons were confirmed as 1106 bp and 1070 bp, respectively.

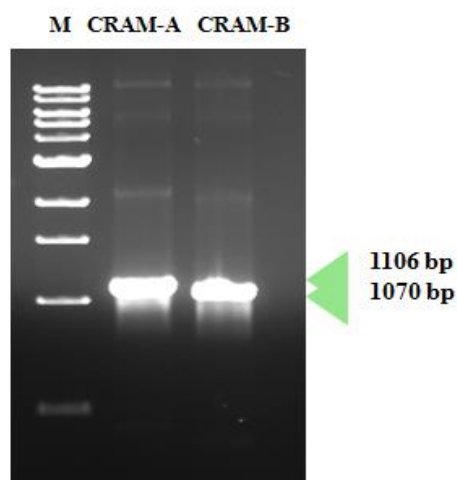


Figure 4.7. Amplification of CRAM-A and CRAM-B insert DNA molecules by *Pfu* DNA polymerase and visualization on agarose gel. M, 1 kb DNA size marker.

Amplified insert DNA molecules were isolated from agarose gel. In order to generate sticky ends at 5' and 3' ends of the DNA molecules, both the insert DNA and the vector were cut by *NheI* and *XmaI* restriction digestion enzymes. Inserts and the vector were isolated either from agarose gel or from tube. Insert and the vector were ligated by T4 DNA ligase enzyme. In order to amplify the recombinant plasmids, they were transferred into *E.coli* by heat shock transformation. Later, *E.coli* colonies that possibly harbored the recombinant CCRL2 constructs were selected due to kanamycin resistance (Figure 4.8) and recombinant plasmids were isolated.

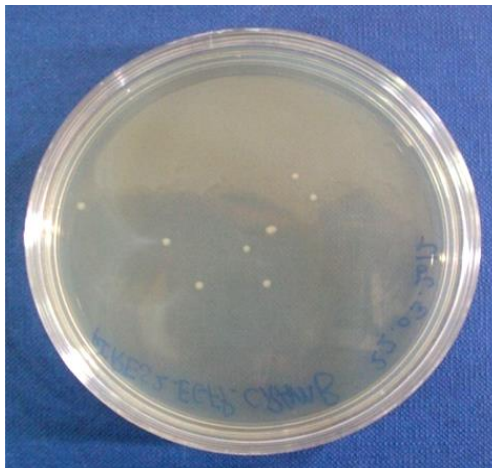
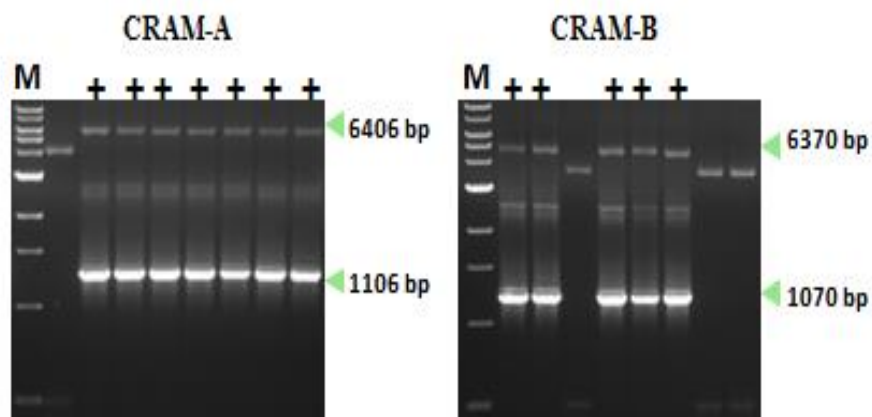


Figure 4.8. Kanamycin resistant *E.coli* colonies on an LB agar petri dish possibly containing recombinant CCRL2 constructs.

The presence of CRAM-A or CRAM-B inserts in recombinant plasmid DNA constructs were confirmed by PCR (Figure 4.9A). In addition, the clones that gave positive PCR results were further confirmed by *NheI* and *XmaI* restriction digestion (Figure 4.9B) and by DNA sequencing analysis (Supplement 1).

A)



B)

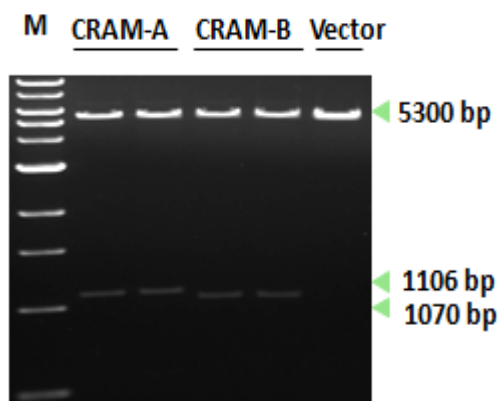


Figure 4.9. A) Confirmation of recombinant DNA products by PCR (Left panel shows CRAM-A, right panel shows CRAM-B PCR amplifications) and **B)** by *NheI-XmaI* restriction digestion. Results of agarose gel electrophoresis are shown. +, Recombinant clones containing CRAM-A (left panel) or CRAM-B (right panel) inserts; M, 1 kb DNA size marker.

Confirmation of recombinant constructs by PCR showed 6406 bp total size of recombinant construct on top of the agarose gel and at 1106 bp for CRAM-A, and 6370 bp total size of recombinant construct and 1070 bp for

CRAM-B (Figure 4.9A). 1106 bp CRAM-A insert or 1070 bp CRAM-B insert was released by *NheI-XmaI* restriction digestion from 5300 bp pIRES2-EGFP vector (Figure 4.9B).

DNA sequencing analyses revealed the presence of single nucleotide polymorphisms (SNPs) in the cloned CCRL2 genes (Table 4.1). The functional consequences of these SNPs in the protein product were assessed by using *PolyPhen-2* computer program.

Table 4.1. The SNPs detected in cloned CCRL2 genes.

Gene	SNP position	Nucleotide change	Amino acid position	Amino acid change	Damage probability	NCBI SNP database no.
CRAM-A	+444	A → C	148	G → G	none	rs11266744
CRAM-A	+536	T → A	179	F → Y	yes	rs3204849
CRAM-B	+59	T → C	20	L → P	yes	novel SNP
CRAM-B	+533	A → G	178	K → R	low or none	novel SNP
CRAM-B	+727	A → G	243	I → V	low or none	rs3204850
CRAM-B	+827	A → G	276	Y → C	yes	novel SNP
CRAM-B	+925	A → G	309	K → E	yes	novel SNP

Certain SNPs has been determined previously and were matched in the National Center for Biotechnology Information (NCBI) SNP database. In addition, four novel SNPs were also identified in the CCRL2 gene. Because of the presence of these SNPs in the cloned products, cloning steps were repeated till the recombinant constructs without any SNPs that could hamper the protein function were obtained. In total, among the 96 isolated colonies, 12 were CRAM-A positive clones. Among the 60 isolated colonies, 10 were

CRAM-B clones. The recombinant CRAM-A or CRAM-B clones selected for further steps of the study were sequenced and no seriously damaging SNPs were observed.

Hereafter, the recombinant plasmids carrying CRAM-A coding sequence were named as **pCRAM-A-IRES2-EGFP**. Whereas, the recombinant plasmids carrying CRAM-B coding sequence were named as **pCRAM-B-IRES2-EGFP**.

4.5. De Novo Expression and Functional Analysis of CRAM-A and CRAM-B

In order to check the expression and to perform functional analyses on recombinant CRAM-A or CRAM-B genes, pCRAM-A-IRES2-EGFP or pCRAM-B-IRES2-EGFP plasmids were transfected into human embryonic kidney (HEK293T) cell line. Since these cells are easily grown and are good transfection hosts, they were preferentially used for initial expression and functional analyses. In addition, HEK293T cells carry SV40 large T antigen, which allows the efficient amplification and expression of SV40 origin of replication-containing plasmids [105].

Before using HEK293T cells, they were examined for the expression of CCRL2-related genes (See Figure 4.4). Since HEK293T cells do not express CRAM-A or CRAM-B, CRAM-A or CRAM-B recombinant constructs were supposed to be transferred into these cells to generate their *de novo* expression. In addition, the absence of CCRL2-related genes in HEK293T cells was important for this study to prevent complexities in the experiments because of the interactions between CCRL2's cognate ligands and other receptors binding the same ligands. By using RT-PCR, we found that only CCRL1 was expressed in these cells (Figure 4.10). Since most of the

CCRL2-related genes were not expressed by HEK293T cells, we decided that working with these cells would generate consistent results.

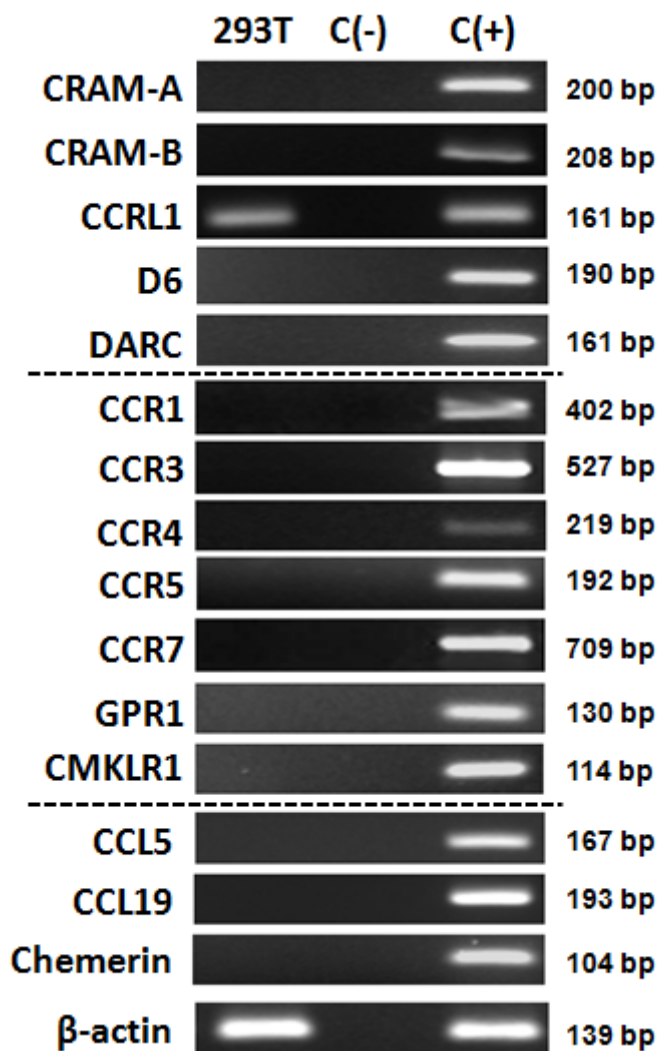


Figure 4.10. Gene expression analysis of CCRL2-related genes in HEK293T cells. 293T, HEK293T cell line; C(-), negative control; C(+), positive control. cDNA obtained from MDA-MB-231 cell line or LPS-stimulated PBMCs was used as positive control.

pIRES2-EGFP is a bicistronic vector and allows the expression of two intact proteins from a single mRNA. EGFP is the reporter protein and EGFP-positive cells indicate successfully transfected cells. HEK293T cells were transfected with empty vector pIRES2-EGFP as the control. In order to investigate the expression of the recombinant plasmids in successfully transfected cells, flow cytometry gate was selected over the EGFP-positive region. Untransfected HEK293T cells were used as autofluorescence controls in order to determine the gate for EGFP⁺ cells (Figure 4.11A). The cells that were transfected with the empty vector showed high EGFP expression (65-86%) (Figure 4.11B). On the other hand, the cells that were transfected with pCRAM-A-IRES2-EGFP or pCRAM-B-IRES2-EGFP recombinant plasmids showed lower EGFP expression (45-62%) (Figure 4.11B). EGFP⁺ HEK293T cells transfected with recombinant CRAM-A or CRAM-B constructs were also identified with CCRL2 surface expression (Figure 4.11B). The cells were labeled with APC-labeled anti-human CCRL2 antibody. By the flow cytometric analysis in HEK293T cells, *de novo* expression of the recombinant plasmids in eukaryotic cells was shown. Thus, pCRAM-A-IRES2-EGFP or pCRAM-B-IRES2-EGFP could be efficiently transcribed, translated, and translocated to the cell surface.

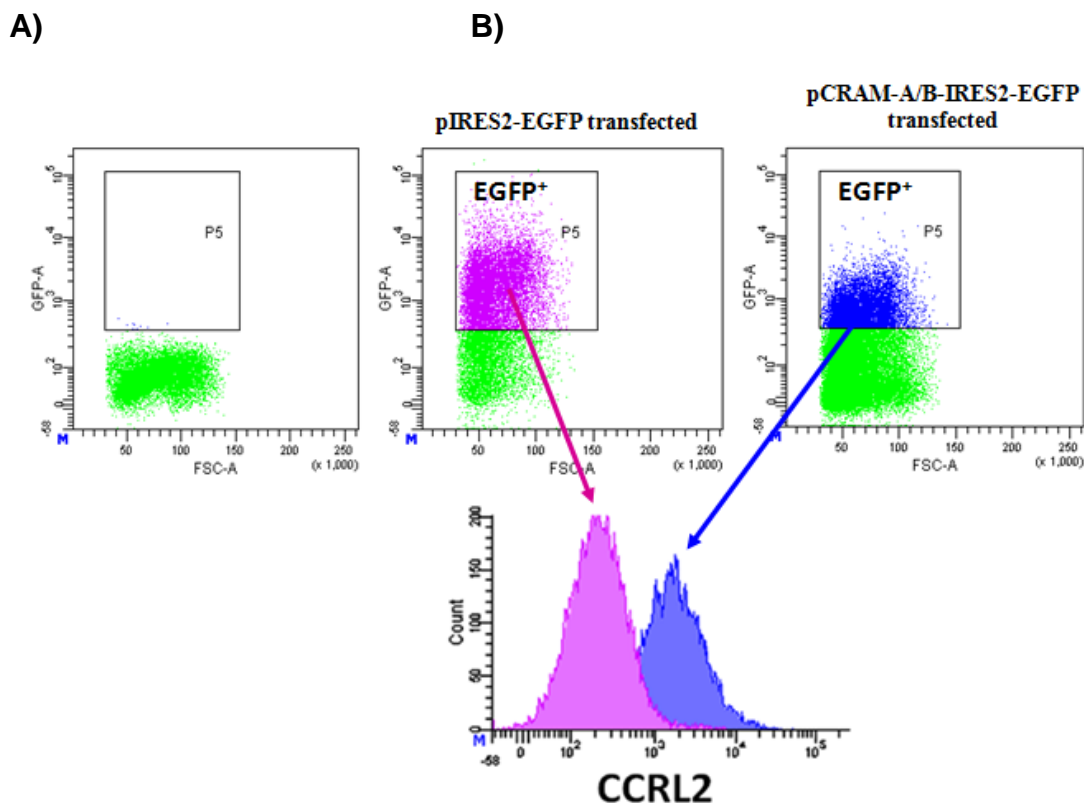


Figure 4.11. Surface expression analysis of recombinant CRAM-A or CRAM-B constructs transfected into HEK293T cells. **A)** The gate P5 was taken according to the untransfected HEK293T cells displaying auto-fluorescence. **B)** EGFP⁺ HEK293T cells transfected with the empty vector pIRES2-EGFP (left panel) or with the recombinant plasmid pCRAM-A/B-IRES2-EGFP (right panel) were gated. CCRL2 expression in pCRAM-A/B-IRES2-EGFP transfected cells are shown in the histogram overlaid with that of control vector transfected cells. Pink color shows the cells transfected with pIRES2-EGFP. Blue color shows the cells transfected with pCRAM-A/B-IRES2-EGFP recombinant construct. Representative histograms out of at least 3 independent experiments are shown.

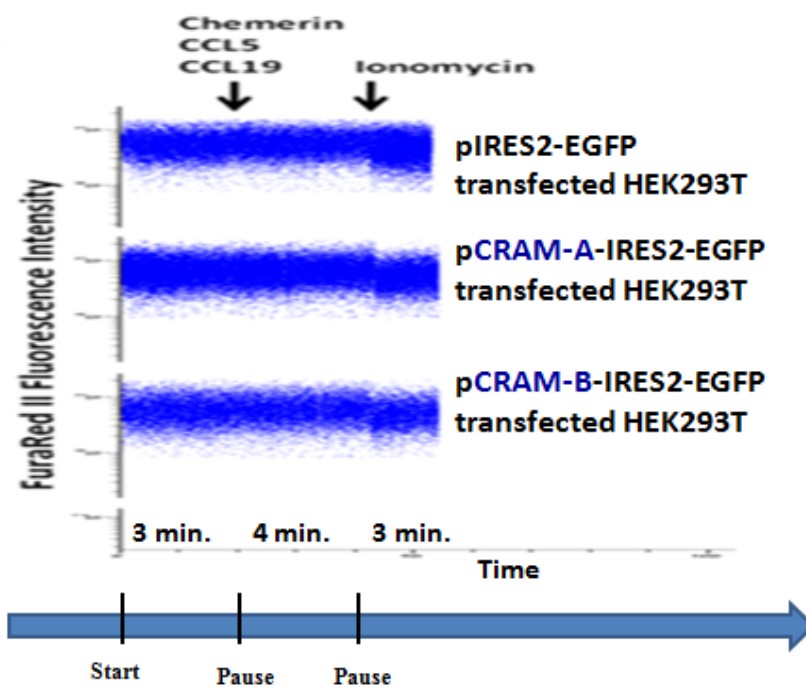
Ca²⁺ Mobilization Assay

Upon engagement with their cognate ligands, decoy chemokine receptors do not transduce signals. Therefore, they cannot affect the intracellular calcium dynamics [103]. In order to validate the unresponsiveness of pCRAM-A/B-IRES2-EGFP or pIRES2-EGFP-transfected HEK293T cells to CCRL2 ligands, CCL5, CCL19, and chemerin, flow cytometric Ca²⁺ ion mobilization assay with the FuraRedII fluorescent probe was performed. The changes in fluorescence intensity were read against the time. The calcium ionophore, ionomycin, was used as a positive control.

At the 48 h post-transfection, HEK293T cells either transfected with pIRES2-EGFP or pCRAM-A-IRES2-EGFP or pCRAM-B-IRES2-EGFP were stained with FuraRedII agent. Cells were read for 3 minutes at 37°C; then, CCL5, CCL19, and chemerin chemokine cocktail was added into the tubes, and the assay was continued for 4 minutes. This was followed by the addition of ionomycin and the cells were read for another 3 minutes (Figure 4.12A). The change in the MFI values of FuraRedII was also quantified and plotted in Figure 4.12B.

Intracellular Ca²⁺ mobilization was not changed in the absence or presence of CCRL2's specific chemokine ligands either in CRAM-A or in CRAM-B or empty vector transfected cells. On the other hand, addition of Ca²⁺ ionophore resulted in a decrease in FuraRedII fluorescence indicating that the experimental setup was working properly.

A)



B)

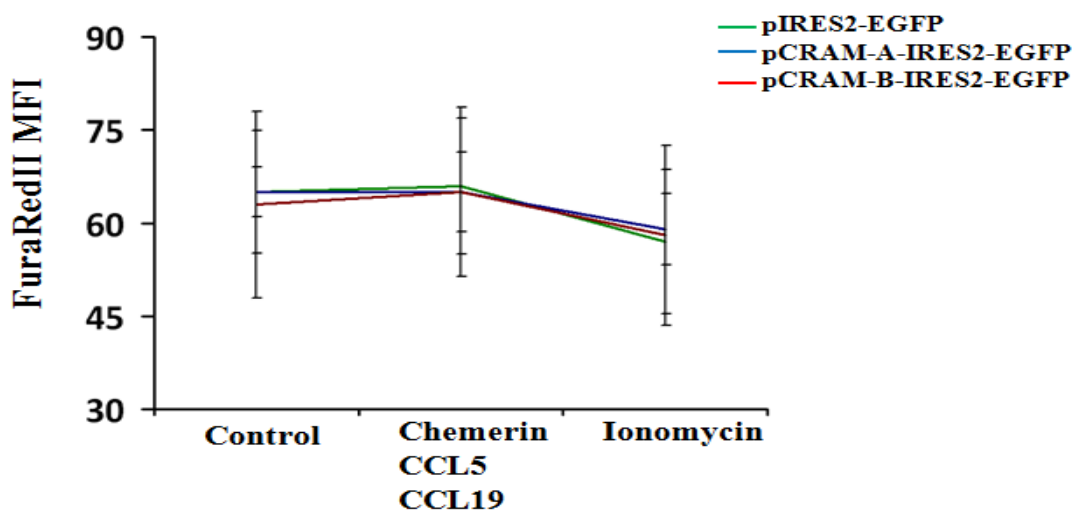


Figure 4.12. Ca²⁺ mobilization analysis in HEK293T cells transfected with the control empty vector pIRES2-EGFP and recombinant plasmids pCRAM-A-IRES2-EGFP or pCRAM-B-IRES2-EGFP. **A)** Representative dot-plots are shown. **B)** The change in FuraRedII MFI values are given.

4.6. Construction of GFP Hybrids of CRAM-A or CRAM-B Genes

Production of hybrid proteins conjugated with GFP is a feasible approach that facilitates tracing of the target protein. Cloning into pcDNA3.1/CT-GFP provided the covalent binding of GFP protein to the C-terminal of CRAM-A or CRAM-B (Figure 4.13).

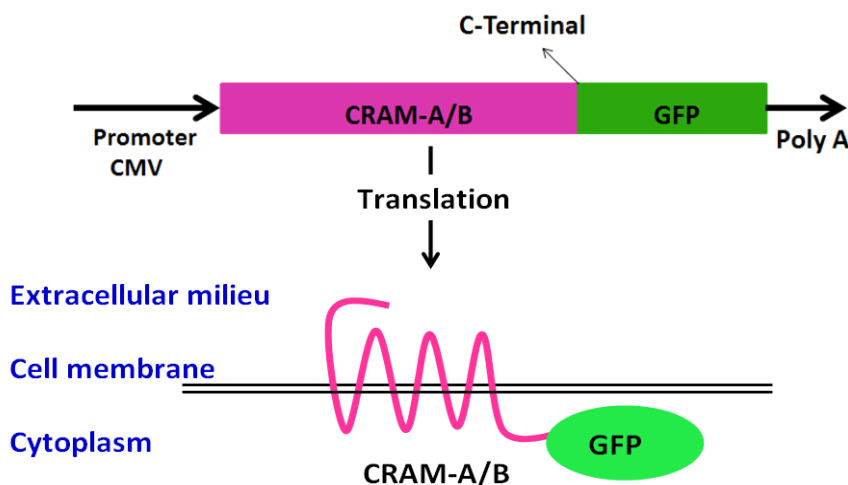


Figure 4.13. Schematic presentation of human CRAM-A or CRAM-B cloning into pcDNA3.1/CT-GFP eukaryotic expression vector and the resulting CRAM-A/B-GFP hybrid recombinant protein. GFP, Green fluorescent protein.

For the construction of CRAM-A- or CRAM-B-GFP recombinant DNA, RNA was isolated from peripheral blood and/or MDA-MB-231 breast cancer cell line. cDNA was synthesized by RT-PCR. CRAM-A and CRAM-B genes were amplified with specific forward and reverse (without stop codon) primers by using *Taq* DNA polymerase (Figure 4.14).

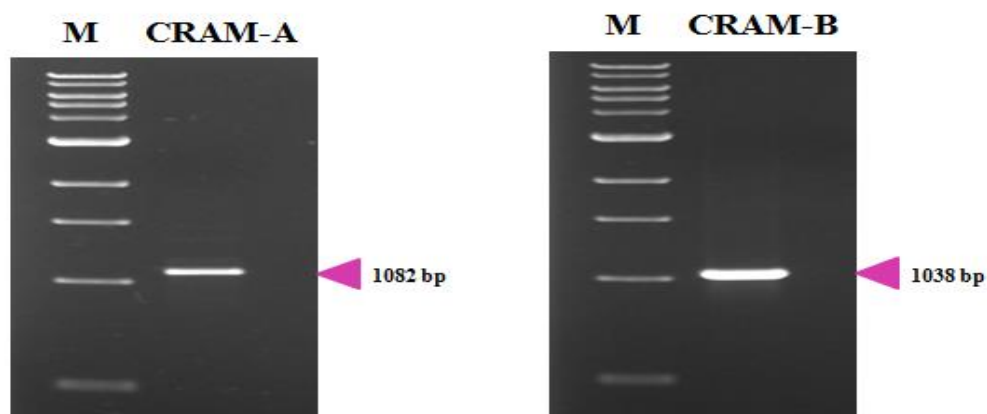


Figure 4.14. Amplification of CRAM-A and CRAM-B DNA inserts by *Taq* DNA polymerase. Photographs taken under UV transilluminator are shown after agarose gel electrophoresis. M, 1 kb DNA size marker.

CRAM-A amplicon was confirmed at 1082 bp and CRAM-B amplicon was obtained at 1038 bp. CRAM-A and CRAM-B genes were isolated from agarose gel. The vector and the insert DNA molecules were cloned into pcDNA3.1/CT-GFP vector by using topoisomerase TA cloning (GFP Fusion TOPO[®] TA Expression Kit, Invitrogen, USA). In order to amplify the recombinant plasmids, they were transferred into *E.coli* by heat shock transformation. *E.coli* colonies that were resistant to ampicillin due to the resistance gene on the vector were selected (Figure 4.15) and plasmids were purified.



Figure 4.15. Ampicillin resistant *E.coli* colonies on an LB agar petri dish possibly containing recombinant CCRL2 variants hybridized with GFP.

The presence of CRAM-A or CRAM-B insert DNA in the recombinant plasmids were confirmed by using PCR (Figure 4.16A), *MluI* restriction digestion (Figure 4.16B), and DNA sequencing analysis (Supplement 2). Confirmation of recombinant constructs by PCR revealed 7239 bp total size of recombinant construct, 1082 bp for CRAM-A, and 7195 bp total size of recombinant construct, 1038 bp for CRAM-B (Figure 4.16A). The constructs that were confirmed to be positive by PCR were later digested by *MluI* endonuclease for the analysis of inserts' orientation. *MluI* restriction digestion gives 5000, 1199, and 985 bp bands for 5'-3' correct orientation of CRAM-A; and, 5000, 1199, and 941 bp bands for 5'-3' correct orientation of CRAM-B inserts (Please refer to Materials and Methods Section 3.3.10, Figure 3.5). *MluI* digestion results of pcDNA3.1/CRAM-A-CT-GFP and pcDNA3.1/CRAM-B-CT-GFP are shown in Figure 4.16B).

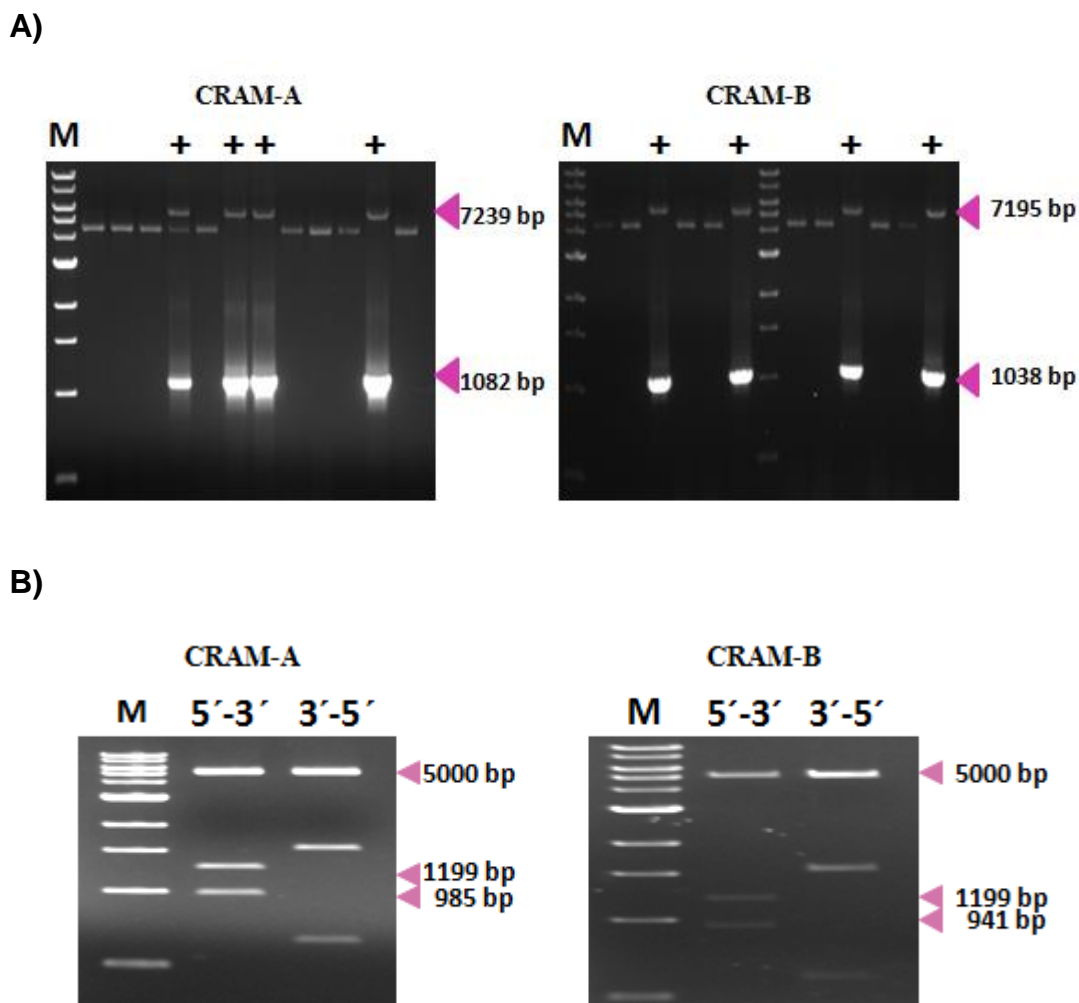


Figure 4.16. Confirmation of recombinant DNA products **A)** by PCR, and **B)** confirmation of inserts' orientation by *MluI* restriction digestion, and examination on agarose gel. +, Recombinant clones containing CRAM-A or CRAM-B inserts; 5'-3', Recombinant clones with correct insert orientation.

DNA sequencing analyses showed that no SNPs that may hamper the expression or function of CRAM-A or CRAM-B proteins were found in the pcDNA3.1/CRAM-A-CT-GFP or pcDNA3.1/CRAM-B-CT-GFP constructs. In addition, the hybridization with GFP was also confirmed by DNA sequencing analysis.

Until the recombinant products with 5'-3' orientation were obtained, whole TA cloning procedures were repeated for 3 times. Among 107 ampicillin-resistant *E.coli* colonies that plasmids were purified, 24 were harboring CRAM-A inserts, 2 were correct oriented, and one was sequenced. Among 142 ampicillin-resistant *E.coli* colonies that plasmids were purified, 22 were harboring CRAM-B inserts, 2 were correct oriented, and one was sequenced.

For the expression analyses, pcDNA3.1/CRAM-A-CT-GFP or pcDNA3.1/CRAM-B-CT-GFP recombinant plasmids were transfected into HEK293T cells. Here, GFP protein will be covalently bound to the C-terminus of CRAM-A or CRAM-B proteins. GFP is the reporter protein indicating the successfully transfected cells. HEK293T cells were transfected with empty vector pcDNA3.1/CT-GFP as the control. In order to investigate the expression of the recombinant plasmids in successfully transfected cells, flow cytometry gate was selected over the GFP-positive region. Untransfected HEK293T cells were used as autofluorescence controls in order to determine the gate for GFP⁺ cells (Figure 4.17A). The cells that were transfected with the empty vector showed high GFP expression (55-75%) (Figure 4.17B). On the other hand, the cells that were transfected with pcDNA3.1/CRAM-A-CT-GFP or pcDNA3.1/CRAM-B-CT-GFP recombinant plasmids showed low GFP expression (20-37%) (Figure 4.17B). GFP⁺ HEK293T cells transfected with recombinant CRAM-A or CRAM-B constructs were identified with CCRL2 surface expression (Figure 4.17B). The cells were labeled with APC-conjugated anti-human CCRL2 antibody and only low amounts of CCRL2 could be detected in GFP⁺ cells.

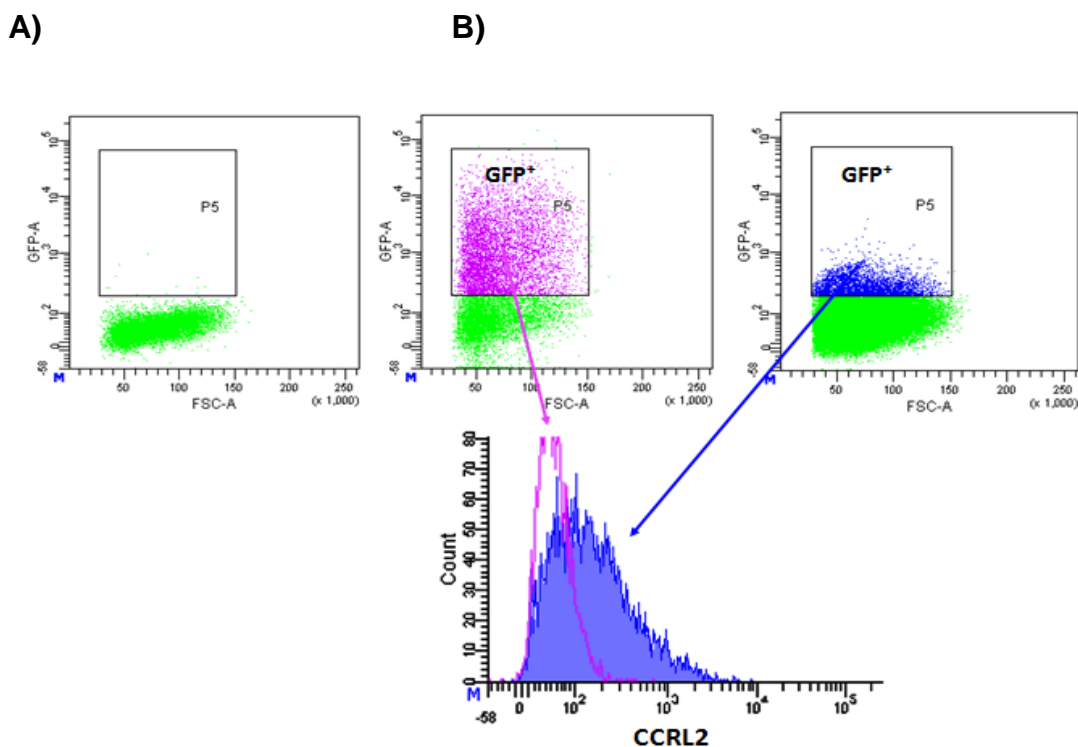


Figure 4.17. A) The gate P5 was taken according to the untransfected HEK293T cells displaying auto-fluorescence. **B)** GFP⁺ HEK293T cells transfected with the empty vector pcDNA3.1/CT-GFP (left panel) or with the recombinant plasmid pcDNA3.1/CRAM-A/B-CT-GFP (right panel) were gated. CCRL2 expression in pcDNA3.1/CRAM-A/B-CT-GFP transfected cells are shown in the histogram overlaid with that of control vector transfected cells. Pink color shows the cells transfected with pcDNA3.1/CT-GFP. Blue color shows the cells transfected with pcDNA3.1/CRAM-A/B-CT-GFP recombinant construct. Representative histograms out of at least 3 independent experiments are shown.

Empty vector pcDNA3.1/CT-GFP and recombinant hybrid constructs pcDNA3.1/CRAM-A-CT-GFP- and pcDNA3.1/CRAM-B-CT-GFP- transfected HEK293T cells were observed under fluorescent microscopy (Figure 4.18).

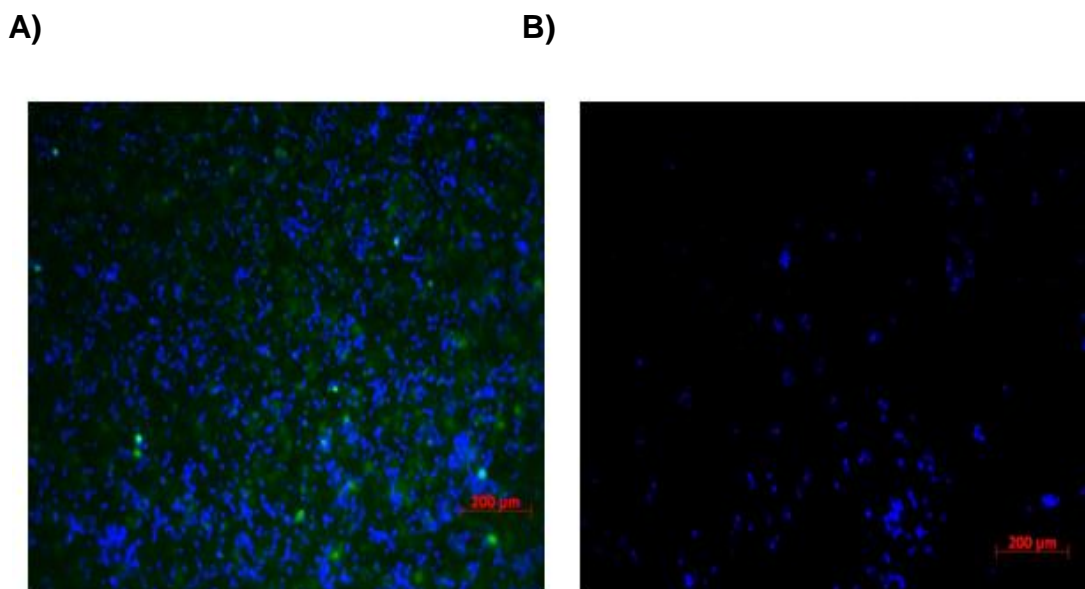


Figure 4.18. Fluorescence microscopic observation of **A)** HEK293T cells transfected with the empty vector pcDNA3.1/CT-GFP and **B)** HEK293T cells transfected with pcDNA3.1/CRAM-A/B-CT-GFP recombinant plasmids. Green, Green fluorescent protein (GFP) expressing cells; Blue, DAPI staining of nuclei.

Since GFP fluorescence was very dim in HEK293T cells transfected with CRAM-A/B-GFP hybrid DNA to be clearly visualized by fluorescent microscopy, this approach was abandoned for the intracellular tracing of CCRL2.

4.7. Determination of the Binding Capacity of anti-CCRL2 mAb 152254 in the Presence of CCRL2 Ligands

According to the gene expression results obtained in Section 4.1, the long variant of CCRL2, CRAM-A, was primarily modulated by IFN- γ

stimulation. Since this observation might indicate a preferential modulation of inflammatory responses by CRAM-A, further experiments were focused on this CCRL2 variant.

As there are restricted numbers of monoclonal antibodies recognizing CCRL2, initially, the binding capacity of mAb 152254 was assessed in the presence of recombinant human CCL5, CCL19, and chemerin. Thus, the convenience of this antibody for functional assays was examined. For this purpose, HEK293T cells were transfected with pCRAM-A-IRES2-EGFP plasmid. At 48 h post-transfection, cells were incubated with CCRL2 ligands and then stained with APC-labeled mAb 152254. The incubations were performed on ice to avoid internalization and the membrane trafficking of the receptor.

None of the chemokine ligands completely abrogated mAb 152254's binding capacity. However, in the presence of CCL19 thus, anti-CCRL2 antibody recognized CRAM-A with a significantly higher ratio in comparison to those of CCL5 or chemerin (Figure 4.19).

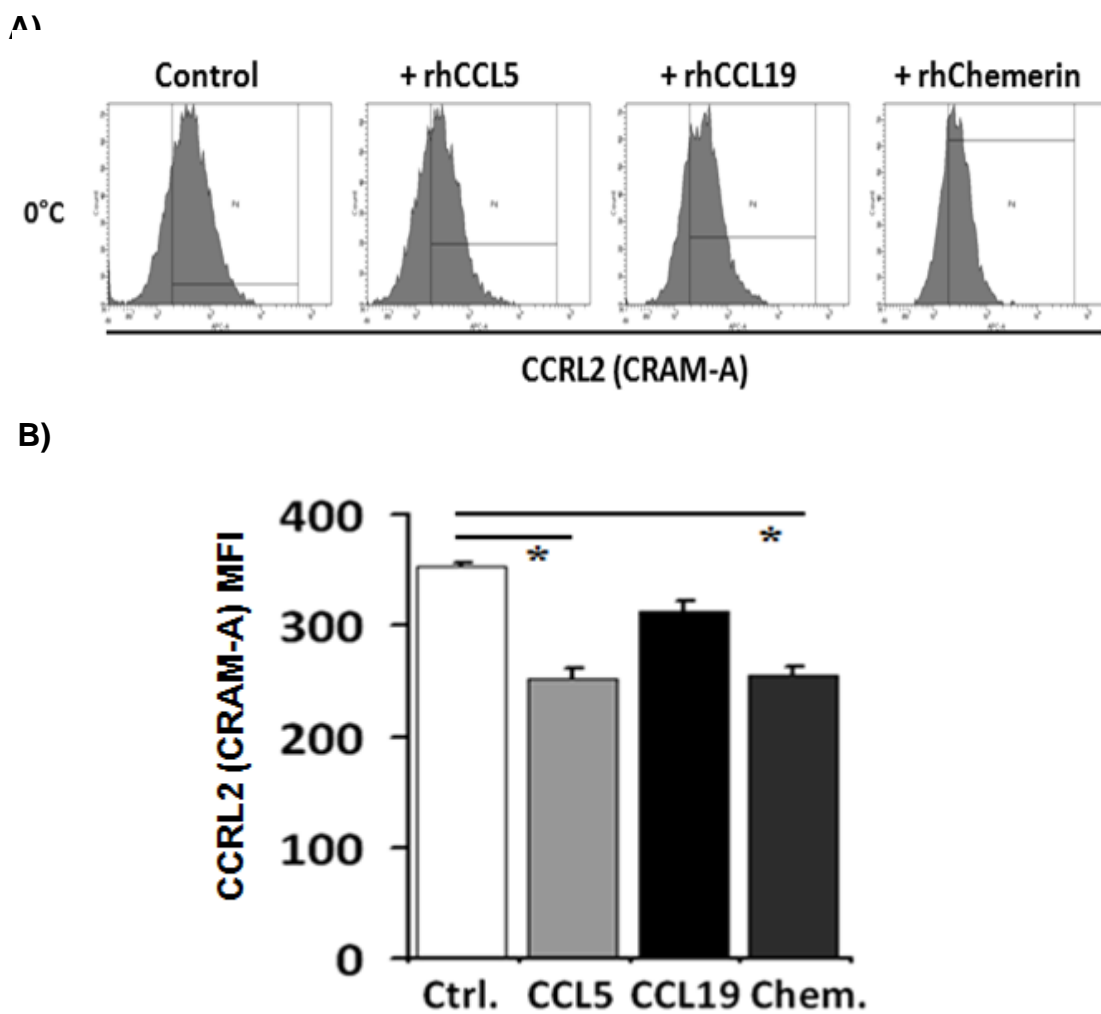


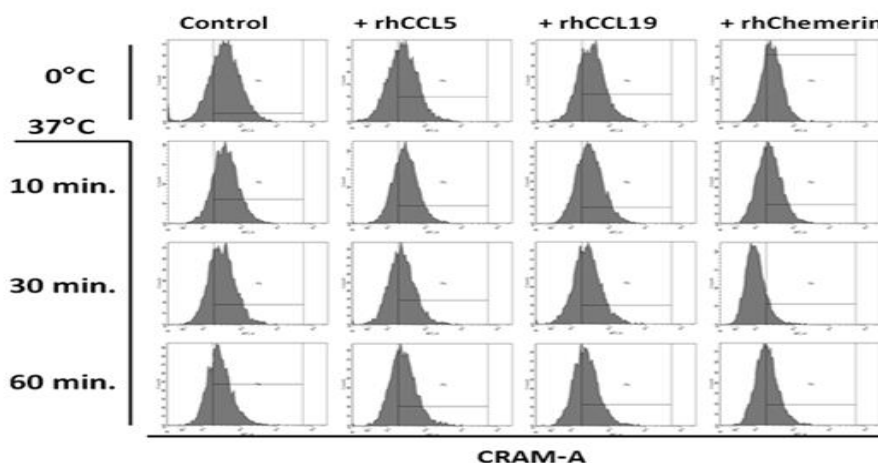
Figure 4.19. Binding capacity of anti-CCRL2 antibody 152254 in the presence of CCRL2-specific chemokine ligands. HEK293T cells transfected with pCRAM-A-IRES2-EGFP were used in the experiments. **A)** Flow cytometric histograms and **B)** bar graphics showing the CRAM-A MFI values are shown. Data were obtained from two independent experiments and are shown as mean \pm SD (* P <0.05). rh, recombinant human; Ctrl., Control; Chem., Chemerin.

4.8. Determination of Surface Expression Changes of CRAM-A in the Presence of CCL5, CCL19, or Chemerin

Surface expression changes of the receptor, CRAM-A-transfected HEK293T cells were analyzed in the presence of CCRL2-specific chemokine ligands, CCL5, CCL19, and chemerin.

Initially, the cells were kept on ice, then incubated in 37°C water bath for 10 min, 30 min, or 1 h and immediately transferred back into ice following the completion of the incubation. When the control cells without ligand incubation kept on the ice throughout the experiment were transferred from 0°C to 37°C, a slight rise in the receptor surface expression was observed (Figure 4.20). The change in CRAM-A surface expression in the presence of CCL5 showed a similar trend as that of observed with no-ligand control. On the other hand, upon binding CCL19, CRAM-A surface levels were steadily decreased up to ~ 25% (* $P < 0.05$). In the presence of chemerin, CRAM-A surface expression change was also significantly downregulated when compared with the control, especially at 30 min. However, at 60 min incubation with chemerin the surface level of CRAM-A tended to increase, indicating a possible recircularization of the receptor to the cell surface.

A)



B)

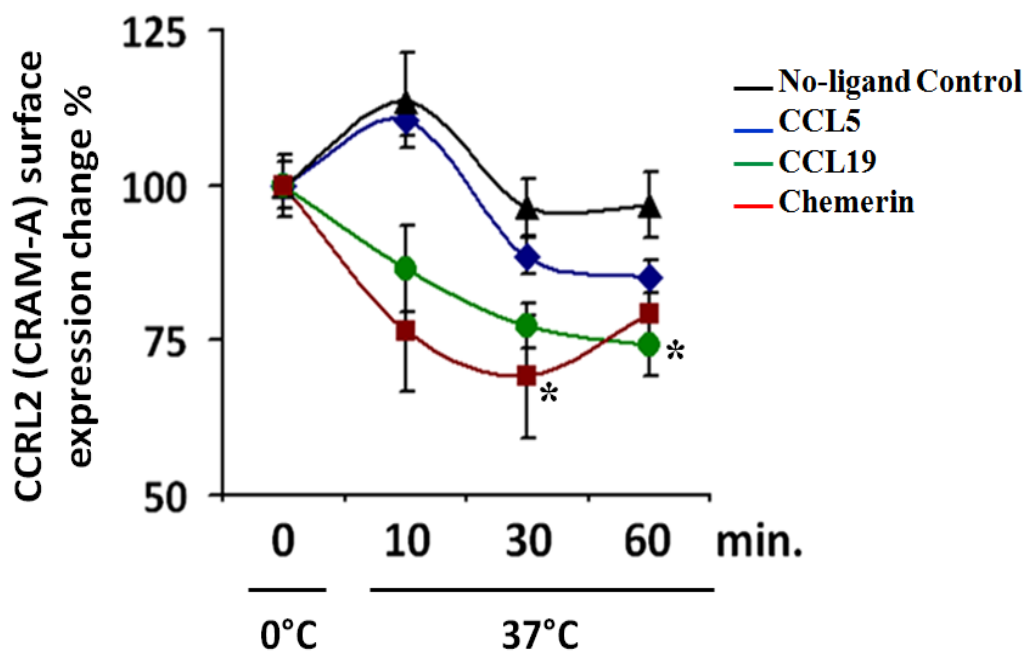


Figure 4.20. CRAM-A surface levels in the presence of CCL5, CCL19, or chemerin. **A)** Flow cytometric histograms representing the CCRL2 surface level at different time points following the addition of recombinant chemokines. **B)** The change in the MFI values of CCRL2 staining is shown as percentages of initial value obtained at 0°C for each chemokine ligand. Data were obtained from two independent experiments and are shown as mean \pm SD (* $P < 0.05$).

4.9. The Analysis of CCL5 and CCL19 Chemokine Removal Capacity of CRAM-A

HEK293T cells and representative breast cancer cell lines MDA-MB-468 or BT-474 were used for this approach. However, because of the low MDA-MB-468 viability under DNA transfection conditions, the assays were continued with HEK293T and BT-474 cells.

4.9.1. In HEK293T Cells

HEK293T cells were transfected with pCRAM-A-IRES2-EGFP recombinant plasmid as described in Section 4.5 and in Section 3.4.7. Prior to incubation with CCL5 or CCL19, transfected cells were incubated with unconjugated anti-CCRL2 152254 or with the isotypic IgG mAb. Since anti-CCRL2 antibody is specific for the receptor, it can alter the ligand binding capacity of the receptor; therefore, higher amounts of its ligands would remain in the cell culture media. After the addition of appropriate amounts of recombinant chemokine ligands, considering the sensitivity of the ELISA kits, supernatants were collected following 20 min of incubation. ELISAs were performed for CCL5 and CCL19.

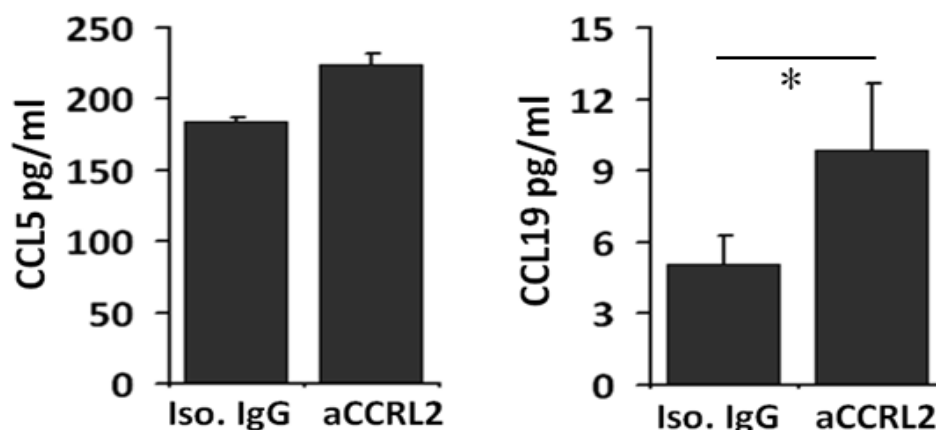


Figure 4.21. ELISA results for CCL5 (left panel) and CCL19 (right panel). (* $P < 0.05$). Iso, isotypic IgG antibody; aCCRL2, anti-CCRL2 mAb 152254.

In the HEK293T cells transfected with pCRAM-A-IRES2-EGFP, hampering the binding of CRAM-A to its chemokine ligands with the mAb modulated chemokine concentration in the cell culture media. Even though binding of CRAM-A with anti-CCRL2 antibody resulted CCL5 to remain higher in the medium, the difference did not reach to statistical significance level (Figure 4.21, left panel). On the other hand, when CRAM-A was bound with anti-CCRL2 antibody, CCL19 levels remained significantly higher in the environment (Figure 4.21, right panel) in comparison to the cells incubated with the isotypic IgG. Thus, CCL19 was more effectively removed from the extracellular milieu than CCL5 by CRAM-A.

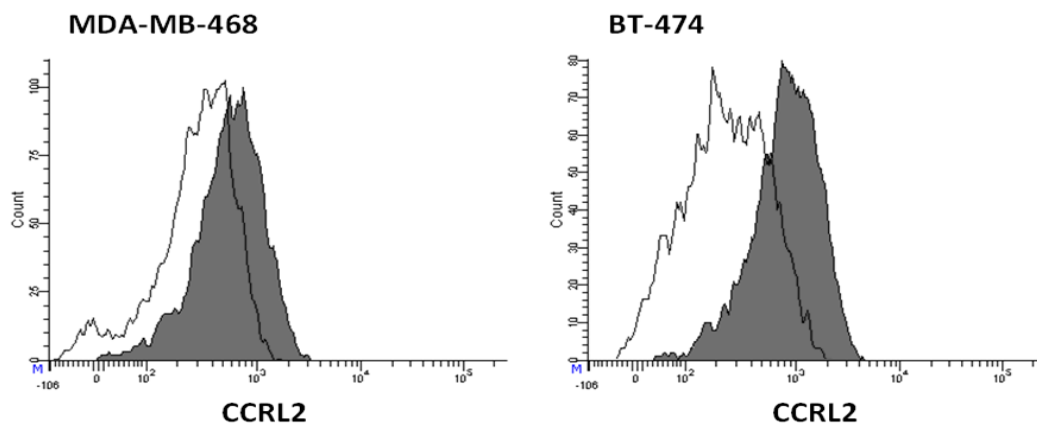
4.9.2. In BT-474 Breast Cancer Cells

In order to investigate the chemokine removal capacity of CRAM-A expressed on breast cancer cells, the breast cancer cell lines MDA-MB-468 and BT-474 which were able to highly express CRAM-A upon IFN- γ stimulation, were transfected with pCRAM-A-IRES2-EGFP recombinant

plasmid. The increase in the CCRL2 expression in these cell lines can be seen in Figure 4.22.

In approximately 15% of untransfected control MDA-MB-468 and BT-474 breast cancer cell lines were CCRL2⁺. This expression was regarded as CRAM-B, since no CRAM-A gene expression was observed in these cell lines under normal (control) conditions (Please refer to Section 4.2). There was no significant difference between untransfected and empty vector-transfected cells in CCRL2 expression. After transfection with pCRAM-A-IRES2-EGFP, CCRL2 (i.e. CRAM-A) expression was increased mostly in BT-474 cells (up to 60%). CRAM-A expression in MDA-MB-468 was lower (approximately 35%) and liposomal transfection procedure was cytotoxic for these cells. Thus, the experiments were continued with BT-474 cells.

A)



B)

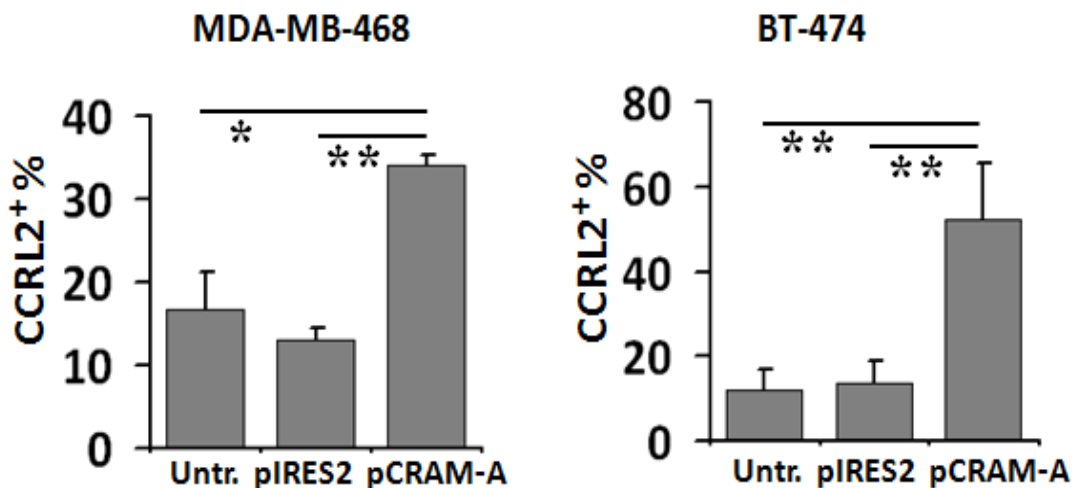


Figure 4.22. A) Analysis of CCRL2 expression in CRAM-A-transfected MDA-MB-468 and BT-474 breast cancer cell lines by flow cytometry. Empty histogram, empty vector pIRES2-EGFP-transfected cells; Filled histogram, pCRAM-A-IRES2-EGFP-transfected cells. **B)** The percentage of CCRL2 positivity in CRAM-A-transfected MDA-MB-468 and BT-474 breast cancer cell lines. (* $P < 0.05$, ** $P < 0.01$). Untr., untransfected control; pIRES2, empty vector pIRES2-EGFP transfected cells; pCRAM-A, pCRAM-A-IRES2-EGFP transfected cells.

In order to verify the convenience of BT-474 cells for CCRL2 functional analyses, CCRL2-related genes (CCL5, CCL19, Chemerin, CCR1, CCR3, CCR4, CCR5, CCR7, CCRL1, DARC, D6, CMKLR1, and GPR1) (Figure 4.4) were analyzed in BT-474 cell line (Figure 4.23). In control BT-474 cells, CRAM-B (as previously determined in Figure 4.3) and CCRL1 were the only CCRL2-related genes expressed. Therefore, BT-474 cells were used for chemokine removal analyses.

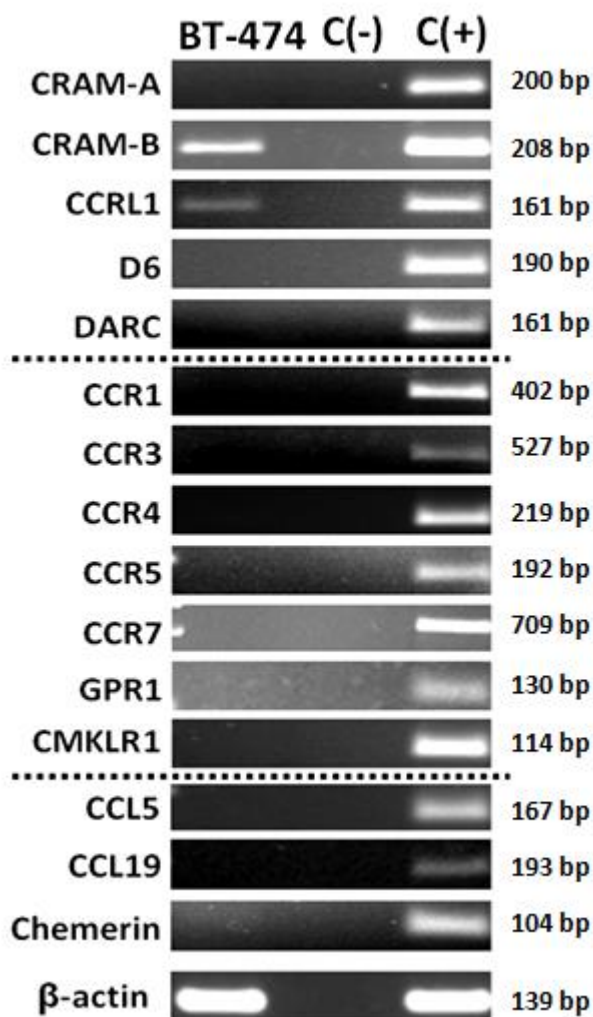


Figure 4.23. Expression analysis of CCRL2-related genes in control BT-474 breast cancer cell line. C(-), negative control; C(+), positive control. cDNA obtained from MDA-MB-231 cell line or LPS-stimulated PBMCs was used as template for positive control.

Similar to HEK293T cells, BT-474 breast cancer cells were transfected with pCRAM-A-IRES2-EGFP recombinant plasmid as described in Section 4.5 and in Section 3.4.7. Prior to incubation with CCL5 or CCL19, transfected cells were incubated with unconjugated anti-CCRL2 152254 or with the

isotypic IgG mAb. Since anti-CCRL2 antibody is specific for the receptor, it can alter the ligand binding capacity of the receptor; therefore, higher amounts of its ligands would remain in the cell culture media. After the addition of appropriate amounts of recombinant chemokine ligands, considering the sensitivity of the ELISA kits, supernatants were collected following 20 min of incubation. ELISAs were performed for CCL5 and CCL19.

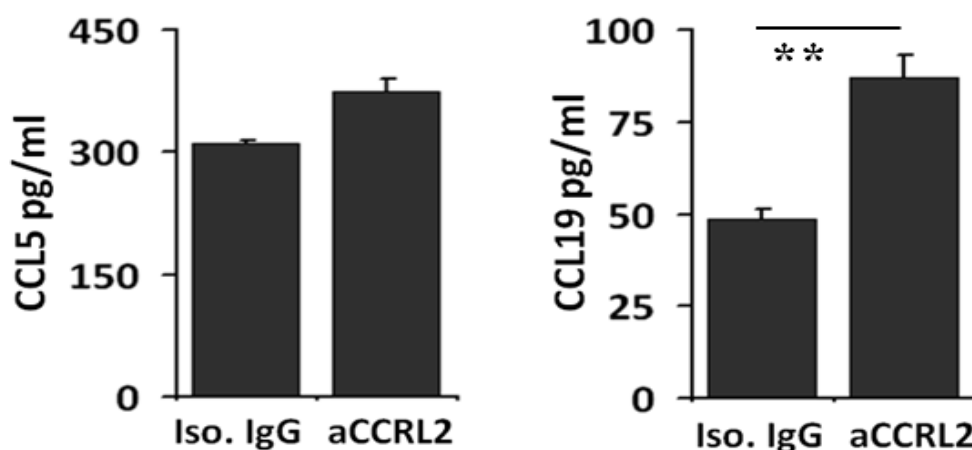


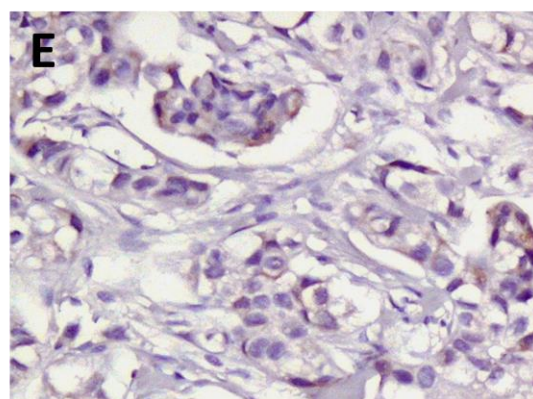
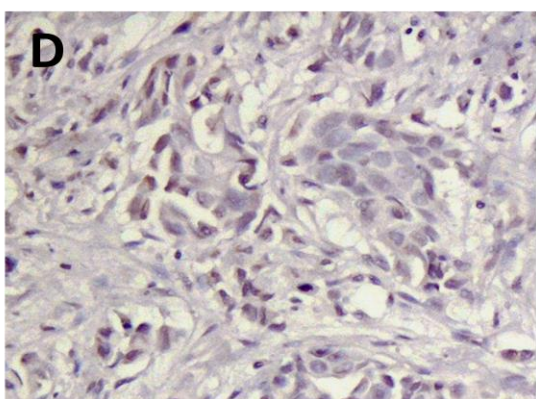
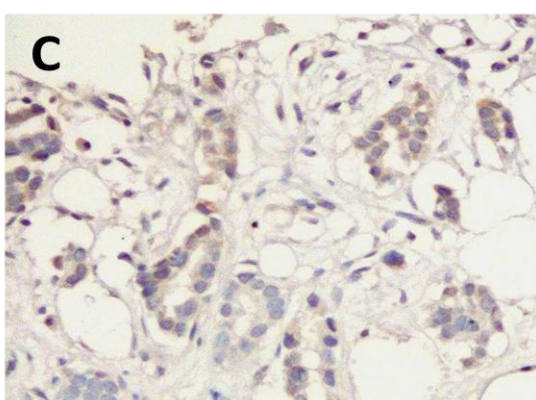
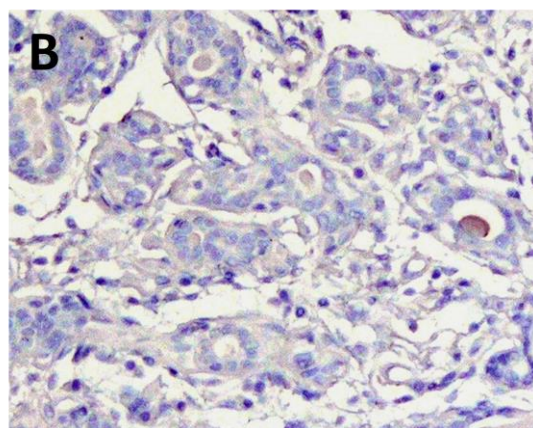
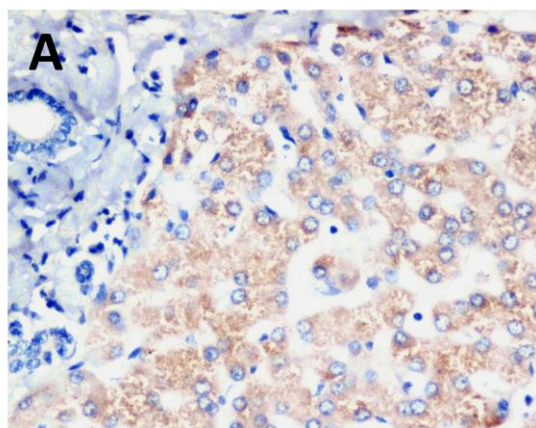
Figure 4.24. ELISA results for CCL5 (left panel) and CCL19 (right panel). (** $P < 0.01$). Iso, isotypic IgG antibody; aCCRL2, anti-CCRL2 mAb 152254.

In the BT-474 cells transfected with pCRAM-A-IRES2-EGFP, hampering the binding of CRAM-A to its chemokine ligands modulated chemokine concentration in the cell culture media. Even though binding of CRAM-A with anti-CCRL2 antibody resulted CCL5 to remain higher in the medium, the difference did not reach to statistical significance level (Figure 4.24, left panel). On the other hand, when CRAM-A was bound with anti-CCRL2 antibody, CCL19 levels remained significantly higher in the environment (Figure 4.24, right panel) in comparison to the cells incubated with isotypic control antibody. Thus, CCL19 was more effectively removed

from the extracellular milieu than CCL5 by CRAM-A. These data were consistent with the results obtained with HEK293T cells transfected with CRAM-A construct.

4.10. CCRL2 Expression in Breast Cancer Tissues

When the patient normal breast tissue samples were stained with CCRL2, no staining was observed; whereas, the immunohistochemistry (IHC) protocol was properly working as the positive control liver tissue (cytoplasm of hepatocytes) was successfully stained, (Figure 4.25 A and B). In the breast cancer tissues obtained from ER⁺ tumors, invasive ductal carcinomas, grade I or II cancers were stained with a similar distribution (2/10 diffuse with low staining intensity, 4/10 focal with low staining intensity, and 4/10 negative) (Figure 4.25 C and D). On the other hand, all of the grade III ER⁺ invasive ductal carcinomas were diffusely stained at low intensity with CCRL2 antibody (Figure 4.25 E). Triple-negative invasive breast cancers were again heterogeneously but more prominently positive for CCRL2 (Figure 4.25 F, G, and H). Of the patient samples, 1/9 was diffusely and strongly positive; whereas, 3/9 stained diffuse and moderate, 1/9 stained diffuse and low, 3/9 showed focal and low staining and only one sample showed no staining for CCRL2.



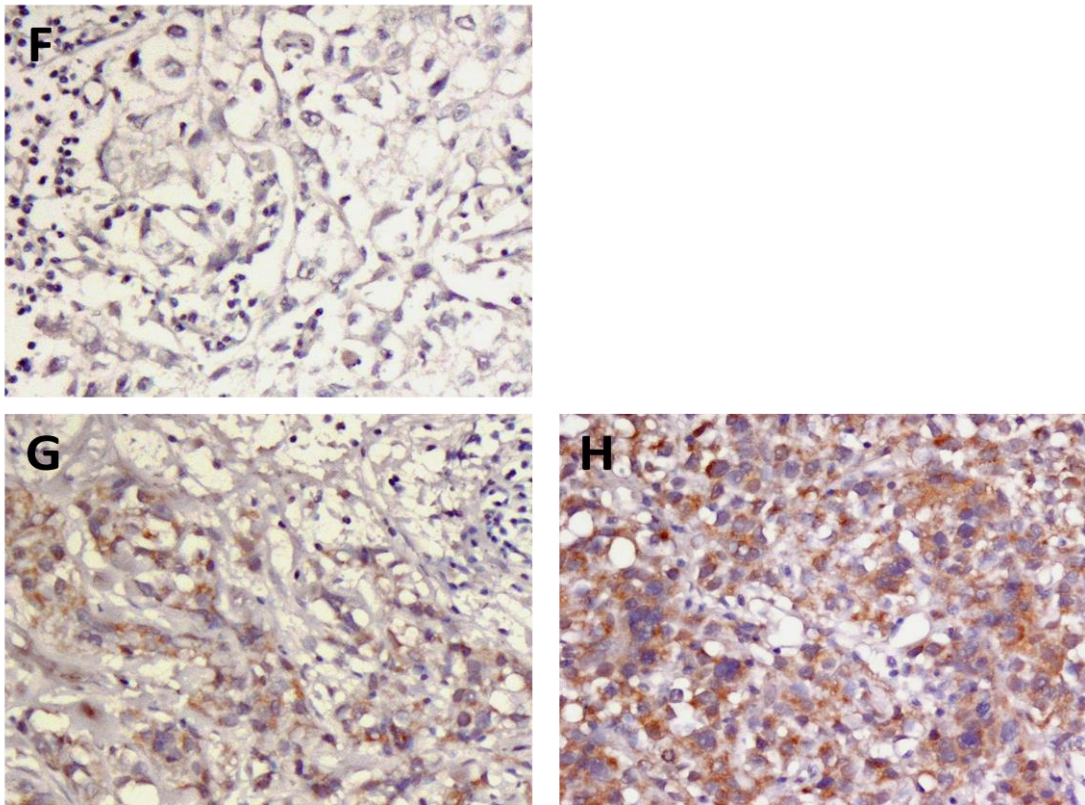


Figure 4.25. Immunohistochemical determination of CCRL2 on breast cancer tissues. Representative micrographs are shown. CCRL2 staining in **A)** normal liver tissue (positive control), **B)** normal breast tissue, **C)** grade I invasive ductal carcinoma (IDC), **D)** grade II IDC, **E)** grade III IDC, and in triple-negative breast cancer tissues with **F)** low, **G)** moderate, and **H)** high CCRL2 expression levels are shown, (100X).

5. DISCUSSION

In the literature, many studies investigating CCRL2 gene expression do not generally address which isoform, CRAM-A or CRAM-B, is transcribed or translated. In addition, it appears that generally the short isoform, CRAM-B, has been implied when CCRL2 expression is mentioned. To our reasoning, this might be due to; I. CRAM-B is widely expressed in many cell types under physiological conditions. Thus, the alternative transcription start site for CRAM-A is not preferentially used in resting cells. II. To our knowledge, there is no CCRL2-specific antibodies that can discriminate between the isoforms, CRAM-A and CRAM-B. In addition, Western-Blot technique is not sensitive enough to reveal 12 amino acid-long size difference between these isoforms. Therefore, it is not feasible or possible to discriminate the protein expression levels of CRAM-A and CRAM-B. III. According to comparative transcript analysis, the long isoform, CRAM-A, is mainly restricted to primates and has no murine homolog. Alternatively, the mouse homolog of CCRL2, L-CCR, shares identity with CRAM-B (51% homology). Therefore, the murine studies on CCRL2 would not properly model the human situation. The overall data obtained from this thesis study, indicates the importance of CRAM-A isoform under inflammatory conditions. CRAM-A was identified to be the preferential isoform expressed especially upon exposure to IFN- γ , the primary anti-tumor cytokine.

It has been previously shown that CCRL2 is expressed in almost all human hematopoietic cells including monocytes, macrophages, PMNs [106], basophils, mast cells [43], CD4⁺ and CD8⁺ T cells, pre- and pro-B cells (depending on the maturation stage) [7], DCs, NK cells, and CD34⁺ progenitor cells [44, 107]. Correspondingly, its expression can be found in lymphoid (spleen, lymph node, fetal liver, and bone marrow) but also in non-lymphoid (lung, heart) tissues [107]. The murine homolog of CCRL2, L-CCR, has been shown to be expressed in macrophages, microglia, astrocytes, and

lung tissue [108, 109]. On the other hand, these studies rarely address which isoform of CCRL2 is expressed. Hartmann et al. found human CCRL2 expression with a preferential expression of CRAM-B splice variant in pre-B cells. Only two B-CLL (pre-B) cell lines out of 6 (Nalm6 and G2) were expressing CRAM-A together with CRAM-B. In addition, the expression of CCRL2 was higher in pro- and pre-B cells than in immature and mature B lymphocytes [7]. Alternatively, Migeotte et al. reported no CCRL2 expression on the B cells obtained from peripheral blood [44].

Here, distribution of CRAM-A and CRAM-B in immune cells was investigated. CRAM-A was not expressed in freshly isolated Th, B, NK, CTL, and PMN cells from healthy donors. This result shows that CRAM-A is not preferentially expressed in these immune cells under steady state (physiological) conditions. However, CRAM-B gene can be constitutively expressed in unstimulated immune cells. As demonstrated by Hartmann et al. [7], we also found that CCRL2 expression in B cells was only observed for CRAM-B. Although, Galligan et al. could not detect CCRL2 mRNA in freshly isolated PMNs by Northern blotting [110], we demonstrated CRAM-B mRNA expression in PMNs. Accordingly, CCRL2 was initially isolated from a cDNA library generated from PMN cells [107] and PMN was determined as CCRL2⁺ cells [44]. In addition, the cytokine-rich environment of synovial fluid from rheumatoid arthritis patients induces CRAM-A and CRAM-B expression on PMNs found in this fluid [110]. Indeed, in our study, LPS recapitulating the TNF and IL-1 pathways and IFN- γ amongst the factors found in synovial fluid up-regulated CCRL2 (especially CRAM-A) expression in PBMCs.

Our analysis of CRAM-A and CRAM-B distribution in cDNA samples obtained from whole PBMCs showed that upon LPS or IFN- γ stimulation, CRAM-A expression was induced or up-regulated, while there was no obvious change in CRAM-B expression. Additional real-time PCR analyses would have been done to quantitatively reveal the exact change in CRAM-B

expression. Even though no CRAM-A expression was detected with individually purified immune cells (Th, CTL, B, NK, PMN cells), CRAM-A was slightly amplified in control PBMC samples. This CRAM-A expression may be deriving from monocytes (found amongst the PBMCs), which could not be separately analyzed due to technical problems. Alternatively, the template cDNA of purified immune cells was synthesized from 290 ng total RNA, but 350 ng RNA was used for that of PBMCs. Thus, increasing the amount of template cDNA might have resulted in the amplification of CRAM-A mRNA found at low levels under steady state condition.

Monnier et al. reported that the combination of TNF- α , LPS and IFN- γ induced robust mCCRL2 (mouse CCRL2) expression in bEND.3, mouse endothelial cell line. Primary human umbilical vein and dermal microvascular endothelial cells, and a human brain endothelial cell line (hCMEC/D3) expressed CCRL2 and significantly upregulated upon TNF- α , LPS, and IFN- γ stimulation. Only the combination of such potent proinflammatory mediators could significantly induce CCRL2 expression [41]. Even though the combination of LPS and IFN- γ was not tested in our study, the increase in CRAM-A expression was evident with single-agent induction of PBMCs. Moreover, the addition of immune suppressive factors such as TGF- β or IL-10 cannot inhibit the upregulated CCRL2 [41]. Galligan et al. reported that inflammatory products present in the synovial fluid can upregulate CCRL2 expression on synovial neutrophils in rheumatoid arthritis patients [110]. Total mRNA of CCRL2 can be upregulated in a mouse microglial cell line infected with rabies virus [111]. Collectively, together with the data produced in this thesis study, CRAM-B is explicitly detected in resting hematopoietic cells. On the other hand, CCRL2 expression can be augmented and shifts to CRAM-A variant under inflammatory conditions.

The relationship between CCRL2 and cancer has previously been investigated in glioblastoma and B cell chronic lymphocytic leukemia (CLL)

but not in breast cancer. Generally, by internalizing and decreasing the chemokine gradient, atypical chemokine receptors play an important role in attenuating inflammation. Since DARC, D6, and CCX-CKR have been shown to decrease tumor invasion, metastasis, and proliferation and are a sign for good prognosis in different types of cancers including breast cancer, it was wondered whether as an atypical chemokine receptor CCRL2 also plays a regulatory role in breast cancer. CCRL2-specific ligands CCL5 [112], CCL19 [113], and chemerin [114] and the other CCRL2-related genes CCR1, CCR3, CCR4, CCR5, CCR7, CCRL1, DARC, D6, CMKLR1, and GPR1 have been found to play important roles in breast cancer [2, 49, 51, 115-117]. NK cells expressing CCRL2 and CMKLR1; CD4⁺ helper T lymphocytes expressing CCR5 and CCR7; and, CD8⁺ CTLs expressing CCR5 and CCR7 [41, 118, 119], and many other immune cells possessing CCRL2-related molecules can also be found in breast tumors. Thus, since these immune cells respond to the same chemokine ligands (putatively) specific for CCRL2, their motility or even functions may be modulated by CCRL2. Therefore, we focused on the relationship between CCRL2 and breast cancer.

In a wide panel of breast cancer cell lines, including MCF-12A normal basal; MDA-MB-468, MDA-MB-231, and HCC38 basal-like; and, MCF-7, SK-BR-3, BT-474, T-47D, and ZR-75-1 luminal cells, CRAM-A and CRAM-B expression was investigated under normal steady state conditions or after LPS or IFN- γ stimulation. CRAM-B was expressed in certain breast cancer cell lines and LPS or IFN- γ stimulation did not modulate its expression levels distinctly. Intriguingly, CRAM-A expression was only detected in unstimulated or LPS-stimulated MDA-MB-231 cells. However, it became the most frequently expressed CCRL2 variant when these cell lines were stimulated with IFN- γ . A prominent increase in CRAM-A expression was also evidenced in IFN- γ -stimulated MDA-MB-231 cells. These results indicate that CRAM-A and CRAM-B expression may not be restricted either to basal-like or luminal subtypes of breast cancer cells.

It was exclusive that both CRAM-A and CRAM-B were constitutively expressed in MDA-MB-231 cells. It has been previously evidenced that the autocrine interaction between chemokine and chemokine receptors can increase the expression of decoy receptors specific for that chemokine. For example, stimulation with CCL5 increased CCRL2 expression in human pro-B and pre-B cells [7] or the loop between CCL19 and CCR7 on B-CLL cells was accompanied with high CCRL2 levels [6]. In order to check if such an autocrine mechanism is present in MDA-MB-231 cells, CCRL2-related genes were assayed. However, none of the ligands or the canonical receptors except for GPR1 (under LPS stimulation) and CMKLR1, the cognate receptors of chemerin were found in this cell line. MDA-MB-231 has been regarded as one with the most aggressive and malignant breast cancer cell lines. These cells are of triple-negative basal-B subtype [120], showing epithelial-to-mesenchymal transition (EMT) [120] and are enriched in CD24⁻CD44⁺ cancer stem cell (CSC) sub-population [121]. In addition, a recent work showed the capacity of MDA-MB-231 cells to maintain helper T cell responses including Th1 cell activation, proliferation, and IFN- γ secretion [122]. Thus, MDA-MB-231 might be involved in or directly constitute a pro-inflammatory microenvironment that results in the constitutive expression of CRAM-A.

As cancer is an inflammatory disease, it has been found that high CCRL2 mRNA level both in glioma cell lines and in glioblastoma patient samples where it may play an immune regulatory role [5]. However, CCRL2 was associated with increased tumor cell migration and invasion capacity. This is an interesting report since CCRL2 does not induce signals. IFN- γ is one of the major mediators of anti-tumor immune responses and it is primarily secreted by NK cells, Th1 cells, and CTLs [13]. As a result, since CRAM-A was up-regulated upon treatment with IFN- γ , this study was further focused on CRAM-A variant.

It may be speculated that chemerin found in the breast tumor microenvironment [85] may act in a paracrine manner through CMKLR1 or GPR1 and influence CCRL2 expression which remained constitutive on MDA-MB-231 cells. Since CMKLR1 and GPR1 are expressed in these cells, CCRL2 regulation may be more related with chemerin than with other ligands. However, this observation is made with a single cell line with very aggressive properties and needs to be expanded by using many other cell lines with similar properties. Accordingly, CCRL2 staining on human triple-negative (basal-like) breast cancer tissues was prominent on the samples with most aggressive features (grade III). Basal-like breast cancers are correlated with inflammatory responses and identified with a conspicuous lymphocytic infiltration. Therefore, it might be the microenvironment effect upregulating the level of CCRL2 (it is not known whether CRAM-A or CRAM-B was the dominant isoform due to antibody specificity) on human triple-negative breast tumors. However, to clearly associate the presence or the level of CRAM-B or CRAM-A transcripts with the molecular sub-types of the breast cancer, i. the number of human tissue samples must be increased, ii. CCRL2 protein expression in breast cancer cell lines must be determined, and/or iii. The level of CRAM-A and CRAM-B gene expression must be determined in the fresh tumor tissues.

In inflammatory diseases including rheumatoid arthritis [110] and ischemic brain injury [123] and in malignant diseases including glioblastoma [5] and B-CLL [6], high level expression of CCRL2 was reported. CRAM-A-specific up-regulation upon IFN- γ stimulation was observed in breast cancer cell lines. Thus, in order to constitute an *in vitro* model, genetically modification with recombinant CRAM-A gene for *de novo* expression was performed. Also, this *in vitro* model could be used for the determination whether CRAM-A binds the same ligands (CCL5, CCL19, and chemerin) arguably proposed for CRAM-B or mCCRL2. Indeed, in the literature, there is no or a few data on CRAM-A expression or functions.

Moreover, previous studies show controversy in the CCRL2-specific ligands, especially about CCL5 [46].

In this study, human CRAM-A and CRAM-B coding DNA sequences were cloned into the eukaryotic expression vector pIRES2-EGFP. However, many cloning attempts were interfered by SNPs which were predicted to hamper protein expression and function. There are some studies in the literature indicating SNPs in CCRL2 gene, which is located in a polymorphic gene locus [124]. It was not unexpected to find many SNPs in our cloning experiments. In summary, either previously reported or novel SNPs were determined; however, we did not focus on these sequence variations. Upon functional computer-based prediction, SNPs that did not modulate protein functions were acceptable for further experiments. Thus, cloning of CCRL2 isoforms were continued till the clones without deleterious SNPs were constructed.

In order to express the recombinant constructs, HEK293T cells were used as hosts for transferring the CRAM-A or CRAM-B plasmids. It was important that these cells do not endogenously express CRAM-A or CRAM-B. Also, to avoid interference with other CCRL2-related chemokines or chemokine receptors, it was important that these genes are not expressed in HEK293T cells. The only gene expressed in HEK293T cells was CCRL1 that can bind CCL19, but its expression level was low. We did not expect that the significance of our results be interfered by CCRL1, since empty vector-transfected cells were used as the controls. Therefore, HEK293T cells were suitable for our experimental design. After the transfection of recombinant CRAM-A or CRAM-B constructs, CCRL2 surface protein expression was observed. Therefore, the recombinant constructs were efficiently transcribed, translated, and translocated to the cell surface. EGFP expression ratio in the control empty vector-transfected cells shows a higher expression than that of the recombinant CRAM-A/B-transfected cells. This observation was expected

because in the CRAM-A or CRAM-B recombinant plasmid-transfected cells two proteins (CCRL2 and EGFP) were being expressed.

In order to examine the recombinant protein functionality and again functionally confirm the suitability of HEK293T cells as hosts, Ca^{2+} mobilization analysis was performed. As an atypical chemokine receptor CCRL2 should not induce Ca^{2+} mobilization in the presence of its ligands [125]. In the HEK293T cells transfected with recombinant CRAM-A or CRAM-B constructs or with the empty control vector, CCRL2-specific chemokine ligands (CCL5, CCL19, and chemerin) did not induce Ca^{2+} flux. Therefore, neither CCRL2 nor any other molecules that might have been found on HEK293T cells possessed the capacity to transduce signals upon engagement with CCL5, CCL19, or chemerin. In other words, there was no canonical signal transducer receptor to bind these ligands. Overall, HEK293T cells were appropriate hosts for functional assays with successfully cloned and expressed recombinant CCRL2 variants.

Galligan et al. suggested that CRAM-A or CRAM-B transfected HEK293 cells migrate chemotactically towards synovial fluid collected from rheumatoid arthritis patients. They stated that rheumatoid arthritis synovial fluid contains TNF, IL-1, IFN- γ , GM-CSF, CCL2, MIP-1, CCL5, CCL19, and complement proteins. They implied that CCRL2 plays a role in this migration. However, there might be some other signaling chemokine receptors on HEK293 cells, which were not determined in their study that could bind rheumatoid arthritis synovial fluid components, promoting their migration. Accordingly, Hartmann et al. reported that they could not reproduce the Galligan et al. results using CRAM-A or CRAM-B transfected HEK293 cells in the presence of rheumatoid arthritis synovial fluid from several patients [7].

There are not several different monoclonal anti-CCRL2 antibodies commercially available and there is no antibody clone that can discriminate between the two variants of CCRL2. Among them, we used the monoclonal

antibody mAb clone 152254, which can recognize the extracellular region of both CRAM-A and CRAM-B, but cannot discriminate between the two variants.

The binding of ligands can cover the target epitope or change the conformation of the receptor; therefore, can interfere with the binding capacity/affinity of an antibody specific for that receptor. Thus, the binding capacity of mAb 152254 was assessed in the presence of CCRL2 cognate chemokine ligands in order to validate its usefulness in the current experimental setups. Upon the addition of the ligands, the decoy chemokine receptor can be rapidly internalized [126]. Therefore, we did this analysis at 0°C to prevent receptor internalization. Since 0°C can make antibody binding difficult, we performed the antibody recognition assay in a 60 min time interval. CCL5 and chemerin minimally decreased antibody binding that might not interfere with the further experimental analyses. Presence of CCL19 did not affect antibody binding capacity. This may be due to the small size of CCL19 (8.8 kDa) in comparison with chemerin (16 kDa) that occupies more space upon receptor binding (Recombinant Human Proteins Certificate of Analysis, R&D, USA). Chemerin's high affinity for CCRL2 blocks binding of some other clone of anti-CCRL2 mAb [43]. On the other hand, CCL5 is also a small (7.8 kDa) chemokine (Recombinant Human Proteins Certificate of Analysis, R&D, USA).

In order to investigate ligand-receptor internalization and CCRL2 surface expression change in the presence of ligands, recombinant protein-transfected cells were incubated for different time periods to see in which time point internalization is more efficient. Recombinant protein ligands were added according to the effective dose (ED) factor recommended by the supplier (R&D, USA).

Upon release from 0°C into 37°C, the level of CCRL2 was slightly increased and later decreased to normal levels in the control pCRAM-A-

IRES2-EGFP-transfected HEK293T cells. This was not unexpected as the membrane trafficking of proteins was resustained quickly by restoring 37°C condition. Similar observations were previously reported in similar assay setups [43]. In order to exclude differential antibody recognition capacity in the presence of ligands, each experiment was normalized relative to its own control at 0°C.

Since the presence of CCL5 gave similar results as with the change of CRAM-A surface levels in “no ligand control” group, our results supported the studies suggesting that CCL5 may not be a ligand that induces CCRL2 (CRAM-A) internalization [8, 43]. In a study performed by Hartmann et al., CCL5 was identified with a capacity to bind CRAM-A or CRAM-B, it did not induce Ca²⁺ mobilization or cellular migration, but led to actin polymerization and ERK1/2 phosphorylation, which may indicate active translocation of the receptor from the cell surface. Therefore, these authors suggested CCL5 to be a specific ligand for CCRL2 [7]. But to date no study has been demonstrated a direct ligation between CCL5 and CCRL2. Several investigations have been done to identify CCRL2 ligands. CCRL2 was initially thought to activate chemotaxis and calcium flux in response to CCL2, CCL5, CCL7, and CCL8 or to bind CCL19 with no signaling [40, 42]. However, since other studies have not detected any CCRL2 functional activation by these chemokines, those results remain controversial [40]. Accordingly, the results of this thesis study, showed a slight binding and chemokine removal activity of CCL5 to CRAM-A.

Upon binding CCL19, CRAM-A surface level showed a time dependent gradual decrease, suggesting that it is internalizing CCL19. The originality of our study is that we demonstrated this ability of CRAM-A, while other studies only state CCRL2 or CRAM-B [6, 8, 40].

Although previous studies might have suggested that CCRL2 concentrates and presents its ligands without internalizing them, Leick et al.

demonstrated constitutive internalization of CCRL2 upon CCL19 binding. They showed that about 60% of the receptor internalized after only 5 min and almost the same amount replaced at the same time, keeping cell surface levels constant [8]. Accordingly, in our study, CCL19 had a higher capacity to induce internalization of CRAM-A and CRAM-A was efficiently removing CCL19 from extracellular milieu. Thus, through the controversial reports in the literature, our data support CCL19 as a specific ligand for CCRL2 (i.e. CRAM-A).

In the presence of chemerin, CRAM-A surface level was initially down-regulated but later tended to increase. This implies that chemerin can induce the internalization of CRAM-A, but later CRAM-A recirculates back to the cell surface. It was previously demonstrated both in mice and in human endothelial cells and mast cells that CCRL2 (CRAM-B) does not internalize chemerin, but instead binds and concentrates it on the cell surface to present chemerin to nearby cells expressing CMKLR1, chemerin's canonical signal transducer receptor [41, 43, 127]. On the other hand, our results showed a transient down-regulation of CRAM-A levels upon engagement with the recombinant chemokine protein. Thus, this may indicate the recircularization capacity of chemerin-bound CRAM-A or may imply a reluctance of the receptor internalization upon chemerin ligation. Therefore, our data is distinct from Monnier et al. [41]. However, it needs to be more precisely assayed to show cellular trafficking of chemerin bound to CRAM-A.

In order to investigate intracellular localization of the ligand-receptor pair after internalization, it is a feasible approach to generate fusion products with fluorescent properties, e.g. GFP. The cellular localization of the GFP-hybrid recombinant protein, whether on the cell membrane, inside a vesicle after internalization, or again on the cell membrane after recirculation, can be directly analyzed. For this purpose, the hybrid protein's GFP part should be very bright. In order to generate GFP-hybrid CRAM-A or CRAM-B proteins,

we used pcDNA3.1/CT-GFP eukaryotic expression vector. Unfortunately, both the flow cytometric and fluorescent microscopic results showed very low and dim GFP expression by CRAM-A/B-GFP hybrids and were not enough for intracellular localization experiments. This was not actually an unexpected problem. For example, the resultant hybrid protein from this cloning is a large protein that can be difficult to be functionally expressed due to translational and post-translational problems, and the protein stability and conformation may be imperfect [128].

In order to investigate chemokine removal capacity of CCRL2 and to further confirm CRAM-A receptor down-regulation, we used CRAM-A-transfected HEK293T cells and BT-474 breast cancer cells. We investigated CCRL2 cognate chemokine ligands especially CCL5 and CCL19, which are very important in tumor immunology and breast cancer. The production of these chemokines in breast cancer microenvironment cells mediates the infiltration of NK cells, Th1 cells, and CTLs, commonly producing IFN- γ . They are the most important immune cells in the elimination phase of tumor immunology. Here, these CRAM-A-modified cells were initially incubated with the CCRL2 blocking antibody and ligands were added after a while. The isotopic antibody was not specific for CCRL2 and served as a control.

Upon IFN- γ stimulation, CRAM-A was highly induced in MDA-MB-468 and BT-474 breast cancer cell lines. Since CRAM-B is endogenously expressed in these cell lines, CRAM-B function on chemokine removal was simultaneously assayed. To examine the convenience of BT-474 cells for CRAM-A gene transfer and following functional analyses, CCRL2-related gene expression was also tested in BT-474 cells. Absence of CRAM-A and other genes except for CRAM-B and CCRL1 (as in HEK293T cells) was observed. Since we blocked CCRL2 with mAb 152254, CCRL1 expression was not expected to interfere with our analyses. Approximately, 15% of BT-474 cells express CRAM-B and nearly five times more CCRL2 expression

was determined in BT-474 cells transfected with CRAM-A plasmid in comparison with untransfected or empty vector transfected BT-474 cells. Thus, with the transfection, CRAM-A became the dominant CCRL2 isotype in BT-474 cells. Similar to the results obtained with CRAM-A-expressing HEK293T cells, CCL19 was the chemokine efficiently removed by CCRL2 (CRAM-A) from the culture media. In this way, the presence of CCRL2 in breast cancer, especially CRAM-A overexpression, can result in the efficient CCL19 removal from the tumor microenvironment.

In a recent study, it was shown that IFN- γ -mediated Th responses constrained basal-like breast cancer cells to adopt a more immune suppressive character [122]. Also, the melanoma cells residing in close proximity to CD8⁺ T cells which are also capable of IFN- γ production [129] or the myeloid leukemia cells directly providing co-stimulatory signals for Th1 responses [130] have been demonstrated to acquire PD-L1 and/or PD-L2 positivity. Similar to melanoma and myeloid leukemia, it may be speculated that basal-like breast cancer cells can utilize an adaptive resistance mechanism that employs inhibitory signaling [122]. Similar to these studies, in our study, CRAM-A overexpression in different IFN- γ -stimulated breast cancer cells can also indicate an adaptation to IFN- γ -mediated signals to evade immunity.

In the light of the current findings presented in this study, we propose that CRAM-A expression in breast cancer upon IFN- γ stimulation may constitute an immune modulatory mechanism. By functioning as an atypical chemokine receptor, CRAM-A, especially and efficiently internalizes CCL19 (compared to CCL5). Accordingly, CCL5 might have pro-tumor functions such as mediating the infiltration of TAMs and formation of new blood vessels [131]. On the other hand, CCL19 down-regulation and reduction in its gradient in the breast tumor microenvironment can directly interfere with the infiltration of CCR7⁺ immune cells including CD4⁺ helper T lymphocytes,

CD8⁺ cytotoxic T lymphocytes (CTLs), and NK cells. Tumor cells can use this mechanism as a tactic to avoid further immune cell chemotaxis in response to initial IFN- γ -mediated anti-tumor immune responses. Therefore, IFN- γ -induced CRAM-A expression in breast cancer may indicate an adaptive resistance mechanism to escape the anti-tumor immunity (Figure 5.1).

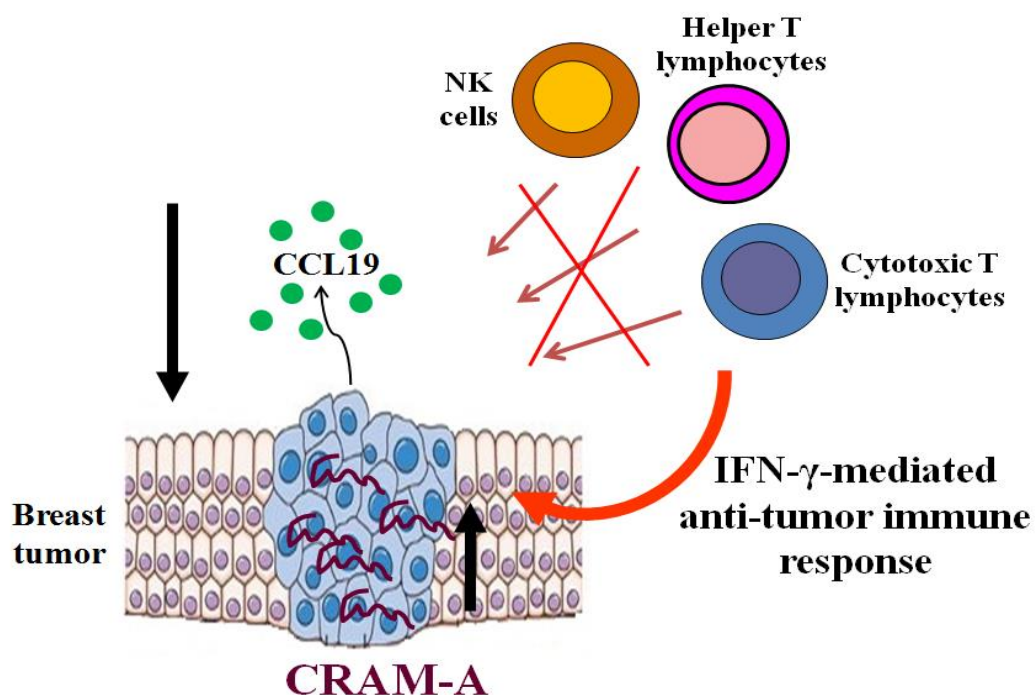


Figure 5.1. Schematic presentation of the hypothesis proposed. NK cells, Th1, and cytotoxic lymphocytes migrate towards CCL19 gradient supplied by the breast tumors. IFN- γ , the common product of these immune cells, leads to the upregulation of CRAM-A in the breast tumor cells. This results in the CCL19 chemokine level reduction; therefore, hampering the infiltration of these anti-tumor effectors.

6. RESULTS AND RECOMMENDATIONS

- CRAM-B gene expression was shown to be frequent and constitutive in immune cells and in certain breast cancer cell lines.
- CRAM-A expression was upregulated or induced upon LPS and IFN- γ stimulation in PBMCs.
- IFN- γ specifically upregulated CRAM-A expression in breast cancer cell lines, independent of their molecular subtypes.
- Triple-negative breast cancer tissues showed higher CCRL2 expression than that of ER⁺ cancers.
- Recombinant CRAM-A and CRAM-B genes were successfully cloned into bicistronic eukaryotic expression vector, and expressed *de novo* in HEK293T and BT-474 and MDA-MB-468 cells.
- In CCRL2-transfected HEK293T cells, no Ca²⁺ mobilization was observed in the presence of CCRL2-specific ligands.
- CRAM-A was specifically internalized in the presence of CCL19.

- CRAM-A was internalized and then showed a trend indicating a recirculation back to the cell surface in the presence of chemerin.
- CRAM-A specifically removed CCL19 from the extracellular milieu.
- Constitutive expression of both CRAM-A and CRAM-B on MDA-MB-231 cells and CRAM-B in BT-474 cells were not associated with the expression of CCRL2-related genes (CCL5, CCL19, chemerin, CCRL1, DARC, D6, CMKLR1, GPR1, CCR1, CCR3, CCR4, CCR5, CCR7).
- Receptor internalization and removal of CCL5 was not efficient in CRAM-A-expressing HEK293T cells and BT-474 breast cancer cells.
- Our results indicate a link between long isoform of CCRL2, CRAM-A, and the regulation of inflammatory response in breast cancer.
- Other than IFN- γ and LPS, different pro-inflammatory mediators such as IL-1, IL-6, TNF- α , GM-CSF, MIP can be used to mimic inflammation *in vitro* in order to determine which CCRL2 variant will be preferentially expressed in different types of breast cancer cell lines.
- The effect of CCRL2 upregulation on breast cancer cell survival, proliferation, invasion and metastasis can be analyzed.

- Especially, the change in CRAM-B expression after inflammatory stimulation can be quantified by real time PCR.
- In order to correlate CCRL2 expression with sub-types of breast cancer, the number of breast cancer tissue samples from different breast cancer sub-types can be increased.
- CCRL2 protein expression level can be determined in breast cancer cell lines.
- The presence of CRAM-A and CRAM-B gene expression can be determined in fresh tumor tissues, in order to determine the dominant isoform.
- SNPs' effects on CCRL2 protein expression and function can be investigated.
- For expression and functional analyses of CRAM-A and CRAM-B, specific antibodies can be generated and used that can distinguish between the two variants.
- ELISA and chemokine removal assay for chemerin can be performed.
- For intracellular localization analysis, GFP-hybrid plasmids can be reconstructed with another cloning strategy; or multicolor confocal microscopy should be performed.

REFERENCES

1. Raman D, Sobolik-Delmaire T, Richmond A: Chemokines in health and disease. *Exp Cell Res* 2011, 317(5):575-589.
2. Feng LY, Ou ZL, Wu FY, Shen ZZ, Shao ZM: Involvement of a novel chemokine decoy receptor CCX-CKR in breast cancer growth, metastasis and patient survival. *Clin Cancer Res* 2009, 15(9):2962-2970.
3. Nibbs RJ, Graham GJ: Immune regulation by atypical chemokine receptors. *Nat Rev Immunol* 2013, 13(11):815-829.
4. Anders HJ, Sayyed SA, Vielhauer V: Questions about chemokine and chemokine receptor antagonism in renal inflammation. *Nephron Exp Nephrol* 2010, 114(2):e33-38.
5. Yin F, Xu Z, Wang Z, Yao H, Shen Z, Yu F, Tang Y, Fu D, Lin S, Lu G *et al*: Elevated chemokine CC-motif receptor-like 2 (CCRL2) promotes cell migration and invasion in glioblastoma. *Biochem Biophys Res Commun* 2012, 429(3-4):168-172.
6. Catusse J, Leick M, Groch M, Clark DJ, Buchner MV, Zirlik K, Burger M: Role of the atypical chemoattractant receptor CRAM in regulating CCL19 induced CCR7 responses in B-cell chronic lymphocytic leukemia. *Mol Cancer* 2010, 9:297.
7. Hartmann TN, Leick M, Ewers S, Diefenbacher A, Schraufstatter I, Honczarenko M, Burger M: Human B cells express the orphan chemokine receptor CRAM-A/B in a maturation-stage-dependent and CCL5-modulated manner. *Immunology* 2008, 125(2):252-262.
8. Leick M, Catusse J, Follo M, Nibbs RJ, Hartmann TN, Veelken H, Burger M: CCL19 is a specific ligand of the constitutively recycling atypical human chemokine receptor CRAM-B. *Immunology* 2010, 129(4):536-546.

9. Sarvaiya PJ, Guo D, Ulasov I, Gabikian P, Lesniak MS: Chemokines in tumor progression and metastasis. *Oncotarget* 2013, 4(12):2171-2185.
10. Mantovani A: The chemokine system: redundancy for robust outputs. *Immunol Today* 1999, 20(6):254-257.
11. Murphy JW, Yuan H, Kong Y, Xiong Y, Lolis EJ: Heterologous quaternary structure of CXCL12 and its relationship to the CC chemokine family. *Proteins* 2010, 78(5):1331-1337.
12. Ali S, Lazennec G: Chemokines: novel targets for breast cancer metastasis. *Cancer Metastasis Rev* 2007, 26(3-4):401-420.
13. Abul K. Abbas AHL, Shiv Pillai: Cellular and Molecular Immunology In., vol. 7; 2012: 41-42.
14. Zlotnik A, Burkhardt AM, Homey B: Homeostatic chemokine receptors and organ-specific metastasis. *Nat Rev Immunol* 2011, 11(9):597-606.
15. Allen SJ, Crown SE, Handel TM: Chemokine: receptor structure, interactions, and antagonism. *Annu Rev Immunol* 2007, 25:787-820.
16. Nomiya H, Osada N, Yoshie O: Systematic classification of vertebrate chemokines based on conserved synteny and evolutionary history. *Genes Cells* 2013, 18(1):1-16.
17. Murdoch C, Finn A: Chemokine receptors and their role in inflammation and infectious diseases. *Blood* 2000, 95(10):3032-3043.
18. Comerford I, McColl SR: Mini-review series: focus on chemokines. *Immunol Cell Biol* 2011, 89(2):183-184.
19. Graham GJ, Locati M, Mantovani A, Rot A, Thelen M: The biochemistry and biology of the atypical chemokine receptors. *Immunol Lett* 2012, 145(1-2):30-38.
20. Mantovani A, Locati M, Vecchi A, Sozzani S, Allavena P: Decoy receptors: a strategy to regulate inflammatory cytokines and chemokines. *Trends Immunol* 2001, 22(6):328-336.

21. Borroni EM, Bonecchi R: Shaping the gradient by nonchemotactic chemokine receptors. *Cell Adh Migr* 2009, 3(2):146-147.
22. Langenes V, Svensson H, Borjesson L, Gustavsson B, Bemark M, Sjoling A, Quiding-Jarbrink M: Expression of the chemokine decoy receptor D6 is decreased in colon adenocarcinomas. *Cancer Immunol Immunother* 2013, 62(11):1687-1695.
23. Hajrasouliha AR, Sadrai Z, Lee HK, Chauhan SK, Dana R: Expression of the chemokine decoy receptor D6 mediates dendritic cell function and promotes corneal allograft rejection. *Mol Vis* 2013, 19:2517-2525.
24. Maksym RB, Tarnowski M, Grymula K, Tarnowska J, Wysoczynski M, Liu R, Czerny B, Ratajczak J, Kucia M, Ratajczak MZ: The role of stromal-derived factor-1--CXCR7 axis in development and cancer. *Eur J Pharmacol* 2009, 625(1-3):31-40.
25. Shimizu S, Brown M, Sengupta R, Penfold ME, Meucci O: CXCR7 protein expression in human adult brain and differentiated neurons. *PLoS One* 2011, 6(5):e20680.
26. Miao Z, Luker KE, Summers BC, Berahovich R, Bhojani MS, Rehemtulla A, Kleer CG, Essner JJ, Nasevicius A, Luker GD *et al*: CXCR7 (RDC1) promotes breast and lung tumor growth in vivo and is expressed on tumor-associated vasculature. *Proc Natl Acad Sci U S A* 2007, 104(40):15735-15740.
27. Odemis V, Lipfert J, Kraft R, Hajek P, Abraham G, Hattermann K, Mentlein R, Engele J: The presumed atypical chemokine receptor CXCR7 signals through G(i/o) proteins in primary rodent astrocytes and human glioma cells. *Glia* 2012, 60(3):372-381.
28. Burns JM, Summers BC, Wang Y, Melikian A, Berahovich R, Miao Z, Penfold ME, Sunshine MJ, Littman DR, Kuo CJ *et al*: A novel chemokine receptor for SDF-1 and I-TAC involved in cell survival, cell adhesion, and tumor development. *J Exp Med* 2006, 203(9):2201-2213.

29. Boldajipour B, Mahabaleshwar H, Kardash E, Reichman-Fried M, Blaser H, Minina S, Wilson D, Xu Q, Raz E: Control of chemokine-guided cell migration by ligand sequestration. *Cell* 2008, 132(3):463-473.
30. Hartmann TN, Grabovsky V, Pasvolsky R, Shulman Z, Buss EC, Spiegel A, Nagler A, Lapidot T, Thelen M, Alon R: A crosstalk between intracellular CXCR7 and CXCR4 involved in rapid CXCL12-triggered integrin activation but not in chemokine-triggered motility of human T lymphocytes and CD34+ cells. *J Leukoc Biol* 2008, 84(4):1130-1140.
31. Levoye A, Balabanian K, Baleux F, Bachelier F, Lagane B: CXCR7 heterodimerizes with CXCR4 and regulates CXCL12-mediated G protein signaling. *Blood* 2009, 113(24):6085-6093.
32. Grymula K, Tarnowski M, Wysoczynski M, Drukala J, Barr FG, Ratajczak J, Kucia M, Ratajczak MZ: Overlapping and distinct role of CXCR7-SDF-1/ITAC and CXCR4-SDF-1 axes in regulating metastatic behavior of human rhabdomyosarcomas. *Int J Cancer* 2010, 127(11):2554-2568.
33. Wang Y, Li G, Stanco A, Long JE, Crawford D, Potter GB, Pleasure SJ, Behrens T, Rubenstein JL: CXCR4 and CXCR7 have distinct functions in regulating interneuron migration. *Neuron* 2011, 69(1):61-76.
34. Hou T, Liang D, Xu L, Huang X, Huang Y, Zhang Y: Atypical chemokine receptors predict lymph node metastasis and prognosis in patients with cervical squamous cell cancer. *Gynecol Oncol* 2013, 130(1):181-187.
35. Comerford I, Litchfield W, Harata-Lee Y, Nibbs RJ, McColl SR: Regulation of chemotactic networks by 'atypical' receptors. *Bioessays* 2007, 29(3):237-247.

36. Comerford I, Milasta S, Morrow V, Milligan G, Nibbs R: The chemokine receptor CCX-CKR mediates effective scavenging of CCL19 in vitro. *Eur J Immunol* 2006, 36(7):1904-1916.
37. Comerford I, Harata-Lee Y, Bunting MD, Gregor C, Kara EE, McColl SR: A myriad of functions and complex regulation of the CCR7/CCL19/CCL21 chemokine axis in the adaptive immune system. *Cytokine Growth Factor Rev* 2013, 24(3):269-283.
38. Comerford I, Nibbs RJ, Litchfield W, Bunting M, Harata-Lee Y, Haylock-Jacobs S, Forrow S, Korner H, McColl SR: The atypical chemokine receptor CCX-CKR scavenges homeostatic chemokines in circulation and tissues and suppresses Th17 responses. *Blood* 2010, 116(20):4130-4140.
39. Bunting MD, Comerford I, Seach N, Hammett MV, Asquith DL, Korner H, Boyd RL, Nibbs RJ, McColl SR: CCX-CKR deficiency alters thymic stroma impairing thymocyte development and promoting autoimmunity. *Blood* 2013, 121(1):118-128.
40. Del Prete A, Bonecchi R, Vecchi A, Mantovani A, Sozzani S: CCRL2, a fringe member of the atypical chemoattractant receptor family. *Eur J Immunol* 2013, 43(6):1418-1422.
41. Monnier J, Lewen S, O'Hara E, Huang K, Tu H, Butcher EC, Zabel BA: Expression, regulation, and function of atypical chemerin receptor CCRL2 on endothelial cells. *J Immunol* 2012, 189(2):956-967.
42. Biber K, Zuurman MW, Homan H, Boddeke HW: Expression of L-CCR in HEK 293 cells reveals functional responses to CCL2, CCL5, CCL7, and CCL8. *J Leukoc Biol* 2003, 74(2):243-251.
43. Zabel BA, Nakae S, Zuniga L, Kim JY, Ohyama T, Alt C, Pan J, Suto H, Soler D, Allen SJ *et al*: Mast cell-expressed orphan receptor CCRL2 binds chemerin and is required for optimal induction of IgE-mediated passive cutaneous anaphylaxis. *J Exp Med* 2008, 205(10):2207-2220.

44. Migeotte I, Franssen JD, Goriely S, Willems F, Parmentier M: Distribution and regulation of expression of the putative human chemokine receptor HCR in leukocyte populations. *Eur J Immunol* 2002, 32(2):494-501.
45. Yoshimura T, Oppenheim JJ: Chemokine-like receptor 1 (CMKLR1) and chemokine (C-C motif) receptor-like 2 (CCRL2); two multifunctional receptors with unusual properties. *Exp Cell Res* 2011, 317(5):674-684.
46. Otero K, Vecchi A, Hirsch E, Kearley J, Vermi W, Del Prete A, Gonzalvo-Feo S, Garlanda C, Azzolino O, Salogni L *et al*: Nonredundant role of CCRL2 in lung dendritic cell trafficking. *Blood* 2010, 116(16):2942-2949.
47. Allavena P, Germano G, Marchesi F, Mantovani A: Chemokines in cancer related inflammation. *Exp Cell Res* 2011, 317(5):664-673.
48. Lazenec G, Richmond A: Chemokines and chemokine receptors: new insights into cancer-related inflammation. *Trends Mol Med* 2010, 16(3):133-144.
49. Yang C, Yu KD, Xu WH, Chen AX, Fan L, Ou ZL, Shao ZM: Effect of genetic variants in two chemokine decoy receptor genes, DARC and CCBP2, on metastatic potential of breast cancer. *PLoS One* 2013, 8(11):e78901.
50. Shen H, Schuster R, Stringer KF, Waltz SE, Lentsch AB: The Duffy antigen/receptor for chemokines (DARC) regulates prostate tumor growth. *Faseb J* 2006, 20(1):59-64.
51. Wu FY, Ou ZL, Feng LY, Luo JM, Wang LP, Shen ZZ, Shao ZM: Chemokine decoy receptor d6 plays a negative role in human breast cancer. *Mol Cancer Res* 2008, 6(8):1276-1288.
52. Anders HJ, Romagnani P, Mantovani A: Pathomechanisms: homeostatic chemokines in health, tissue regeneration, and progressive diseases. *Trends Mol Med* 2014.

53. Wang J, Shiozawa Y, Wang Y, Jung Y, Pienta KJ, Mehra R, Loberg R, Taichman RS: The role of CXCR7/RDC1 as a chemokine receptor for CXCL12/SDF-1 in prostate cancer. *J Biol Chem* 2008, 283(7):4283-4294.
54. Zhu Z, Sun Z, Wang Z, Guo P, Zheng X, Xu H: Prognostic impact of atypical chemokine receptor expression in patients with gastric cancer. *J Surg Res* 2013, 183(1):177-183.
55. Hanahan D, Weinberg RA: Hallmarks of cancer: the next generation. *Cell* 2011, 144(5):646-674.
56. Raman D, Baugher PJ, Thu YM, Richmond A: Role of chemokines in tumor growth. *Cancer Lett* 2007, 256(2):137-165.
57. Li S, Lin YC, Ho CT, Lin PY, Suzawa M, Wang HC, Chu CL, Chen DY, Lin CC: Formulated extract from multiple citrus peels impairs dendritic cell functions and attenuates allergic contact hypersensitivity. *Int Immunopharmacol* 2014.
58. Mittal D, Gubin MM, Schreiber RD, Smyth MJ: New insights into cancer immunoediting and its three component phases-elimination, equilibrium and escape. *Curr Opin Immunol* 2014, 27C:16-25.
59. Quezada SA, Peggs KS, Simpson TR, Allison JP: Shifting the equilibrium in cancer immunoediting: from tumor tolerance to eradication. *Immunol Rev* 2011, 241(1):104-118.
60. Dunn GP, Bruce AT, Ikeda H, Old LJ, Schreiber RD: Cancer immunoediting: from immunosurveillance to tumor escape. *Nat Immunol* 2002, 3(11):991-998.
61. Muller-Hermelink N, Braumuller H, Pichler B, Wieder T, Mailhammer R, Schaak K, Ghoreschi K, Yazdi A, Haubner R, Sander CA *et al*: TNFR1 signaling and IFN-gamma signaling determine whether T cells induce tumor dormancy or promote multistage carcinogenesis. *Cancer Cell* 2008, 13(6):507-518.

62. Braumuller H, Wieder T, Brenner E, Assmann S, Hahn M, Alkhaled M, Schilbach K, Essmann F, Kneilling M, Griessinger C *et al*: T-helper-1-cell cytokines drive cancer into senescence. *Nature* 2013, 494(7437):361-365.
63. Watt J, Kocher HM: The desmoplastic stroma of pancreatic cancer is a barrier to immune cell infiltration. *Oncoimmunology* 2013, 2(12):e26788.
64. Romero I, Garrido C, Algarra I, Collado A, Garrido F, Garcia-Lora AM: T lymphocytes restrain spontaneous metastases in permanent dormancy. *Cancer Res* 2014.
65. Lam SW, Jimenez CR, Boven E: Breast cancer classification by proteomic technologies: current state of knowledge. *Cancer Treat Rev* 2014, 40(1):129-138.
66. Hollestelle A, Nagel JH, Smid M, Lam S, Elstrodt F, Wasielewski M, Ng SS, French PJ, Peeters JK, Rozendaal MJ *et al*: Distinct gene mutation profiles among luminal-type and basal-type breast cancer cell lines. *Breast Cancer Res Treat* 2010, 121(1):53-64.
67. Kao J, Salari K, Bocanegra M, Choi YL, Girard L, Gandhi J, Kwei KA, Hernandez-Boussard T, Wang P, Gazdar AF *et al*: Molecular profiling of breast cancer cell lines defines relevant tumor models and provides a resource for cancer gene discovery. *PLoS One* 2009, 4(7):e6146.
68. Cadoo KA, Fornier MN, Morris PG: Biological subtypes of breast cancer: current concepts and implications for recurrence patterns. *Q J Nucl Med Mol Imaging* 2013, 57(4):312-321.
69. Lavasani MA, Moinfar F: Molecular classification of breast carcinomas with particular emphasis on "basal-like" carcinoma: a critical review. *J Biophotonics* 2012, 5(4):345-366.
70. Longo DL: Harrison's Hematology and Oncology, vol. 17; 2010.

71. Stephen B. Edge DRB, Carolyn C. Compton, April G. Fritz, Frederick L. Greene, Andy Trotti: AJCC Cancer Staging Manual. *Springer* 2010, Seventh Edition:347-367.
72. Longo DL: Harrison's Hematology and Oncology. In: *Mc Graw Hill*. vol. 17; 2010: 459-471.
73. Vinay Kumar AKA, Jon C. Aster: Robbins Basic Pathology. In., Nineth Edition edn: Elsevier; 2013: 704-714.
74. Hagop M. Kantarjian RAW, Charles A. Koller: The MD Anderson Manual of Medical Oncology. *Mc Graw Hill Medical* 2010, Second Edition:635-673.
75. Chen EP, Markosyan N, Connolly E, Lawson JA, Li X, Grant GR, Grosser T, Fitzgerald GA, Smyth EM: Myeloid COX-2 deletion reduces mammary tumor growth through enhanced cytotoxic T lymphocyte function. *Carcinogenesis* 2014.
76. Jang JY, Lee JK, Jeon YK, Kim CW: Exosome derived from epigallocatechin gallate treated breast cancer cells suppresses tumor growth by inhibiting tumor-associated macrophage infiltration and M2 polarization. *BMC Cancer* 2013, 13:421.
77. Zhang Y, Lv D, Kim HJ, Kurt RA, Bu W, Li Y, Ma X: A novel role of hematopoietic CCL5 in promoting triple-negative mammary tumor progression by regulating generation of myeloid-derived suppressor cells. *Cell Res* 2013, 23(3):394-408.
78. Gonzalez-Martin A, Gomez L, Lustgarten J, Mira E, Manes S: Maximal T cell-mediated antitumor responses rely upon CCR5 expression in both CD4(+) and CD8(+) T cells. *Cancer Res* 2011, 71(16):5455-5466.
79. Mulligan AM, Raitman I, Feeley L, Pinnaduwege D, Nguyen LT, O'Malley FP, Ohashi PS, Andrulis IL: Tumoral lymphocytic infiltration and expression of the chemokine CXCL10 in breast cancers from the Ontario Familial Breast Cancer Registry. *Clin Cancer Res* 2013, 19(2):336-346.

80. Cunningham HD, Shannon LA, Calloway PA, Fassold BC, Dunwiddie I, Vielhauer G, Zhang M, Vines CM: Expression of the C-C chemokine receptor 7 mediates metastasis of breast cancer to the lymph nodes in mice. *Transl Oncol* 2010, 3(6):354-361.
81. Phan-Lai V, Kievit FM, Florczyk SJ, Wang K, Disis ML, Zhang M: CCL21 and IFN γ recruit and activate tumor specific T cells in 3D scaffold model of breast cancer. *Anticancer Agents Med Chem* 2014, 14(2):204-210.
82. Wang C, Wu WK, Liu X, To KF, Chen GG, Yu J, Ng EK: Increased serum chemerin level promotes cellular invasiveness in gastric cancer: a clinical and experimental study. *Peptides* 2014, 51:131-138.
83. Wang N, Wang QJ, Feng YY, Shang W, Cai M: Overexpression of chemerin was associated with tumor angiogenesis and poor clinical outcome in squamous cell carcinoma of the oral tongue. *Clin Oral Investig* 2014, 18(3):997-1004.
84. Dupont J, Reverchon M, Cloix L, Froment P, Rame C: Involvement of adipokines, AMPK, PI3K and the PPAR signaling pathways in ovarian follicle development and cancer. *Int J Dev Biol* 2012, 56(10-12):959-967.
85. Rama D, Esendagli G, Guc D: Expression of chemokine-like receptor 1 (CMKLR1) on J744A.1 macrophages co-cultured with fibroblast and/or tumor cells: modeling the influence of microenvironment. *Cell Immunol* 2011, 271(1):134-140.
86. Lanca T, Costa MF, Goncalves-Sousa N, Rei M, Grosso AR, Penido C, Silva-Santos B: Protective role of the inflammatory CCR2/CCL2 chemokine pathway through recruitment of type 1 cytotoxic gammadelta T lymphocytes to tumor beds. *J Immunol* 2013, 190(12):6673-6680.
87. Thakur A, Schalk D, Sarkar SH, Al-Khadimi Z, Sarkar FH, Lum LG: A Th1 cytokine-enriched microenvironment enhances tumor killing by

- activated T cells armed with bispecific antibodies and inhibits the development of myeloid-derived suppressor cells. *Cancer Immunol Immunother* 2012, 61(4):497-509.
88. Olkhanud PB, Baatar D, Bodogai M, Hakim F, Gress R, Anderson RL, Deng J, Xu M, Briest S, Biragyn A: Breast cancer lung metastasis requires expression of chemokine receptor CCR4 and regulatory T cells. *Cancer Res* 2009, 69(14):5996-6004.
 89. Shiao SL, Coussens LM: The tumor-immune microenvironment and response to radiation therapy. *J Mammary Gland Biol Neoplasia* 2010, 15(4):411-421.
 90. Zhang Y, Cheng S, Zhang M, Zhen L, Pang D, Zhang Q, Li Z: High-infiltration of tumor-associated macrophages predicts unfavorable clinical outcome for node-negative breast cancer. *PLoS One* 2013, 8(9):e76147.
 91. Strachan DC, Ruffell B, Oei Y, Bissell MJ, Coussens LM, Pryer N, Daniel D: CSF1R inhibition delays cervical and mammary tumor growth in murine models by attenuating the turnover of tumor-associated macrophages and enhancing infiltration by CD8 T cells. *Oncoimmunology* 2013, 2(12):e26968.
 92. de la Cruz-Merino L, Barco-Sanchez A, Henao Carrasco F, Nogales Fernandez E, Vallejo Benitez A, Brugal Molina J, Martinez Peinado A, Grueso Lopez A, Ruiz Borrego M, Codes Manuel de Villena M *et al*: New insights into the role of the immune microenvironment in breast carcinoma. *Clin Dev Immunol* 2013, 2013:785317.
 93. Obeid E, Nanda R, Fu YX, Olopade OI: The role of tumor-associated macrophages in breast cancer progression (review). *Int J Oncol* 2013, 43(1):5-12.
 94. Emens LA: Breast cancer immunobiology driving immunotherapy: vaccines and immune checkpoint blockade. *Expert Rev Anticancer Ther* 2012, 12(12):1597-1611.

95. Whiteside TL: Immune responses to cancer: are they potential biomarkers of prognosis? *Front Oncol* 2013, 3:107.
96. Loi S, Michiels S, Salgado R, Sirtaine N, Jose V, Fumagalli D, Kellokumpu-Lehtinen PL, Bono P, Kataja V, Desmedt C *et al*: Tumor infiltrating lymphocytes is prognostic and predictive for trastuzumab benefit in early breast cancer: results from the FinHER trial. *Ann Oncol* 2014.
97. Gameiro SR, Jammeh ML, Wattenberg MM, Tsang KY, Ferrone S, Hodge JW: Radiation-induced immunogenic modulation of tumor enhances antigen processing and calreticulin exposure, resulting in enhanced T-cell killing. *Oncotarget* 2014, 5(2):403-416.
98. Chen X, Yang Y, Zhou Q, Weiss JM, Howard OZ, McPherson JM, Wakefield LM, Oppenheim JJ: Effective chemoimmunotherapy with anti-TGFbeta antibody and cyclophosphamide in a mouse model of breast cancer. *PLoS One* 2014, 9(1):e85398.
99. Goodman WA, Cooper KD, McCormick TS: Regulation generation: the suppressive functions of human regulatory T cells. *Crit Rev Immunol* 2012, 32(1):65-79.
100. Sun S, Fei X, Mao Y, Wang X, Garfield DH, Huang O, Wang J, Yuan F, Sun L, Yu Q *et al*: PD-1(+) immune cell infiltration inversely correlates with survival of operable breast cancer patients. *Cancer Immunol Immunother* 2014, 63(4):395-406.
101. Becton DaC: pIRES2-EGFP Vector Information. *BD Biosciences Clontech* 2002:1-3.
102. Manual IU: GFP Fusion TOPO TA Expression Kits. *Invitrogen* 2004:1-38.
103. Bailey S, Macardle PJ: A flow cytometric comparison of Indo-1 to fluo-3 and Fura Red excited with low power lasers for detecting Ca(2+) flux. *J Immunol Methods* 2006, 311(1-2):220-225.
104. <http://genetics.bwh.harvard.edu/pph2/>.

105. http://www.lgcstandards-atcc.org/products/all/CRL-11268.aspx?geo_country=tr.
106. Patel L, Charlton SJ, Chambers JK, Macphee CH: Expression and functional analysis of chemokine receptors in human peripheral blood leukocyte populations. *Cytokine* 2001, 14(1):27-36.
107. Fan P, Kyaw H, Su K, Zeng Z, Augustus M, Carter KC, Li Y: Cloning and characterization of a novel human chemokine receptor. *Biochem Biophys Res Commun* 1998, 243(1):264-268.
108. Oostendorp J, Hylkema MN, Luinge M, Geerlings M, Meurs H, Timens W, Zaagsma J, Postma DS, Boddeke HW, Biber K: Localization and enhanced mRNA expression of the orphan chemokine receptor L-CCR in the lung in a murine model of ovalbumin-induced airway inflammation. *J Histochem Cytochem* 2004, 52(3):401-410.
109. Zuurman MW, Heeroma J, Brouwer N, Boddeke HW, Biber K: LPS-induced expression of a novel chemokine receptor (L-CCR) in mouse glial cells in vitro and in vivo. *Glia* 2003, 41(4):327-336.
110. Galligan CL, Matsuyama W, Matsukawa A, Mizuta H, Hodge DR, Howard OM, Yoshimura T: Up-regulated expression and activation of the orphan chemokine receptor, CCRL2, in rheumatoid arthritis. *Arthritis Rheum* 2004, 50(6):1806-1814.
111. Zhao P, Yang Y, Feng H, Zhao L, Qin J, Zhang T, Wang H, Yang S, Xia X: Global gene expression changes in BV2 microglial cell line during rabies virus infection. *Infect Genet Evol* 2013, 20:257-269.
112. Velasco-Velazquez M, Pestell RG: The CCL5/CCR5 axis promotes metastasis in basal breast cancer. *Oncoimmunology* 2013, 2(4):e23660.
113. Nguyen-Hoai T, Baldenhofer G, Ahmed MS, Pham-Duc M, Gries M, Lipp M, Dorken B, Pezzutto A, Westermann J: CCL19 (ELC) improves TH1-polarized immune responses and protective immunity in a murine Her2/neu DNA vaccination model. *J Gene Med* 2012, 14(2):128-137.

114. Bozaoglu K, Curran JE, Stocker CJ, Zaibi MS, Segal D, Konstantopoulos N, Morrison S, Carless M, Dyer TD, Cole SA *et al*: Chemerin, a novel adipokine in the regulation of angiogenesis. *J Clin Endocrinol Metab* 2010, 95(5):2476-2485.
115. Berndt B, Haverkamp S, Reith G, Keil S, Niggemann B, Zanker KS, Dittmar T: Fusion of CCL21 non-migratory active breast epithelial and breast cancer cells give rise to CCL21 migratory active tumor hybrid cell lines. *PLoS One* 2013, 8(5):e63711.
116. Swamydas M, Ricci K, Rego SL, Dreau D: Mesenchymal stem cell-derived CCL-9 and CCL-5 promote mammary tumor cell invasion and the activation of matrix metalloproteinases. *Cell Adh Migr* 2013, 7(3):315-324.
117. Li JY, Ou ZL, Yu SJ, Gu XL, Yang C, Chen AX, Di GH, Shen ZZ, Shao ZM: The chemokine receptor CCR4 promotes tumor growth and lung metastasis in breast cancer. *Breast Cancer Res Treat* 2012, 131(3):837-848.
118. Sato W: Chemokine receptor expression of T cells in the cerebrospinal fluid of relapsing multiple sclerosis. *Nihon Rinsho Meneki Gakkai Kaishi* 2014, 37(2):83-89.
119. Galkina E, Thatte J, Dabak V, Williams MB, Ley K, Braciale TJ: Preferential migration of effector CD8+ T cells into the interstitium of the normal lung. *J Clin Invest* 2005, 115(12):3473-3483.
120. Taube JH, Herschkowitz JI, Komurov K, Zhou AY, Gupta S, Yang J, Hartwell K, Onder TT, Gupta PB, Evans KW *et al*: Core epithelial-to-mesenchymal transition interactome gene-expression signature is associated with claudin-low and metaplastic breast cancer subtypes. *Proc Natl Acad Sci U S A* 2010, 107(35):15449-15454.
121. Cufi S, Vazquez-Martin A, Oliveras-Ferraros C, Martin-Castillo B, Vellon L, Menendez JA: Autophagy positively regulates the CD44(+)

- CD24(-/low) breast cancer stem-like phenotype. *Cell Cycle* 2011, 10(22):3871-3885.
122. Karasar P, Esendagli G: T helper responses are maintained by basal-like breast cancer cells and confer to immune modulation via upregulation of PD-1 ligands. *Breast Cancer Res Treat* 2014, 145(3):605-614.
 123. Douglas RM, Chen AH, Iniguez A, Wang J, Fu Z, Powell FL, Jr., Haddad GG, Yao H: Chemokine receptor-like 2 is involved in ischemic brain injury. *J Exp Stroke Transl Med* 2013, 6:1-6.
 124. Clark VJ, Dean M: Characterisation of SNP haplotype structure in chemokine and chemokine receptor genes using CEPH pedigrees and statistical estimation. *Hum Genomics* 2004, 1(3):195-207.
 125. Rajagopal S, Kim J, Ahn S, Craig S, Lam CM, Gerard NP, Gerard C, Lefkowitz RJ: Beta-arrestin- but not G protein-mediated signaling by the "decoy" receptor CXCR7. *Proc Natl Acad Sci U S A* 2010, 107(2):628-632.
 126. O'Hayre M, Salanga CL, Handel TM, Allen SJ: Chemokines and cancer: migration, intracellular signalling and intercellular communication in the microenvironment. *Biochem J* 2008, 409(3):635-649.
 127. Yoshimura T, Oppenheim JJ: Chemerin reveals its chimeric nature. *J Exp Med* 2008, 205(10):2187-2190.
 128. Abedi MR, Caponigro G, Kamb A: Green fluorescent protein as a scaffold for intracellular presentation of peptides. *Nucleic Acids Res* 1998, 26(2):623-630.
 129. Taube JM, Anders RA, Young GD, Xu H, Sharma R, McMiller TL, Chen S, Klein AP, Pardoll DM, Topalian SL *et al*: Colocalization of inflammatory response with B7-h1 expression in human melanocytic lesions supports an adaptive resistance mechanism of immune escape. *Sci Transl Med* 2012, 4(127):127ra137.

130. Dolen Y, Esendagli G: Myeloid leukemia cells with a B7-2(+) subpopulation provoke Th-cell responses and become immunosuppressive through the modulation of B7 ligands. *Eur J Immunol* 2013, 43(3):747-757.
131. Siveen KS, Kuttan G: Role of macrophages in tumour progression. *Immunol Lett* 2009, 123(2):97-102.

APPENDICES

Appendix 1. Research Ethics Approval



Sayı: B.30.Z.HAC.0.05.06.00/

64

09 Eylül 2011

HAYVAN DENEYLERİ YEREL ETİK KURUL KARARI

TOPLANTI TARİHİ : 08.09.2011 (PERŞEMBE)
TOPLANTI SAYISI : 2011/5
DOSYA KAYIT NUMARASI : 2011/46
KARAR NUMARASI : 2011/46-2
ARAŞTIRMA YÜRÜTÜCÜSÜ : Dr. Güneş Esendağlı
HAYVAN DENEYLERİNDEN SORUMLU ARAŞTIRMACI : Dr. Güneş Esendağlı
YARDIMCI ARAŞTIRMACILAR : Uzm. Biol. Bahar Çamurdanoğlu
ONAYLANAN HAYVAN TÜRÜ ve SAYISI : 64 adet CD-1 nude fare
ONAY GEÇERLİLİK SÜRESİ : 36 ay

Üniversitemiz Onkoloji Enstitüsü Temel Onkoloji Anabilim Dalı öğretim görevlilerinden Dr. Güneş Esendağlı'nın yürüttüğü olduğu 2011/46 dosya numaralı ve "*Meme Kanseri Hücrelerinde CCRL2 Ekspresyonu ve Anti-Tümör İmmün Yanıtları Üzerine Etkisi*" isimli çalışmada, Hayvan Deneyleri Yerel Etik Kurulu Yönergesi'ne göre uygun bulunarak oy birliği ile onaylanmasına karar verilmiştir.

Sorumlu araştırmacı deneylere başlangıç tarihini Etik Kurula bildirmekle yükümlüdür.

Prof. Dr. Hakan S. ORER
Etik Kurul Başkanı



T.C
GAZİ ÜNİVERSİTESİ TIP FAKÜLTESİ YEREL ETİK KURULU
RESEARCH ETHICS COMMITTEE OF MEDICAL FACULTY, GAZI UNIVERSTY
ANKARA-TÜRKİYE
ARAŞTIRMA BAŞVURUSU ONAYI
İLAÇ DIŞI KLİNİK ÇALIŞMALAR

BAŞVURU BİLGİLERİ	PROTOKOL ADI	"Proliferatif ve tümöral meme lezyonlarına eşlik eden kolumnar hücreli lezyonların proliferasyon, diferansiyasyon ve invazyon potansiyeli profilinin immünhistokimyasal yöntemle değerlendirilmesi"		
	SORUMLU ARAŞTIRICI UNVANI, / ADI	Yrd.Doç.Dr.Güldal Yılmaz		
DEĞERLENDİRİLEN İLGİLİ BELGELER	Belge Adı	Tarihi / değişiklik No.su	Dili Türkçe	
	ARAŞTIRMA PROTOKOLÜ			
KARAR BİLGİLERİ	Karar No: 361	Tarih : 15 Haziran 2009		
	Üniversitemiz Tıp Fakültesinde yapılması tasarlanan ve yukarıdaki künyede kayıtlı araştırma projesine ait dosya; araştırmanın gerekçe, amaç, yaklaşım, yöntemler ve aydınlatılmış onamın yeterliliği yönünden incelenmiş, bütçe dışında uygun olduğuna karar verilmiştir. Etik Kurul kararı; projenin bütçesi BAP tarafından kabul edildiği takdirde yürürlüğe girecek olup, BAP kararının Etik Kurula bildirilmesi gerekmektedir.			
ETİK KURUL BİLGİLERİ				
ÇALIŞMA ESASI	İYİ KLİNİK UYGULAMALAR KILAVUZU, HELSİNKİ BELGESİ, BİYOETİK SÖZLEŞMESİ			

ÜYELER

Ünvanı / Adı / Soyadı Uyeliği	Uzmanlık Dalı	Kurumu	Cinsiyeti	İlişki (*)		Katılım (**)		İmza
				x	E	xx	E	
Prof.Dr.Necla BUYAN BAŞKAN	Çocuk Sağlığı ve Hastalıkları - Nefroloji	G.Ü.T.F Çocuk Sağ.ve Hast.A.D.	K	x	H	xx	E	
Prof. Dr.Firdevs Aktaş UYE	Enfeksiyon	G.Ü.T.F Enfeksiyon Hast. A.D.	K	x	H	xx	E	
Prof. Dr.Aysel ARICIOĞLU UYE	Tıbbi Biyokimya	G.Ü.T.F Tıbbi Biyokimya A.D.	K	x	H	xx	E	
Prof.Dr.Fatma ATALAY UYE	Fiziksel Tıp ve Rehabilitasyon	G.Ü.T.F Fiziksel Tıp ve Reha.A.D.	K	x	H	X	H	Katılmadı
Prof.Dr.Çağatay ÇİFTER UYE	Genel Cerrahi	G.Ü.T.F Genel Cerrahi A.D.	E	x	H	xx	E	
Prof.Dr.Seyhan ERSAN UYE	Farmasötik Kimya Ecz. Fak.	G.Ü.E.F (Ecz.Fak.) Farmasötik Kimya	K	x	H	X	H	Katılmadı
Prof.Dr.Reha KURUOĞLU UYE	Noroloji	G.Ü.T.F Noroloji A.D.	E	x	H	xx	E	
Doç.Dr.Nesrin ÇOBANOĞLU UYE	Tıp Etiği ve Tıp Tarihi	G.Ü.T.F Tıp Etiği ve Tıp tarihi A.D.	K	x	H	xx	E	
Doç.Dr.Mehmet Ali Ergun UYE	Tıbbi Genetik	G.Ü.T.F Tıbbi Genetik A.D.	E	x	H	xx	E	
Doç.Dr.Aylar POYRAZ UYE	Tıbbi Patoloji	G.Ü.T.F Tıbbi Patoloji A.D.	K	x	H	xx	E	
Doç.Dr.Canar ULUOĞLU UYE	Tıbbi Farmakoloji	G.Ü.T.F Tıbbi Farmakoloji A.D.	K	x	H	xx	E	
Doç.Dr.Münci YAĞCI UYE	İç Hastalıkları - Hematoloji	G.Ü.T.F İç Hastalıkları A.D.	E	x	H	xx	E	
Doç.Dr.Birol DEMİREL UYE	Adli Tıp	G.Ü.T.F Adli Tıp A.D.	E	x	H	xx	E	
Hukuk Müşaviri Adem GELİR UYE	Hukuk Müşavirliği	Rektörlük Hukuk Müşavirliği	E	x	H	xx	E	

*Araştırma ile İlişki

** Toplantıda Bulunma



Sayı: B.30.2.HAC.0.05.07.00 1961

ARAŞTIRMA PROJESİ DEĞERLENDİRME RAPORU

Toplantı Tarihi : 28 KASIM 2012 ÇARŞAMBA
Toplantı No : 2012/11
Proje No : LUT 12/153 (Değerlendirme Tarihi 28.11.2012)
Karar No : LUT 12/153 - 35

Üniversitemiz Kanser Enstitüsü Temel Onkoloji Anabilim Dalı öğretim üyelerinden Doç. Dr. Güneş Esendağlı'nın sorumlu araştırmacı olduğu Uzm. Biol. Gürcan Tunalı ile birlikte çalışacakları Biol. Pınar Karasar'ın tezi olan LUT 12/153 kayıt numaralı ve "**Meme Kanseri Hücrelerinde Kostimülatör B7 Ailesi Ligandlarının Ekspresyonu ve Yardımcı T Hücre Yanıtları Üzerine Etkisi**" başlıklı proje önerisi Kurulumuzda değerlendirilmiş olup, etik açıdan uygun bulunmuştur.

- | | |
|---|--|
| 1. Prof. Dr. Nurten Akarsu (Başkan) | 9 Prof. Dr. Songül Varzoğlu (Üye) |
| 2. Prof. Dr. Nüket Örnek Buken (Üye) | 10. Prof. Dr. Melahat Görduysus (Üye) |
| İZİNLİ | |
| 3. Prof. Dr. Hakan S. Ozer (Üye) | 11. Doç. Dr. R. Köksal Özgül (Üye) |
| 4. Prof. Dr. Sevdâ F. Müftüoğlu (Üye) | 12. Doç. Dr. Cansın Saçkesen (Üye) |
| 5. Prof. Dr. Cenk Sökmensüer (Üye) | 13 Doç. Dr. Ayşe Lale Doğan (Üye) |
| 6. Prof. Dr. Kafiye Eroğlu (Üye) | 14. Doç. Dr. S. Kutay Demirkan (Üye) |
| İZİNLİ | |
| 7. Prof. Dr. Volga Bayrakçı Tunay (Üye) | 15. Yrd. Doç. Dr. H. Hüsrev Turnagöl (Üye) |
| GÖREVLİ | |
| 8. Prof. Dr. Yılmaz Selim Erdal (Üye) | 16. Av. Meltem Onurlu (Üye) |



T.C.
HACETTEPE ÜNİVERSİTESİ
Girişimsel Olmayan Klinik Araştırmalar Etik Kurulu

Sayı : 16969557 - (925)

ARAŞTIRMA PROJESİ DEĞERLENDİRME RAPORU

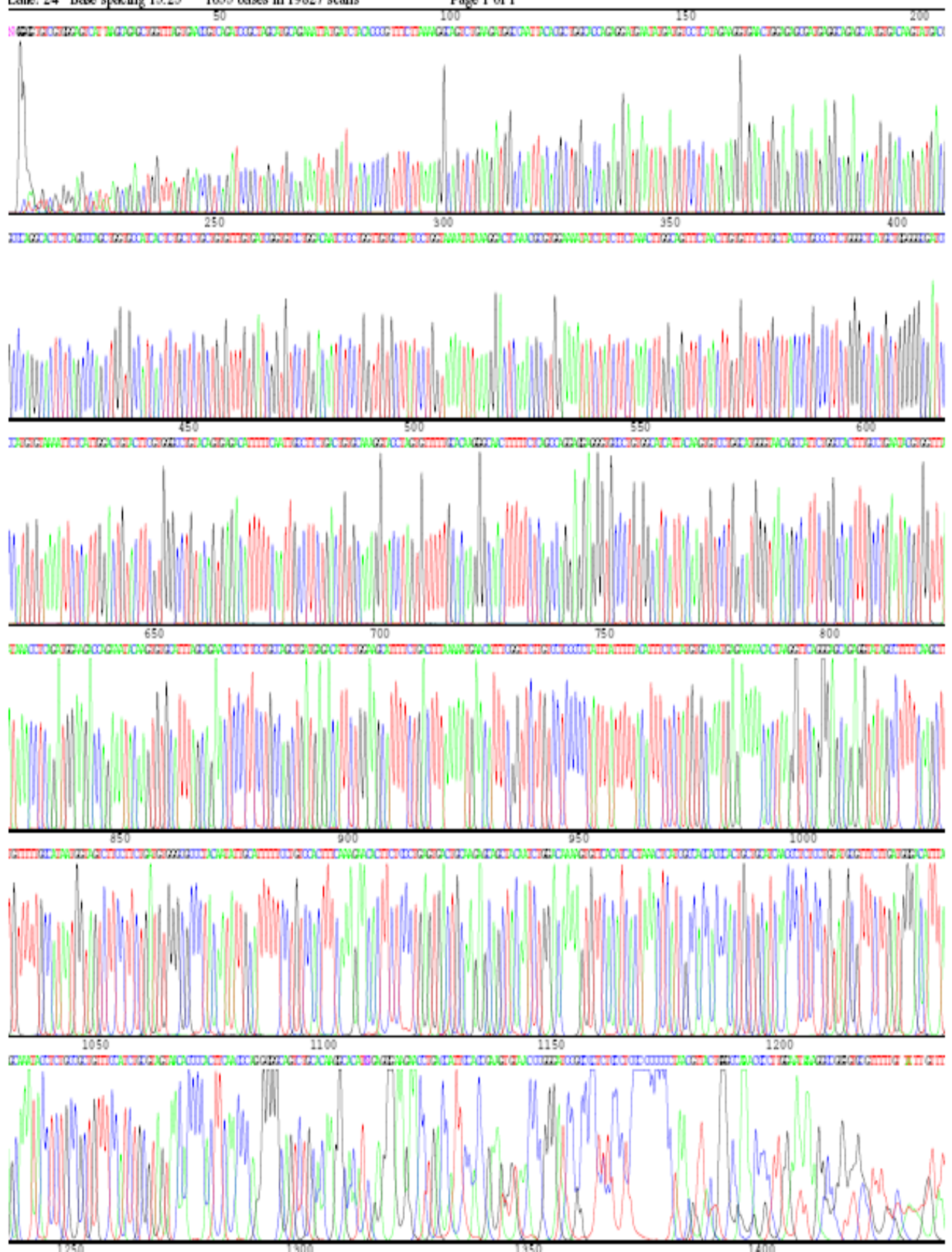
Toplantı Tarihi : 03.09.2014 ÇARŞAMBA
Toplantı No : 2014/13
Proje No : GO 14/440 (Değerlendirme Tarihi 03.09.2014)
Karar No : GO 14/440 - 32

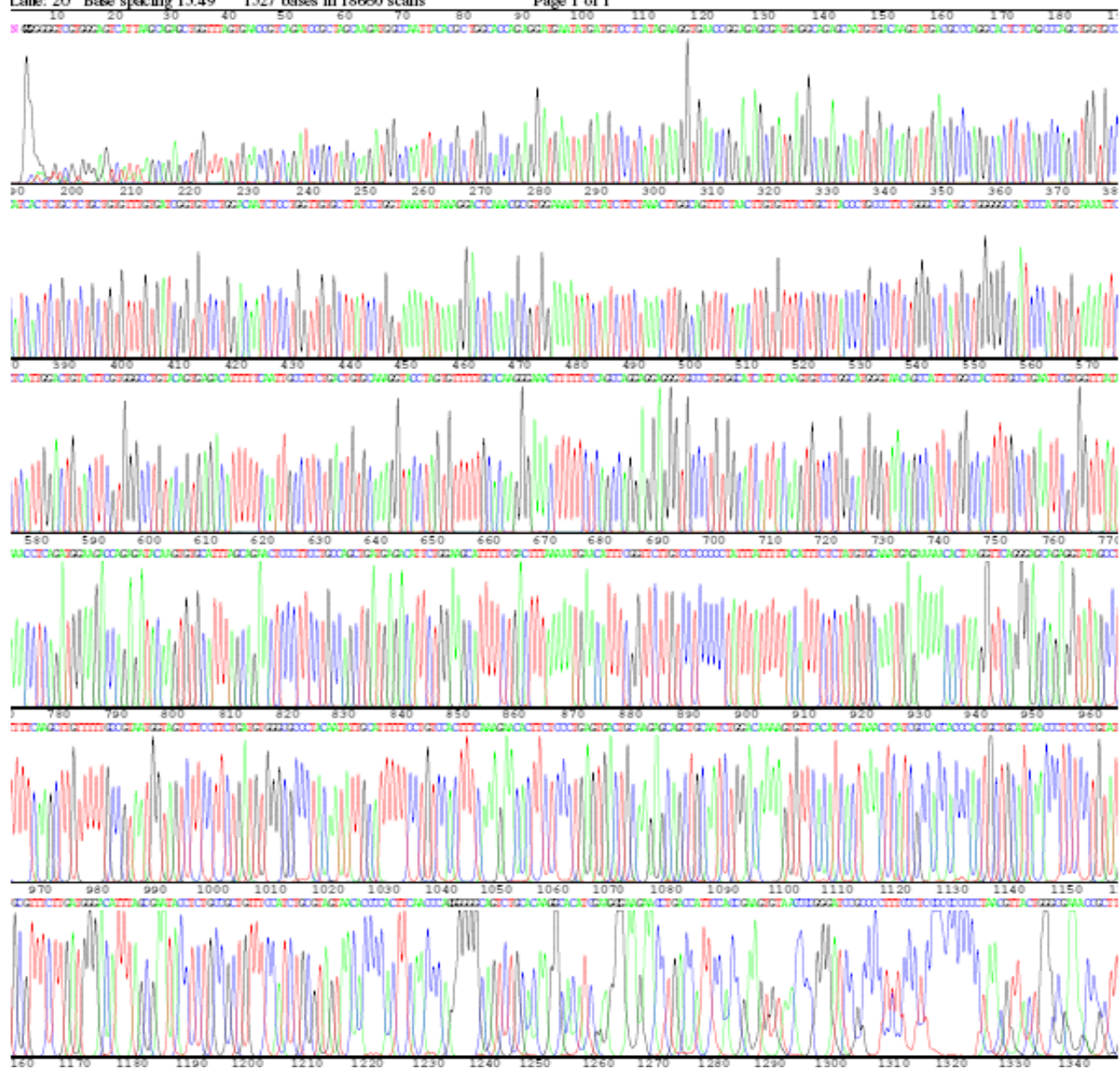
Üniversitemiz Kanser Enstitüsü Temel Onkoloji Anabilim Dalı öğretim üyelerinden Doç.Dr.Güneş ESENDAĞLI'nın sorumlu araştırmacısı olduğu Doç.Dr.Güldal YILMAZ ile birlikte çalışacakları Uzm.Biol.Parisa SARMADI'nin tezi olan GO 14/440 kayıt numaralı ve "**CCRL2 Atipik Kemokin Reseptörü Varyantlarının Meme Kanseri Hücrelerinde Ekspresyonu ve Fonksiyonel Analizi**" başlıklı proje önerisi araştırmanın gerekeçe, amaç, yaklaşım ve yöntemleri dikkate alınarak incelenmiş olup, etik açıdan uygun bulunmuştur.

- | | | |
|---|---------|--|
| 1.Prof. Dr. Nurten Akarsu (Başkan) | İZİNLI | 9 Prof. Dr. Melahat Görduysus (Üye) |
| 2. Prof. Dr. Nuket Örnek Buken (Üye) | GÖREVLİ | 10. Prof. Dr. Cansın Saçkesen (Üye) |
| 3. Prof. Dr. M. Yıldırım Sarı (Üye) | İZİNLI | 11. Prof. Dr. R. Köksal Özgül (Üye) |
| 4. Prof. Dr. Sevda F. Müftüoğlu (Üye) | İZİNLI | 12. Prof. Dr. Ayşe Lale Doğan (Üye) |
| 5. Prof. Dr. Cenk Sokmensüer (Üye) | İZİNLI | 13 Doç. Dr. S. Kutay Demirkan (Üye) |
| 6. Prof. Dr. Volga Bayrakçı Tunay (Üye) | İZİNLI | 14. Prof. Dr Leyla Dinç (Üye) |
| 7. Prof. Dr. Songül Vaizoğlu (Üye) | İZİNLI | 15. Yrd. Doç. Dr. H. Hüsrev Turnagöl (Üye) |
| 8. Prof. Dr. Yılmaz Selim Erdal (Üye) | İZİNLI | 16. Av. Meltem Onurlu (Üye) |

Appendix 2. Results of DNA sequencing analyses.

Appendix Figure 1. Results of DNA sequencing analysis for pCRAM-A-IRES2-EGFP and pCRAM-B-IRES2-EGFP recombinant plasmids.





Appendix Figure 2. Results of DNA sequencing analysis for pcDNA3.1/CRAM-A-CT-GFP and pcDNA3.1/CRAM-B-CT-GFP recombinant plasmids.

Appendix 3. Scientific meetings where the data of this thesis were presented and the related prize.

Poster and Oral Presentations

Sarmadi P., Esendagli G. (2014) CCRL2 atypical chemokine receptor variants' expression and functional analysis in breast cancer cells. **2nd International Molecular Immunology & Immunogenetics Congress (MIMIC-II)**, Antalya, Turkey, P-086, P89.

Sarmadi P., Esendagli G. (2013) CRAM-A ve CRAM-B atipik kemokin reseptörlerinin klonlanması ve fonksiyonel analizi. **22. Ulusal İmmünoloji Kongresi**, Çeşme, Türkiye, P-117, Ref. No: 36, S131.

Sarmadi P., Esendagli G. (2013) Meme kanseri hücrelerine aktarılmak üzere CRAM-A ve CRAM-B atipik kemokin reseptörlerinin klonlanması ve fonksiyonel analizi. **20. Ulusal Kanser Kongresi**, Antalya, Türkiye, Ref. No: S031, S15.

Sarmadi P., Esendagli G. (2012) Cloning of atypical chemokine receptors CRAM-A and CRAM-B for comparative functional analysis. **3rd European Congress of Immunology**, Glasgow, Scotland, P0010, P188, 137 (Suppl. 1), 185-772.

Sarmadi P., Esendagli G. (2012) Cloning of atypical chemokine receptors CRAM-A and CRAM-B for comparative functional analysis. **Molecular Immunology & Immunogenetics Congress**, Antalya, Turkey, PP-29, P118, Turkish Journal of Immunology, Volume: 1, Number: 17.



2nd International Molecular Immunology & Immunogenetics Congress (MIMIC-II)

April 27-30, 2014
Ramada Plaza Hotel
Antalya - TURKEY

PROGRAMME & ABSTRACT BOOK

www.mimic2014.org

cell proliferation. Unexpectedly CXCR2 blockage significantly increased MIP-2 secretion.

CONCLUSIONS: These results demonstrated for the first time that MIP-2 and CXCR2 receptors are involved in growth of brain and liver metastatic cells of breast carcinoma and CXCR-2 antagonist might have therapeutic potential in metastatic breast cancer.

Keywords: MIP-2, Breast cancer, CXCR2, chemokines

P-086

[ABSTRACT REF.: 014

CCRL2 ATYPICAL CHEMOKINE RECEPTOR VARIANTS' EXPRESSION AND FUNCTIONAL ANALYSIS IN BREAST CANCER CELLS

Parisa Sarmadj, Gunes Esendagli

Department of Basic Oncology, Hacettepe University Cancer Institute, Ankara, Turkey

Atypical chemokine receptors play role in the termination of inflammatory responses and CCRL2 is the newest member. CCRL2 binds CCL5, CCL19 and chemerin and decreases their local concentration. Therefore, immune cell migration is hampered. Human CCRL2 gene has two variants; namely, CRAM-A and CRAM-B. The aim of this work is to investigate the expression and the functions of these variants in breast cancer cells.

CRAM-A and CRAM-B expression were determined with RT-PCR in breast cancer cell lines, PBMCs, and purified-immune cells under IFN- γ or LPS stimulation. pCRAM-A-IRES2-EGFP and pCRAM-B-IRES2-EGFP recombinant DNAs were constructed and confirmed by PCR, restriction-digestion and DNA-sequencing. These recombinant-plasmids and the empty-vector were transfected into HEK293T cell line and MDA-MB-468 and BT-474 breast cancer cell lines. Transfection efficiency (GFP-expression) and recombinant CRAM expression were examined by flow cytometry. For functional analyses; Ca²⁺ flux (FuraRed II staining), ligand-binding, receptor-internalization and ligand-removal assays were performed with or without CCRL2-blocking antibodies. Recombinant CCRL2 constructs were successfully expressed in HEK293T cells (GFP+ CCRL2+ 66.3-84.22%). As expected, CCL5, CCL19 and chemerin did not stimulate intracellular Ca²⁺ flux, whereas ionomycin Ca²⁺ ionophore did. On breast cancer cells, CRAM-A expression was specifically increased upon IFN- γ stimulation. In the presence of chemokine ligands, CRAM-A internalization was determined in ~30 minute-intervals. In addition, CCL19 was the most efficiently removed chemokine from the environment. This effect was observed both in HEK293T and BT-474 cell lines transfected with recombinant CCRL2. Therefore, CRAM-A expression may serve as an immune evasion mechanism that mitigates T cell infiltration towards the tumor.

Keywords: Atypical chemokine receptor, CCRL2, Chemokine, Recombinant DNA technology.

P-087

ABSTRACT REF.: 080

T HELPER RESPONSES ARE MAINTAINED BY BASAL-LIKE BREAST CANCER CELLS AND CONFER TO IMMUNE MODULATION VIA UPREGULATION OF PD-1 LIGANDS

Pinar Karasay, Güneş Esendağlı

Department of Basic Oncology, Hacettepe University, Ankara, Turkey

INTRODUCTION: Even though a high cytotoxic T cell infiltration is generally associated with favorable prognosis, the immunological course of breast cancer is explicitly directed by helper T cells. This study aims to determine the influence of BLBCs on CD4+ T cell responses.

METHODS: Co-cultures were established between breast cancer cell lines and CD4+ T cells under stimulatory conditions. Helper T cell activation, proliferation, cytokine secretion, and differentiation were assessed. Protein and mRNA expression of PD-1 ligands were determined on breast cancer cell lines. Blockage assays were performed in order to determine the functional assets of PD-1 ligation.

RESULTS: In contrast to luminal breast cancer cells, BLBC cells allowed CD4+ T cell activation, proliferation, and IFN- γ secretion, but only to a certain extent. In return, IFN- γ stimulated the upregulation of PD-L1 and/or PD-L2 on the basal-like cells. A substantial population of CD25+CD127low/- regulatory T (Treg) cells was also induced in BLBC co-cultures. Accordingly, in prolonged periods of co-culturing, blockage of PD-1 ligands on BLBC cell lines impaired Treg differentiation, restored IL-2 secretion, and increased CD8+ T cell activation. **CONCLUSIONS:** T helper responses were permitted by BLBC cells. On the other hand, IFN- γ secreted from Th1 and other immune cells upregulated the expression of PD-1 ligands on BLBC cells and modulated the immune reactions. Our results indicate the capacity of BLBCs to adapt to IFN- γ -mediated immune responses and to evade immunity via upregulation of PD-1 ligands.

Keywords: Basal-like breast cancer; T lymphocyte; immune modulation; PD-1.

P-088

ABSTRACT REF.: 077

TYROSINE 416 IS PHOSPHORYLATED IN THE CLOSED, REPRESSED CONFORMATION OF C-SRC

Sevgi Irtegun¹, Rebecca J Wood², Angeliqe R Ormsby², Terrence D Mulhern², Danny M Hatters²

¹*Department of Medical Biology, Dicle University, Diyarbakir, Turkey*

²*Department of Biochemistry and Molecular Biology, The University of Melbourne, Australia*

c-Src signaling controls many cellular events such as cell growth, proliferation, differentiation, motility and cell adhesion. The kinase activity of c-Src depends on whether the protein is in the more expanded "open" active conformation or in the more compact "closed" repressed conformation. Phosphorylation of Y527 facilitates the formation of the closed conformation by enabling high affinity binding of the SH2 domain to the C-tail. This interaction, as well as binding between the SH3 domain and the SH2-kinase linker, creates a compact structure that represses kinase activity. Dephosphorylation of Y527 releases SH2 binding to the C-tail leading to a more open conformation with far greater kinase activity. Here we investigated the correlation of Y416 phosphorylation with c-Src activity when c-Src was locked into the open and closed conformations (by mutations Y527F and Q528E, P529E, G530I respectively). Consistent with prior findings, we found Y416 to be more greatly phosphorylated when c-Src was in an open, active conformation. However, we also observed an appreciable amount of Y416 was phosphorylated when c-Src was in a closed, repressed conformation under conditions by which c-Src was unable to phosphorylate substrate STAT3. The phosphorylation of Y416 in the closed conformation arose by autophosphorylation, since abolishing kinase activity by mutating the ATP binding site (K295M) prevented phosphorylation. Basal Y416 phosphorylation correlated positively with cellular levels of c-Src suggesting autophosphorylation depended on self association. Using sedimentation velocity analysis on cell lysate with fluorescence detection optics, we confirmed that c-Src forms monomers and dimers, with the open conformation also forming a minor population of larger mass complexes. Collectively, our studies suggest a model by which dimerization of c-Src primes

22.

ULUSAL İMMÜNOLOJİ KONGRESİ

27-30 Nisan 2013
Radisson Blu Çeşme Oteli



1974
Türk İmmünoloji Derneği

BİLDİRİ ve ÖZET KİTABI

www.ulusalimmunoloji2013.com

leri ile tümörün diferansiyasyonu, hacmi, T evresi, nöral ve peri-nöral invazyon varlığı arasında istatistiksel anlamlı bir ilişki tespit edilemedi. Ancak, T evresi arttıkça IL-32 ekspresyon düzeyinin de artma eğiliminde olduğu görüldü.

SONUÇ: Kolon kanserli hastaların tümör dokularında IL-32 gen ekspresyon düzeylerinin artmış olarak bulunması, invazyon parametreleri ile ilişki gösterilemese de T-evresi ile aradaki korelasyon, IL-32'nin kolon kanseri etyopatogenezinde rol oynayabileceğini düşündürmektedir. Tümörlü dokularda IL-32 proteinin ekspresyon düzeyini göstermek üzere çalışmalara devam edilecektir.

Anahtar Kelimeler: IL-32, Kolon Kanseri, Gen Ekspresyonu,

P-117

Ref. No: 36

CRAM-A VE CRAM-B ATİPİK KEMOKİN RESEPTÖRLERİNİN KLONLANMASI VE FONKSİYONEL ANALİZİ

Parisa Sarmadı, Güneş Esendağlı

Hacettepe Üniversitesi, Temel Onkoloji AD, Ankara

Genel bilgiler: Atipik kemokin reseptörleri, inflamatuvar yanıtların sonlandırılmasında rol oynar. CCRL2 atipik kemokin reseptör ailesinin en yeni üyesidir. İnsan CCRL2 geninin CRAM (Chemokine Receptor on Activated Macrophages) -A ve -B olarak adlandırılan iki farklı transkript varyantı bulunmaktadır. Bu reseptörler CCL5, CCL19 ve chemerin ligandlarına bağlanarak ortamdaki kemokin miktarını azaltır ve immün hücre migrasyonu engellenir.

AMAÇ: Bu çalışmanın amacı, insan CRAM-A ve CRAM-B genlerini ökaryotik ekspresyon vektörüne klonlamak ve bu farklı varyantların fonksiyonelliğini ve kemokin gradyanı üzerindeki etkisini araştırmaktır.

YÖNTEM: Total cDNA RT-PCR ile sentezlendi. CRAM-A ve CRAM-B protein kodlayan cDNA dizileri, özel primerler ve pfu DNA polimeraz ile çoğaltıldı ve NheI-XmaI restriksiyon enzimleri ile kesildi. CRAM-A ve CRAM-B ampliconları ve pIRES2-EGFP ökaryotik ekspresyon vektörünün kesim ve izolasyonundan sonra T4 DNA ligaz reaksiyonu ile birleştirildi. Daha sonra, kompetan E.coli bakterilerine transforme edildi. Koloni seçimi ve plazmid izolasyonundan sonra, rekombinant DNA ürünleri PCR, restriksiyon kesim ve DNA dizilim analizleri ile doğrulandı. Bu rekombinant plazmidler ve boş vektör lipozomal transfeksiyonla HEK293T hücrelerine aktarıldı. Transfeksiyon verimliliği (GFP ekspresyonu) ve rekombinant CRAM ekspresyonu analizleri akim sitometri yöntemi ile incelendi. Klonlanan rekombinant CRAM genlerinin fonksiyonel analizleri, Ca²⁺ flux (FuraRed II boyası) ile, ligand bağlanma ve reseptör internalizasyon deneyleri CRAM geni aktarılan HEK293T hücrelerinde akim sitometri yöntemi ile yapıldı.

BULGULAR-SONUÇ: Rekombinant klonlar pCRAM-A-IRES2-EGFP ve pCRAM-B-IRES2-EGFP, CRAM ve EGFP'nin bisiystronik ekspresyonunu sağladı. pCRAM-A/B-IRES2-EGFP ekspresyon düzeylerine göre transfeksiyon verimliliği %66.3-84.22, CRAM-A ekspresyonu %83.8 ve CRAM-B ekspresyonu %15.4 olarak bulunmuştur. Kemokin bağlanma deneyinden elde edilen sonuçta göre, kemokinlerle uyandırılmamış kontrol hücreleri ve CCL5, CCL19 ve chemerin kokteyli eklenen hücrelerde hücre-içi Ca²⁺ miktarında bir değişim görülmezken pozitif kontrol olarak kullanılan ionomycin iyonoforu varlığında hücre içine Ca²⁺ akümüülasyonu gözlemlendi. Bu kemokinler varlığında CRAM reseptörünün de etkin bir şekilde yaklaşık 30 dk'lık periyotlarda internalize olduğu belirlendi. Bu rekombinant klonlar meme kanserli hücrelerine aktarılabilecek ve ilerde CCRL2'nin meme kanserinde oynadığı rolü araştırılacaktır.

Anahtar Kelimeler: Atipik kemokin reseptörü, CCRL2, Kemokin, Rekombinant DNA teknolojisi

P-118

Ref. No: 38

MEME KANSERİ HÜCRELERİNDE FARKLI CD40 İZOFORMLARINA AİT GEN EKSPRESYONUNUN İNCELENMESİ

Neşe Ünver¹, Diğdem Yöyen Ermiş², Bahar Çamurdanoğlu¹, Esra Kuzuca², Güneş Esendağlı¹

¹Hacettepe Üniversitesi Kanser Enstitüsü, Temel Onkoloji AD, Ankara

²Hacettepe Üniversitesi Kanser Enstitüsü, Temel Onkoloji Anabilim Dalı, Yaz Dönemi Staj Grubu 2011, Ankara

CD40, tümör nekroz faktörü reseptör (TNF-R) süperalesinin bir üyesidir. B hücre, makrofaj, dendritik hücrelerin yanı sıra meme kanserli hücrelerinin yüzeyinde de ekspresye olduğu gösterilmiştir. CD40 gen ekspresyonu, "alternative splicing" aracılığıyla post-transkripsiyonel düzeyde düzenlenir ve farklı izoformları oluşur. CD40 geninin 6 farklı mRNA varyantı bulunur. Bu izoformlardan sadece üçü proteine dönüşebilir. CD40 Tip I varyantı en uzun izoformdur, proteine dönüşen diğer varyantlardan Tip II salgılanabilir formdur. CD40 Tip III varyantında ise ligand bağlama bölgesindeki sisteinden zengin altbirim-3 (CRD-3)'ün bir kısmı ile CRD-4 bölgesi eksiktir. Bu nedenle, ligand bağlama afinitesinin düşük olabileceği düşünülmektedir.

AMAÇ: Bu çalışmada meme kanserli hücre hatlarında CD40 mRNA varyantlarının ekspresyonu araştırılmıştır.

YÖNTEM: HCC-38, MDA-MB-468, MDA-MB-231, ZR-75-1, T-47D, BT-474, MCF-7, SK-BR-3 meme kanserli hücre hatlarının ve MCF-12A normal meme hücre hattının kültürü yapıldı. Bunun yanı sıra CD40 ekspresyonunu uyardığı bilinen LPS (1 ug/ml, 24h) varlığında da hücre kültürü gerçekleştirildi. RNA izolasyonunu takiben cDNA sentezlendi. CD40 izoformlarına özgül primerler tasarlandı. CD40 varyant I, II ve III'ün ekspresyonu RT-PCR yöntemiyle araştırıldı.

BULGULAR: MCF-12A, SK-BR-3, MDA-MB-231, T-47D ve HCC-38 hücrelerinde her üç CD40 varyantının da ekspresye olduğu hem LPS içeren hem de içermeyen hücre kültürü koşulunda saptandı. BT-474 hücre hattında ise sadece LPS içermeyen hücre kültürü koşulunda CD40 varyant III belirlendi. LPS varlığında ise BT-474 hücreleri CD40 negatif idi.

SONUÇ: Anti-tümör immün yanıtları destekleyecek fonksiyonlara sahip olmayan CD40 Tip I mRNA varyantı dışındaki izoformların, meme kanserli hücrelerinin immün kaçışında etkili olabileceğini düşünülmektedir. Bu varyantlar tarafından kodlanan CD40 izoformlarının protein düzeyinde belirlenmesi ve fonksiyonel analizleri ancak ileriki çalışmalarla mümkün olabilecektir.

Anahtar Kelimeler: CD40, meme kanserli, alternative splicing

P-119

Ref. No: 64

PEDİYATRİK B HÜCRELİ AKUT LENFLOBLASTİK LÖSEMİ OLGULARDA MİNİMAL REZİDÜEL HASTALIK

Suzan Çınar, Burcin Aydın, İlhan Tahralı, Umur Can Küçüksezer, Abdullah Yılmaz, Günnur Deniz

İstanbul Üniversitesi, Deneysel Tıp Araştırma Enstitüsü, İmmünooloji AD, İstanbul.

Lenfoblastlardan kaynaklanan neoplazilerden Akut Lenfoblastik Lösemi (ALL)'lerin %80-85'i prekürsör B hücrelerinden kaynaklanmaktadır. Tedavinin 15. günündeki kemik iliği (Kİ) submikroskopik lösemi hücreleri (minimal rezidüel hastalık, MRD) ile prognoz ilişkilidir. MRD tanısı, moleküler yöntemlere göre daha hızlı ve ucuz olması nedeniyle birçok merkezde "Flow sitometri" (FCM) ile yapılabilmektedir. MRD'nin FCM ile değerlendirilmesi AIEOP-BFM protokolüne göre, B hücreli (B-) ALL tanısındaki belirgin antijen



20. ULUSAL KANSER KONGRESİ



19 - 23 Nisan 2013
Susesi Otel - ANTALYA

BİLDİRİ ÖZETLERİ KİTABI



www.ukk2013.org

serlerin karsinogenezinde sıklıkla rastlanmaktadır. Transkripsiyonel olarak baskılanan genlerden birçoğunun HNSCC gelişimindeki rolü henüz tanımlanmayı beklemektedir. Bu çalışmada, HNSCC'de epigenetik yolla baskılanan yeni genleri tanımlamak amacıyla farmakolojik demetilasyon ve genişletilmiş mRNA ekspresyon profillemeye yaklaşımı ile mikroarray ekspresyon analizi yöntemleri kullanıldı.

Gereç-Yöntem: İki HNSCC hücre soyu, 5-aza-2'-deoxycytidine (5-Aza-dC) ile muamele edildikten sonra mikroarray analizi yapıldı. 13 HNSCC tümörü ve 5 normal mukozaya örneği Affymetrix 47K mRNA gen ekspresyon array ile incelendi ve hücre soyu verileriyle karşılaştırıldı. Aday genlerin promotör bölgeleri bisülfid DNA dizi analizi yöntemi ile tarandı. Seçilen aday genlerin metilasyon durumları kantitatif metilasyon-spesifik PCR (QMSP) yöntemiyle 22 normal tükürük, 14 normal mukozaya ve 33 HNSCC tümör örneğinde incelendi.

Bulgular: 5-Aza-dC muamelesi sonrası, iki HNSCC hücre soyunda ayrı ayrı ve kombine olarak elde edilen analiz sonuçları değerlendirildiğinde, sırasıyla 1960, 614 ve 427 genin ekspresyonunda artış saptandı. Mikroarray analizi ile normal mukozaya kıyasla HNSCC tümör örneklerinde 7140 genin ekspresyonunda azalma gözlemlendi. Tümör örneklerinde TSG'lerde normal mukozaya örneklerine kıyasla tumorda düşük ekspresyon profilleri elde edildi. 126 aday genin tanımlandığı integratif analiz ve bisülfid dizi analizi sonrası, HNSCC'de farklı seviyelerde hipermetile olan 7 aday gen seçildi. Tümör örneklerinde sadece 7 gene ait promotör bölgede CpG adacıklarında metilasyon gözlenirken, normal mukozaya örneklerinde metilasyona rastlanmadı. QMSP yöntemi ile doğrulama sonrası, HNSCC ile ilişkili 3 gen tanımlandı.

Sonuç: Tanımlanan aday genlerden guanine nucleotide-binding protein gamma-7 (*GNG7*), geni tümör örneklerinde yüksek düzeyde metile ve normal tükürük ile mukozaya örneklerinde ise metillenmemiş olduğundan bu genin, HNSCC tümör dokusuna özgü metilasyon gösterdiği sonucuna varıldı. *TXNIP* ve *TUSC2* genleri ise tümör ve normal tükürük örneklerinde düşük düzeyde metile iken normal mukozada metilasyona rastlanmadı. Sonuç olarak *GNG7* promotör bölgesinde gözlenen yüksek seviyeli metilasyon HNSCC ile kausal ilişkili bulunurken, *TXNIP* ve *TUSC2* genleri de HNSCC için potansiyel biyomarker aday oldukları düşünülmektedir.

Ref No: S031

Tümör Biyolojisi

MEME KANSERİ HÜCRELERİNE AKTARILMAK ÜZERE CRAM-A VE CRAM-B ATİPİK KEMOKİN RESEPTÖRLERİNİN KLONLANMASI VE FONKSİYONEL ANALİZİ

Parisa Sarmadı, Güneş Esendağlı

Hacettepe Üniversitesi, Kanser Enstitüsü, Temei Onkoloji Ana Bilim Dalı, Sıhhiye- Ankara

Genel bilgiler: Atipik kemokin reseptörleri, inflamatuvar yanıtın sonlandırılmasında rol oynar. CCRL2 atipik kemokin reseptör ailesinin en yeni üyesidir. İnsan CCRL2 geninin CRAM (Chemokine Receptor on Activated Macrophages) -A ve -B olarak adlandırılan iki farklı transkript varyantı bulunmaktadır. Bu reseptörler CCL5, CCL19 ve chemerin ligandlarına bağlanarak ortamdaki kemokin miktarını azaltır ve immün hücre migrasyonu engellenir. CCRL2'nin meme kanserindeki rolü henüz araştırılmamıştır.

Amaç: Bu çalışmanın amacı, insan CRAM-A ve CRAM-B genlerini ökaryotik ekspresyon vektörlerine klonlamak ve fonksiyonelliğini araştırmaktır. Klonlanan bu genler daha sonra meme kanseri hücrelerinde CCRL2'nin fonksiyonunu araştırmak için kullanılacaktır.

Gereç-Yöntem: MDA-MB-231 meme kanseri hücrelerinden izole edilen RNA'dan cDNA RT-PCR yöntemi ile sentezlendi. CRAM-A ve CRAM-B protein kodlayan cDNA dizileri, özel primerler ve *pfu* DNA polimeraz ile çoğaltıldı ve *NheI-XmaI* restriksiyon enzimleri ile kesildi. CRAM-A ve CRAM-B ampiklonları pIRES2-EGFP ökaryo-

tik ekspresyon vektörüne T4 DNA ligaz reaksiyonu ile yerleştirildi. Daha sonra, kompetan *E.coli* bakterilerine transforme edildi. Koloni seçimi ve plazmid izolasyonundan sonra, rekombinant DNA ürünleri PCR, restriksiyon kesim ve DNA dizi analizleri ile doğrulandı. Bu rekombinant plazmidler ve boş vektör lipozomal transfeksiyonla HEK293T hücrelerine aktarıldı. Transfeksiyon verimliliği (GFP ekspresyonu) ve rekombinant CRAM ekspresyonu analizleri akım sitometri yöntemi ile incelendi. Klonlanan rekombinant CRAM genlerinin fonksiyonel analizleri, Ca²⁺ flux (FuraRed II boyası ile), ligand bağlanma ve reseptör internalizasyon deneyleri CRAM geni aktarılan HEK293T hücrelerinde akım sitometri yöntemi ile yapıldı.

Bulgular-Sonuç: Yapılan moleküler analizler sonucunda elde edilen rekombinant ürünlerin dizileri doğruluğu NCBI gen bankası verileri ile karşılaştırılarak belirlendi. Rekombinant klonlar pCRAM-A-IRES2-EGFP ve pCRAM-B-IRES2-EGFP, CRAM ve EGFP'nin bisitronik ekspresyonunu sağladı. pCRAM-A/B-IRES2-EGFP ekspresyon düzeylerine göre transfeksiyon verimliliği %66.3-84.22, CRAM-A ekspresyonu %83.8 ve CRAM-B ekspresyonu %15.4 olarak bulunmuştur. Kemokinlerle uyarılmamış kontrol hücreleri ve CCL5, CCL19 ve chemerin kokteyli eklenen hücrelerde hücre-içi Ca²⁺ miktarında bir değişim görülmezken pozitif kontrol olarak kullanılan ionomycin iyonoforu varlığında hücre içine Ca²⁺ akümülasyonu gözlemlendi. Bu kemokinler varlığında CRAM reseptörünün de etkin bir şekilde yaklaşık 30 dk.'lık periyotlarda internalize olduğu belirlendi.

Tartışma: Klonladığımız CCRL2 varyantlarının ökaryotik hücrede ekspresyonu ve kemokinleri bağlayarak ortamdaki uzaklaştırıcı tuzak reseptör fonksiyonunu taşıdığını belirledik. Bu klonlar meme kanseri hücrelerine aktarılacak ve ileride, CCRL2'nin meme kanserinde oynadığı rol araştırılacaktır.

Ref No: S032

Tümör Biyolojisi

ANDROJEN MUAMELE EDİLEN PROSTAT KANSERİ HÜCRELERİNDEN MİKORNA SALINIMININ İN VİTRO KARAKTERİZASYONU

Duygu Tiryakioğlu, Merve Çetinkaya, Emre Özgür, Nejat Dalay, Uğur Gezer
Istanbul Üniversitesi Onkoloji Enstitüsü, Temei Onkoloji Ana Bilim Dalı, İstanbul

Amaç: Prostat kanseri erkeklerde en sık rastlanan malin tümördür ve kanserden ölümlerde akciğer tümörlerinden sonra ikinci en yüksek ölüm nedenidir. Prostat kanseri androjen bağımlı bir malignitedir ve hormonal tedavi, ileri ve/veya metastatik prostat kanserinin en yaygın olarak kullanılan tedavi yöntemidir; ancak hastaların önemli bir bölümünde androjene direnç gelişir ve hastalık hızla ilerler. Bu nedenle diğer kanser türlerinde olduğu gibi prostat kanserinde de hastalığın progresyonunun takibi açısından yeni biyobelirteçlere gereksinim vardır. Son yıllarda yapılan çalışmalar mikroRNA'ların (miRNA'lar), diğer kanserlerde olduğu gibi prostat kanseri patogenezi de rol aldığını ortaya koymaktadır. miRNA'lar ile prostat kanseri arasındaki ilişkiyi araştırmak için yapılmış olan çalışmalar özellikle miR-141 ve miR-375'in artmış plazma düzeylerinin ileri evre/metastatik prostat kanseri ile ilişkili olduğunu ortaya koymaktadır. Bu gözlemler, prostat kanseri progresyonu sürecinde bu iki molekülün androjen hormonu tarafından düzenleniyor olabileceğini düşündürmüştür. Bu noktadan hareketle, çalışmamızda hormona duyarlı bir prostat kanseri hücre soyu olan LNCaP hücreleri model sistem olarak kullanılarak androjen muamelesinin, miR-141 ve miR-375 moleküllerinin ifade düzeylerini nasıl etkilediği ve hücrelerden kültür ortamına salınıp salınmadığı incelendi. miRNA ifadesi ve hücrelerden salınması, prostat spesifik antijen (PSA) ve bir prostat kanser spesifik kodlamayan RNA olan PCA3'ün ekspresyonu ve salınımı ile karşılaştırıldı.

Gereç-Yöntem: Yaklaşık 200.000 hücre 48 saat steroid hormonlardan arındırılmış kültür ortamında büyütüldükten sonra, 0, 1, 10 ve

British Society for
immunology

EUROPEAN CONGRESS OF IMMUNOLOGY
2012 GLASGOW

Scottish Exhibition and Conference Centre (SECC)
Glasgow, Scotland | 5 - 8 September, 2012



INDUSTRY SPONSORSHIP PROSPECTUS



European Federation of
Immunological Societies



www.eci-glasgow2012.com

lower resulting in reduced neutrophil and lymphocyte chemotactic properties. Although citrullination of CXCL8 moderately reduced its signaling properties, no difference in chemotactic activity was detected *in vitro*. However, upon intraperitoneal injection, both citrullinated CXCL5 and CXCL8 had a highly reduced ability to attract neutrophils to the peritoneal cavity. Citrullinated CXCL8 retained its angiogenic activity and efficiently mobilized neutrophils upon intravenous injection.

Conclusions: PAD-dependent citrullination of chemokines dampens their inflammatory activity.

P0008

Chemokine receptor CCR7 on CD4⁺ T cells plays a crucial role in the induction of experimental autoimmune encephalomyelitis

P. Belikan, F. Zipp & V. Siffrin

Department of Neurology, University Medical Center of the Johannes Gutenberg University of Mainz, Mainz, Germany

Purpose/Objective: Experimental autoimmune encephalomyelitis (EAE) is the animal model for the human disease multiple sclerosis. EAE is mediated by myelin-specific CD4⁺ helper T cells. The chemokine receptor CCR7 is an important factor for immune cell trafficking and recirculation not only in the secondary lymphoid organ, but also within target organs of an inflammatory attack. Previous data suggested that CCR7 deficiency influenced clinical disease by altering dendritic cell biology.

Materials and methods: Using different animal models for multiple sclerosis and *in vivo* imaging technique within the CNS, we investigated the role of T cells in animals which lack the CCR7 on T cells.

Results: We demonstrate here that CD4⁺ T cell-specific constitutive deletion of CCR7 led to an impaired clinical course in EAE. In adoptive transfer EAE, mice receiving CCR7^{-/-} myelin antigen T cell receptor transgenic 2d2 TH17 cells showed an earlier disease onset compared to mice adoptively transferred with CCR7^{+/+} 2d2 TH17 cells. Thus CCR7-deficiency on TH17 cells caused an increased encephalitogenicity in adoptive transfer EAE. We monitored the trafficking of CCR7^{-/-} and CCR7^{+/+} 2d2 TH17 cells within the CNS by two-photon laser scanning microscopy in living anaesthetized mice and identified distinct motility patterns. In contrast to the findings in adoptive transfer EAE, CCR7 deficiency on CD4⁺ cells led to a delayed disease onset in active EAE induced with MOG in lymphopenic RAG^{-/-} mice, which had been grafted with CCR7^{-/-}, CCR7^{+/+} or CCR7^{+/+}. This could be attributed to impaired T cell priming in secondary lymphoid organs, which most likely resulted from reduced lymph node homing potential.

Conclusions: Taken together these findings underline a crucial and paradoxical role of CCR7 in neuroinflammation.

P0009

Chemokine-mediated innate immune responses to mosquito bites and their viruses

C. McKimmie,* A. Kohl,* J. K. Fazakerley[†] & G. J. Graham*

*Institute of Infection Immunity and Inflammation, University of Glasgow, Glasgow, UK, [†]Institute of Animal Health, Pirbright, UK

Purpose/Objective: Diseases spread by mosquitoes have a significant impact on human health and include disease caused by viruses such as Chikungunya and West Nile virus. There remains a need to understand the complex interplay between these viruses, their mosquito vectors and their mammalian hosts. The early events of infection are critically important for disease outcome in the host. Strikingly, arbovirus inoculated via bites or accompanied by arthropod saliva induces a more rapid viraemia, higher mortality and higher pathogen load, compared to inoculation via a needle. Although, how virus disseminates from the inoculation site and what role arthropod saliva have in facilitating this process are not understood.

Chemokines have pivotal functions in the immune system, without which coordinated immune responses would not occur. We have studied chemotactic responses during key stages of infection, from the mosquito bite site to target CNS tissue.

Materials and methods: We have used a relevant, tractable *in vivo* model system to study the effects of bites and arbovirus infection on the chemokine system and other key innate immune processes. We have carefully mapped the kinetics of virus spread from skin inoculation sites and assayed the expression of chemokines and innate immune genes during these early stages of infection.

Results: Surprisingly, virus spreads within hours from skin to draining lymph nodes followed by viraemia at 48 h, suggesting that virus primarily disseminates away from bite sites via lymph fluid. Mosquito bites trigger chemotactic responses in the skin and lymph nodes that are qualitatively and temporally distinct from those triggered by virus infection. Bites induce a chemokine response dominated by neutrophil attracting chemokines whilst virus infection induces a later response dominated by the ligands for CXCR3.

Conclusions: In summary, we have developed a new model for studying chemotactic processes *in vivo* and defined a key aspect of innate anti-viral immunity in the initiating stages of a mosquito-borne virus infection.

P0010

Cloning of atypical chemokine receptors CRAM-A and CRAM-B for comparative functional analysis

P. Sarmadi & G. Esendagli

Department of Basic Oncology, Institute of Oncology, Hacettepe University, Ankara, Turkey

Purpose/Objective: Atypical chemokine receptors play an important role in the termination of inflammatory responses. Upon binding to their cognate ligands, chemokine gradient drops and immune cell migration is hampered. CCRL2 is the newest member of atypical chemokine receptor family. The human CCRL2 gene has two transcript variants CRAM-A (Chemokine Receptor on Activated Macrophages) and CRAM-B. The aim of this study is to compare the effect of these different variants on the chemokine gradient.

Materials and methods: Total cDNA was synthesized using RT-PCR. CRAM-A and CRAM-B protein coding cDNAs, specific primers and *Pfu* DNA polymerase were used in amplification and site-directed cloning (*NheI* and *XbaI* restriction enzyme sites). CRAM-A and -B amplicons, pIRES2-EGFP and pcDNA3.1/CT-GFP eukaryotic expression vectors were digested, isolated, ligated, and then transformed into *E. coli* competent bacteria.

Results: The resulting constructs were confirmed by restriction analysis and DNA sequencing. The recombinant clones pCRAM-A-IRES2-EGFP and pCRAM-B-IRES2-EGFP enabled the bicistronic expression of CRAM and EGFP, whereas pcDNA3.1/CRAM-A-CT-GFP and pcDNA3.1/CRAM-B-CT-GFP produced a hybrid GFP-tagged protein. The recombinant plasmids and empty vectors were delivered into HEK293T cell line via liposomal transfection. Transfection efficiency (GFP expression) and recombinant CRAM expression were analyzed by flow cytometry.

Conclusions: In conclusion, the transcript variants of human CCRL2 gene were cloned into different recombinant DNA constructs and *de novo* expression of recombinant CRAM proteins were determined. Next, the ligand binding assays will be performed with CRAM-A or CRAM-B-expressing cells.

Molecular Immunology & Immunogenetics Congress, 2012

TURKISH JOURNAL *of* IMMUNOLOGY

The Official Journal of the Turkish Society of Immunology



Türk İmmünoloji Dergisi – Volume: 1, Number: 17

Supplement (Molecular Immunology & Immunogenetics Congress – Abstract Book), 2012

PP-29

CLONING OF ATYPICAL CHEMOKINE RECEPTORS CRAM-A AND CRAM-B FOR COMPARATIVE FUNCTIONAL ANALYSIS

Parisa SARMADI, Basic Oncology, Oncology, Ankara
Gunes ESENDAGLI, Basic Oncology, Oncology, Ankara

Atypical chemokine receptors play an important role in the termination of inflammatory responses. Upon binding to their cognate ligands, chemokine gradient drops and immune cell migration is hampered. CCRL2 is the newest member of atypical chemokine receptor family. The human CCRL2 gene has two transcript variants CRAM-A and -B. The aim of this study is to compare the effect of these different variants on the chemokine gradient. Total cDNA was synthesized using RT-PCR. CRAM-A and -B protein coding cDNAs, specific primers and Pfu DNA polymerase were used in amplification and site-directed cloning (NheI and XmaI restriction enzyme sites). CRAM-A and -B amplicons, pIRES2-EGFP and pcDNA3.1/CT-GFP eukaryotic expression vector were digested, isolated, ligated, and then transformed into E.coli competent bacteria. The resulting constructs were confirmed by restriction analysis and DNA sequencing. The recombinant clones pCRAM-A-IRES2-EGFP and pCRAM-B-IRES2-EGFP enabled the bicistronic expression of CRAM and EGFP, whereas pcDNA3.1/CRAM-A-CT-GFP and pcDNA3.1/CRAM-B-CT-GFP produced a hybrid GFP-tagged protein. The recombinant plasmids and empty vectors were delivered into HEK293 cell line via liposomal transfection. Transfection efficiency (GFP expression) and recombinant CRAM expression were analyzed by flow cytometry. In conclusion, the transcript variants of human CCRL2 gene were cloned into different recombinant DNA constructs and de novo expression of recombinant CRAM proteins were determined. Next, the ligand binding assays will be performed with CRAM-A or -B-expressing cells.

Keywords: Atypical Chemokine Receptors, CRAM, Chemokine, Recombinant DNA Technology



TÜRK İMMÜNOLOJİ DERNEĞİ

Başkan
Dr. Günnur Deniz

Yeznedar
Dr. Tunç Akkoç

Genel Sekreter
Dr. Gaye Erten

Başkan Yardımcısı
Dr. Barbaros Oral

Üyeler
Dr. Dicle Güç
Dr. Emel Ekşioğlu-Demiralp
Dr. Vedat Bulut

03 Ekim 2012

Sayı: 31

Sayın Parisa Sarmadi,

Derneğimizin 27-29 Nisan 2012 tarihleri arasında Antalya'da düzenlemiş olduğu "Molecular Immunology & Immunogenetics Congress 2012 (MIMIC 2012)" etkinliği çerçevesinde birincilik poster ödülü kazanmış bulunmaktasınız.

Bu ödül 2013 yılında Derneğimiz tarafından düzenlenecek olan 22. Ulusal İmmünoloji Kongresi'ne ulaşım, kayıt ve konaklama içermektedir.

Gereğini bilgilerinize rica ederim.

Saygılarımla.

Prof. Dr. Günnur Deniz

Başkan

İletişim: DETAE, Vakıf Güreba Cad. Şehremini, 34280, İstanbul,

Tel: 0212 414 2232, 0212 414 2000 / 33355

Faks: 0212 532 41 71

gdeniz@istanbul.edu.tr, gerten@istanbul.edu.tr